

**EFFECTS OF SCRATCHING RATE ON CERCHAR
ABRASIVENESS INDEX OF SANDSTONES**



**A Thesis Submitted in Partial Fulfillment of the Requirements for the
Degree of Master of Engineering in Civil, Transportation and
Geo-Resources Engineering
Suranaree University of Technology
Academic Year 2020**

ผลกระทบของอัตราการขาดต่อดัชนีความสึกกร่อนแบบเซอร์คาร์ของหินทราย



นางสาวธราภรณ์ โคตรสมบัติ

วิทยานิพนธ์นี้เป็นส่วนหนึ่งของการศึกษาตามหลักสูตรปริญญาวิศวกรรมศาสตรมหาบัณฑิต

สาขาวิชาวิศวกรรมโยธา ขนส่ง และทรัพยากรธรณี

มหาวิทยาลัยเทคโนโลยีสุรนารี

ปีการศึกษา 2563

EFFECTS OF SCRATCHING RATE ON CERCHAR

ABRASIVENESS INDEX OF SANDSTONES

Suranaree University of Technology has approved this thesis submitted in partial fulfillment of the requirements for a Master's Degree.

Thesis Examining Committee



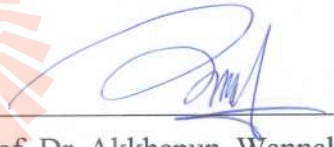
(Assoc. Prof. Dr. Pornkasem Jongpradist)

Chairperson



(Prof. Dr. Kittitep Fuenkajorn)

Member (Thesis Advisor)



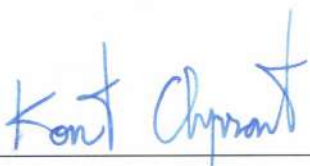
(Asst. Prof. Dr. Akkhapun Wannakomol)

Member



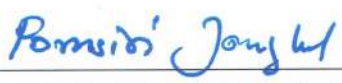
(Dr. Thanittha Thongprapha)

Member



(Assoc. Prof. Ft. Lt. Dr. Kontom Chamniprasart)

Vice Rector for Academic Affairs
and Internationalization



(Assoc. Prof. Dr. Pornsiri Jongkol)

Dean of Institute of Engineering

ธราภรณ์ โศตรสมบัติ : ผลกระทบของอัตราการขูดต่อดัชนีความสึกกร่อนแบบเชอคาร์
ของหินทราย (EFFECTS OF SCRATCHING RATE ON CERCHAR ABRASIVENESS
INDEX OF SANDSTONES) อาจารย์ที่ปรึกษา : ศาสตราจารย์ ดร.กิตติเทพ เฟื่องขจร,
105 หน้า.

วัตถุประสงค์ของการศึกษานี้คือ เพื่อหาผลกระทบของอัตราการขูดต่อดัชนีความสึกกร่อน
แบบเชอคาร์ (CAI) ของหินทรายพระวิหาร ภูพาน และภูกระดึง ภายใต้สภาวะแห้งและสภาวะ
อิมตัวด้วยน้ำ อัตราการขูดผันแปรจาก 0.001 0.01 0.1 และ 1 มิลลิเมตรต่อวินาที ผลการทดสอบ
ระบุว่าค่า CAI เพิ่มขึ้นแบบเชิงเส้นกับแทนด้วยการเพิ่มกำลังอัดแกนเดียวและค่าความเค้นยึดติด
ของหินทรายที่ทดสอบ ภายใต้อัตราการขูดเดียวกัน หินทรายที่อิมตัวด้วยน้ำจะให้ค่า CAI ค่ากำลัง
ของหิน และค่าความเค้นยึดติดต่ำกว่า แต่ให้ปริมาตรร่องที่มากกว่าหินทรายที่ทดสอบแบบแห้ง
งานที่กระทำถูกคำนวณจากการอินทิเกรตแรงต้านข้างกับระยะการขูดมีค่าเพิ่มขึ้น เมื่อค่า CAI และ
อัตราการขูดเพิ่มขึ้น ภายใต้สภาวะการทดสอบเดียวกันหินทรายพระวิหารมีค่า CAI ปริมาตรร่อง
และงานที่กระทำมากที่สุด แต่ใช้พลังงานจำเพาะน้อยที่สุดเมื่อเทียบกับหินทรายอีกสองชนิด
อัตราการขูดที่ต่ำมักจะให้ค่าพลังงานจำเพาะที่ต่ำกว่าแต่ให้ปริมาตรร่องที่มากกว่าเมื่อมีอัตราการขูด
สูงกว่า ผลการศึกษานี้สามารถใช้เป็นข้อมูลประกอบการพิจารณาสำหรับการขูดเจาะในชั้นหิน
ด้วยวิธีแบบต่อเนื่อง



สาขาวิชา เทคโนโลยีธรณี
ปีการศึกษา 2563

ลายมือชื่อนักศึกษา ธราภรณ์ โศตรสมบัติ
ลายมือชื่ออาจารย์ที่ปรึกษา ก. กิตติเทพ

TARAPORN KOTSOMBAT : EFFECTS OF SCRATCHING RATE ON
CERCHAR ABRASIVENESS INDEX OF SANDSTONE. THESIS

ADVISOR : PROF. KITTITEP FUENKAJORN, Ph.D., P.E., 105 PP.

CAI VALUE/SANDSTONE/SCRATCHING GROOVE/SPECIFIC ENERGY

The objective of this study is to determine the effects of scratching rates on CERCHAR abrasiveness index (CAI) of Phra Wihan, Phu Phan and Phu Kradung sandstones under dry and saturated conditions. The scratching rates are varied from 0.001, 0.01, 0.1 to 1 mm/s. Results indicate that CAI values increase linearly with increasing unconfined compressive strength and cohesion of the tested sandstones. Under the same scratching rate, saturated sandstones give lower CAI values, rock strength and cohesion but larger groove volume than dry sandstones do. Work done calculated from integrating lateral force over scratching distance increases with increasing CAI values and scratching rate. Under the same test conditions, Phra Wihan sandstone yields largest CAI values, groove volumes and work done but uses least specific energy, as compared to the other two sandstones. Lower scratching rates tend to give lower specific energy but larger groove volume than higher rates do. The outcomes of this study can be used as an operation consideration for rock excavation with continuous methods.

School of Geotechnology

Academic Year 2020

Student's Signature

Taraporn Kotsombat

Advisor's Signature

K. Fuenkajorn

ACKNOWLEDGEMENTS

I wish to acknowledge the funding support from Suranaree University of Technology (SUT).

I would like to express my sincere thanks to Prof. Dr. Kittitep Fuenkajorn for his valuable guidance and efficient supervision. I appreciate his strong support, encouragement, suggestions and comments during the research period. My heartiness thanks to Assoc. Prof. Dr. Pornkasem Jongpradist, Asst. Prof. Dr. Akkhapun Wannakomol and Dr. Thanittha Thongprapha for their constructive advice, valuable suggestions and comments on my research works as thesis committee members. Grateful thanks are given to all staffs of Geomechanics Research Unit, Institute of Engineering who supported my work.

Finally, I would like to thank beloved parents for their love, support and encouragement.



Taraporn Kotsombat

TABLE OF CONTENTS

	Page
ABSTRACT (THAI)	I
ABSTRACT (ENGLISH)	II
ACKNOWLEDGEMENTS	III
TABLE OF CONTENTS	IV
LIST OF TABLES	VIII
LIST OF FIGURES	IX
SYMBOLS AND ABBRIVIATIONS	XVII
CHAPTER	
I INTRODUCTION	1
1.1 Background and Rationale.....	1
1.2 Research Objectives.....	2
1.3 Scope and Limitations.....	2
1.4 Research Methodology.....	3
1.4.1 Literature review.....	3
1.4.2 Sample preparation.....	3
1.4.3 CERCHAR testing.....	4
1.4.4 Analysis.....	5
1.4.5 Discussions and conclusions.....	5
1.4.6 Thesis writing.....	5

TABLE OF CONTENTS (Continued)

	Page
1.5 Thesis Contents.....	6
II LITERATURE REVIEW.....	7
2.1 Introduction.....	7
2.2 Rock Abrasiveness.....	7
2.3 CERCHAR Testing.....	8
2.3.1 Test apparatus.....	8
2.3.2 Procedure.....	8
2.4 Factor Affecting CERCHAR Abrasiveness Index.....	10
2.4.1 Pin hardness.....	10
2.4.2 Pin speed.....	12
2.4.3 Testing length.....	12
2.4.4 Surface conditions.....	14
2.4.5 Rock moisture content.....	15
2.4.6 Varying applied load.....	15
2.5 Factors Affecting Mechanical Properties of Rock.....	17
2.5.1 Loading rate.....	17
2.5.2 Pore pressure.....	18
2.6 Relation between CERCHAR and Rock Properties.....	24
2.6.1 Physical properties.....	25
2.6.2 Mechanical properties.....	27
2.6.3 Mineral compositions.....	28

TABLE OF CONTENTS (Continued)

	Page
III SAMPLE PREPARATION	30
3.1 Introduction.....	30
3.2 Sample Preparation for CERCHAR Test.....	30
3.3 Equivalent Quartz Content	34
IV TEST APPARATUS AND METHOD	36
4.1 Introduction.....	36
4.2 CERCHAR Testing.....	36
4.3 Lateral Force Measurement.....	39
4.4 Vertical Displacement Measurement.....	40
V TEST RESULTS	42
5.1 Introduction.....	42
5.2 CAI Results.....	42
5.3 Lateral Force and Vertical Displacement.....	48
5.4 Groove volumes.....	48
VI ANALYSIS OF RESULTS	55
6.1 Introduction.....	55
6.2 Mathematical Relationships.....	55
6.3 Work and Energy.....	58
VII DISCUSSIONS AND CONCLUSIONS	69
7.1 Discussions.....	69
7.2 Conclusions.....	71

TABLE OF CONTENTS (Continued)

	Page
7.3 Recommendations for Future Studies.....	72
REFERENCES	73
APENDIX A	80
BIOGRAPHY	105



LIST OF TABLES

Table	Page
2.1 Physical properties of rock specimens (Khamrat et al., 2016)	24
3.1 Physical properties of sandstones (Khamrat et al., 2016)	30
3.2 Mechanical properties of sandstones (Khamrat et al., 2016)	31
3.3 Dry densities of sandstone specimens	33
3.4 Wet densities of sandstone specimens.....	34
3.5 Relationship between Mohs hardness and Rosiwal hardness (Bharti et al., 2017)	35
3.6 Mineral compositions of tested sandstones obtained from X-ray diffraction analysis	35
4.1 CAI classification (ASTM D7625-10)	39
5.1 CAI values under different scratching rates for Phra Wihan sandstones.....	44
5.2 CAI values under different scratching rates for Phu Phan sandstones.....	45
5.3 CAI values under different scratching rates for Phu Kradung sandstones.....	46
5.4 Groove volumes.....	54

LIST OF FIGURES

Figure	Page
1.1	Research methodology.....4
1.2	Test equipment similar to West apparatus..... 5
2.1	Two devices of CERCHAR testing (a) original CERCHAR and (b) West CERCHAR apparatuses (ASTM D7625-10)9
2.2	Relationship of HRC 40 (CAI ₄₀) and HRC 55 (CAI ₅₅) hardness values (Michalakopoulos et al., 2006)11
2.3	CAI values under different pin speeds (a) limestone, (b) sandstone and (c) quartzite (Rostami et al., 2014)13
2.4	Relationship between CAI and testing length of rock specimen surface (Plinninger et al., 2003) 14
2.5	CERCHAR test results for (a) saw-cut surface and (b) rough surface (Rostami et al., 2014)15
2.6	Effect of moisture contents on CAI (Jacobs and Hagan, 2009) 16
2.7	CAI as a function of force on the stylus (Rostami et al., 2014) 16
2.8	Rock strengths as a function of confining pressure at different loading rates for Phra Wihan, Phu Phan and Phu Kradung sandstones (Fuenkajorn and Kenkhunthod, 2010)19
2.9	Shear stresses as a function of shear strain at different loading rates (Fuenkajorn et al., 2012)20

LIST OF FIGURES (Continued)

Figure	Page
2.10 Relationships between dry and saturated UCS for 35 British Sandstones (Vasarhelyi, 2003)	21
2.11 Relationships between dry and saturated Young's modulus for 35 British sandstones (Vasarhelyi, 2003)	21
2.12 Relationships between unconfined compressive strength (UCS) and the tangent Young's modulus (E_{tan}) under dry and saturated conditions (Vasarhelyi, 2003)	22
2.13 Relationships between unconfined compressive strength (UCS) and the secant Young's modulus (E_{sec}) under dry and saturated conditions (Vasarhelyi, 2003)	23
2.14 Relationship between strength (σ_c) as function of water content (w) values up to 5% (Vasarhelyi and Van, 2006)	23
2.15 Relationships between strength (σ_c) as function of water content in only 1% (Vasarhelyi and Van, 2006)	24
2.16 Major principal stress ($\sigma_{1,f}$) as a function of loading rate ($\partial\sigma_1/\partial t$) (Khamrat et al., 2016)	26
2.17 CERCHAR index (1 mm) versus rock strength (Al-Ameen and Waller, 1994)	29
3.1 Some rectangular block specimens of Phra Wihan, Phu Phan and Phu Kradung sandstones used in CERCHAR test on saw-cut surface	32

LIST OF FIGURES (Continued)

Figure	Page
3.2	Nominal dimensions and guideline of scratching of specimens used in CERCHAR test on saw-cut surfaces.....32
3.3	Rock specimens saturated under water in vacuum chamber32
3.4	Water contents as function of time for all specimens33
4.1	Device modified from West CERCHAR apparatus (ASTM D7625-10)37
4.2	Schematic drawing of CERCHAR device used in this study.....37
4.3	Examples of stylus-55 HRC for CERCHAR testing.....39
4.4	Freebody diagram of lead screw..... 40
4.5	Variables used in this study.....41
5.1	CERCHAR stylus pins after testing on Phra Wihan sandstone specimens (a) and their corresponding groove images (b) under scratching rate of 1 mm/s and saturated conditions..... 43
5.2	CAI values as a function of scratching rates ($\partial d_s/\partial t$) for dry (a) and saturated (b) conditions..... 47
5.3	Scratching forces (F) and vertical displacement (d_n) as a function of scratching distance for dry (a) and saturated (b) conditions.....49
5.4	Representative laser-scanned images of grooves on rock surfaces after CAI testing under dry (a) and saturated (b) conditions for Phra Wihan sandstone.....50

LIST OF FIGURES (Continued)

Figure	Page
5.5	Representative laser-scanned images of grooves on rock surfaces after CAI testing under dry (a) and saturated (b) conditions for Phu Phan sandstone.....51
5.6	Representative laser-scanned images of grooves on rock surfaces after CAI testing under dry (a) and saturated (b) conditions for Phu Kradung sandstone.....52
5.7	Mean groove volume (V_m) as a function of scratching rates under dry (a) and saturated (b) conditions.....53
6.1	Relationship between CAI value and compressive strength under dry (a) and saturated (b) conditions.....56
6.2	Relationship between CAI and cohesion under dry (a) and saturated (b) conditions.....57
6.3	Relationship between CAI value and internal friction under dry (a) and saturated (b) conditions.....59
6.4	Relationship between CAI value and groove volume under dry (a) and saturated (b) conditions.....60
6.5	Force as a function of horizontal displacement curve fit of Phra Wihan sandstone under dry (a) and saturated (b) conditions.....63
6.6	Force as a function of horizontal displacement curve fit of Phu Phan sandstone under dry (a) and saturated (b) conditions.....64

LIST OF FIGURES (Continued)

Figure	Page
6.7	Force as a function of horizontal displacement curve fit of Phu Kradung sandstone under dry (a) and saturated (b) conditions.....65
6.8	Work done and CAI under dry (a) and saturated (b) conditions.....66
6.9	Work done as a function of scratching rates under dry (a) and saturated (b) conditions.....67
6.10	CSE and mean groove volume.....68
A.1	CERCHAR stylus pins after testing on Phra Wihan sandstone specimens (a) and their corresponding groove images (b) under scratching rate of 1 mm/s and dry conditions.....81
A.2	CERCHAR stylus pins after testing on Phra Wihan sandstone specimens (a) and their corresponding groove images (b) under scratching rate of 0.1 mm/s and dry conditions.....82
A.3	CERCHAR stylus pins after testing on Phra Wihan sandstone specimens (a) and their corresponding groove images (b) under scratching rate of 0.01 mm/s and dry conditions.....83
A.4	CERCHAR stylus pins after testing on Phra Wihan sandstone specimens (a) and their corresponding groove images (b) under scratching rate of 0.001 mm/s and dry conditions.....84
A.5	CERCHAR stylus pins after testing on Phra Wihan sandstone specimens (a) and their corresponding groove images (b) under scratching rate of 1 mm/s and saturated conditions.....85

LIST OF FIGURES (Continued)

Figure	Page
A.6 CERCHAR stylus pins after testing on Phra Wihan sandstone specimens (a) and their corresponding groove images (b) under scratching rate of 0.1 mm/s and saturated conditions.....	86
A.7 CERCHAR stylus pins after testing on Phra Wihan sandstone specimens (a) and their corresponding groove images (b) under scratching rate of 0.01 mm/s and saturated conditions.....	87
A.8 CERCHAR stylus pins after testing on Phra Wihan sandstone specimens (a) and their corresponding groove images (b) under scratching rate of 0.001 mm/s and saturated conditions.....	88
A.9 CERCHAR stylus pins after testing on Phu Phan sandstone specimens (a) and their corresponding groove images (b) under scratching rate of 1 mm/s and dry conditions.....	89
A.10 CERCHAR stylus pins after testing on Phu Phan sandstone specimens (a) and their corresponding groove images (b) under scratching rate of 0.1 mm/s and dry conditions.....	90
A.11 CERCHAR stylus pins after testing on Phu Phan sandstone specimens (a) and their corresponding groove images (b) under scratching rate of 0.01 mm/s and dry conditions.....	91
A.12 CERCHAR stylus pins after testing on Phu Phan sandstone specimens (a) and their corresponding groove images (b) under scratching rate of 0.001 mm/s and dry conditions.....	92

LIST OF FIGURES (Continued)

Figure	Page
A.13 CERCHAR stylus pins after testing on Phu Phan sandstone specimens (a) and their corresponding groove images (b) under scratching rate of 1 mm/s and saturated conditions.....	93
A.14 CERCHAR stylus pins after testing on Phu Phan sandstone specimens (a) and their corresponding groove images (b) under scratching rate of 0.1 mm/s and saturated conditions.....	94
A.15 CERCHAR stylus pins after testing on Phu Phan sandstone specimens (a) and their corresponding groove images (b) under scratching rate of 0.01 mm/s and saturated conditions.....	95
A.16 CERCHAR stylus pins after testing on Phu Phan sandstone specimens (a) and their corresponding groove images (b) under scratching rate of 0.001 mm/s and saturated conditions.....	96
A.17 CERCHAR stylus pins after testing on Phu Kradung sandstone specimens (a) and their corresponding groove images (b) under scratching rate of 1 mm/s and dry conditions.....	97
A.18 CERCHAR stylus pins after testing on Phu Kradung sandstone specimens (a) and their corresponding groove images (b) under scratching rate of 0.1 mm/s and dry conditions.....	98
A.19 CERCHAR stylus pins after testing on Phu Kradung sandstone specimens (a) and their corresponding groove images (b) under scratching rate of 0.01 mm/s and dry conditions.....	99

LIST OF FIGURES (Continued)

Figure	Page
A.20 CERCHAR stylus pins after testing on Phu Kradung sandstone specimens (a) and their corresponding groove images (b) under scratching rate of 0.001 mm/s and dry conditions.....	100
A.21 CERCHAR stylus pins after testing on Phu Kradung sandstone specimens (a) and their corresponding groove images (b) under scratching rate of 1 mm/s and saturated conditions.....	101
A.22 CERCHAR stylus pins after testing on Phu Kradung sandstone specimens (a) and their corresponding groove images (b) under scratching rate of 0.1 mm/s and saturated conditions.....	102
A.23 CERCHAR stylus pins after testing on Phu Kradung sandstone specimens (a) and their corresponding groove images (b) under scratching rate of 0.01 mm/s and saturated conditions.....	103
A.24 CERCHAR stylus pins after testing on Phu Kradung sandstone specimens (a) and their corresponding groove images (b) under scratching rate of 0.001 mm/s and saturated conditions.....	104

SYMBOLS AND ABBREVIATIONS

EQC	=	Equivalent Quartz Content
CAI	=	CERCHAR abrasiveness index
HRC	=	Rockwell hardness
A	=	Mineral compositions
R	=	Rosinwal abrasiveness
n	=	Number of minerals
$\sigma_{1,f}$	=	Major principal stress
$\partial\sigma_1/\partial t$	=	Loading rate
σ_c	=	Uniaxial compressive strength
c	=	Cohesion
ϕ	=	Friction angle
η	=	Effective porosity
w	=	Water content
w_{ave}	=	Average water content
E_{sec}	=	Secant young's modulus
E_{tan}	=	Tangent young's modulus
τ_{oct}	=	Octahedral shear stress
γ_{oct}	=	Octahedral shear strains
σ_1	=	Major principal stress
σ_3	=	Confining pressure

SYMBOLS AND ABBREVIATIONS (Continued)

E	=	Elastic modulus
ν	=	Poisson's ratio
d_i	=	Average diameter of the scratched flat area
CAI_s	=	CERCHAR index for saw-cut surface
F	=	Lateral force
T	=	Torque
P_s	=	Screw pitch
N	=	Vertical load
d_n	=	Vertical displacement
d_s	=	Scratching distance
$\partial d_s / \partial t$	=	Scratching rate
α	=	Empirical counts
β	=	Empirical counts
V_m	=	Mean groove volume
SW	=	Scratching work done
CSE	=	CERCHAR specific energy

CHAPTER I

INTRODUCTION

1.1 Background and Rationale

Abrasiveness and hardness of rocks are the main factors controlling excavation machinery performance. The wear of cutting tools due to rock/pick interaction is important as the cost and delays incurred for the replacement of the worn-out parts reflects on the machine performance (Atkinson et al., 1986). In addition, the abrasiveness of rock can also be used as a factor for predicting tool wear in all processes of rock excavation on surface and underground. One of the methods for determining rock abrasiveness is CERCHAR abrasiveness test (Thuro and Käsling, 2009). The CAI has been used in tunneling excavation since 1970s. The CAI has become popular due to its simplicity, speed and low cost (Prieto, 2012; Ko et al., 2016). The CERCHAR abrasiveness test is widely used in French coal industry. It is introduced in the British coal mining industry and is also used as a method for determined the abrasiveness of rocks in the tunneling industry (West, 1989).

Many studies have been carried out to assess the factors affecting CAI values, including pin hardness (Michalakopoulos et al., 2006; Stanford and Hagan, 2009; Rostami et al., 2014), pin speed (Hamzaban et al., 2019), testing length (West, 1989; Plinninger et al., 2003; Balani et al., 2017), moisture content (Jacobs and Hagan, 2009) and applied load (Rostami et al., 2014). These investigators reach conclusions that the CAI increases with increasing of the mechanical properties. These include uniaxial

compressive and tensile strengths (Ko et al., 2016; Er and Tuğrul, 2016; Capik and Yilmaz, 2017) and Shore and Schmidt hardness (Ozdogan et al., 2018). CAI also increases with increasing equivalent quartz content (Er and Tuğrul, 2016; Capik and Yilmaz, 2017) However, mathematical relations between CAI and rock compressive strengths remain unclear. This is primary due to the coupled effects of other factors which leads to highly variations of the strength results.

1.2 Research Objectives

The goal of this study is to determine the effects of scratching rate on CERCHAR abrasiveness index of Phra Wihan, Phu Phan and Phu Kradung sandstones under dry and wet conditions. The concept is based on the fact that the rock strength is dependent of the loading rates. The relationships between CAI values and ploughing forces, grooves, and uniaxial compressive strengths of sandstones under various scratching rates are determined for the same rocks, and hence eliminates other coupled effects, such as mineral compositions, and porosity. The findings can be used to predict the abrasivity/wear resistance of devices under different rotational speeds.

1.3 Scope and Limitations

The scope and limitations of the study are as follows:

- 1) Laboratory testing is performed on saw-cut surfaces of Phra Wihan, Phu Phan and Phu Kradung sandstones.
- 2) The nominal dimensions of rectangular specimens are $100 \times 100 \times 50 \text{ mm}^3$.
- 3) The CERCHAR test procedure follows ASTM D7625-10 standard practice.
- 4) The scratching rates are varied from 0.001, 0.01, 0.1 to 1 mm/s.

- 5) The testing is performed under dry and saturated conditions.
- 6) Ploughing forces and groove profiles of CAI specimens are measured by torque wrench and laser scanner.
- 7) Equivalent quartz contents are excluded from the analysis since there are only three sandstone types tested here.

1.4 Research Methodology

The research methodology shown in Figure 1.1 comprises 6 steps: including literature review, samples collection and preparation, CERCHAR testing, analysis and comparison, discussions and conclusions, and thesis writing.

1.4.1 Literature review

Literature reviews are performed to study the researches inducing rock abrasiveness, CERCHAR testing, factor affecting CERCHAR abrasiveness index, factor affecting mechanical properties of rock and the relationship between CERCHAR and rock properties.

1.4.2 Samples preparation

The rock specimens include Phra Wihan, Phu Phan and Phu Kradung sandstones. They belong to the Khorat member and widely exposed in the northeast of Thailand. For each rock type, four specimens have been prepared to obtain rectangular blocks with nominal dimensions of $100 \times 100 \times 50 \text{ mm}^3$ for CERCHAR testing. The specimens are cut and ground to obtain sawn surface to comply with the ASTM D7625-10 standard practice.

1.4.3 CERCHAR testing

The CERCHAR testing has been performed on a saw-cut surface under dry and saturated conditions by using the apparatus similar to the West apparatus, as shown in

Figure 1.2. The test procedures follow the ASTM D7625-10 standard practice. The scratching rates are varied from 0.001, 0.01, 0.1 to 1 mm/s scratching and vertical displacement are measured. The crank rotation torque wrench during the scratching is 1 mm/s rather than the specified standard. The testing is repeated 5 times for each rate and each condition. Under dry condition, the specimens are dried in an oven for 24 hours before testing. For saturated condition, the specimens are submerged under water in vacuum chamber with negative -1 atm until its weight becomes unchanged, which takes about 50 hours. Their weights are measured before and after testing.

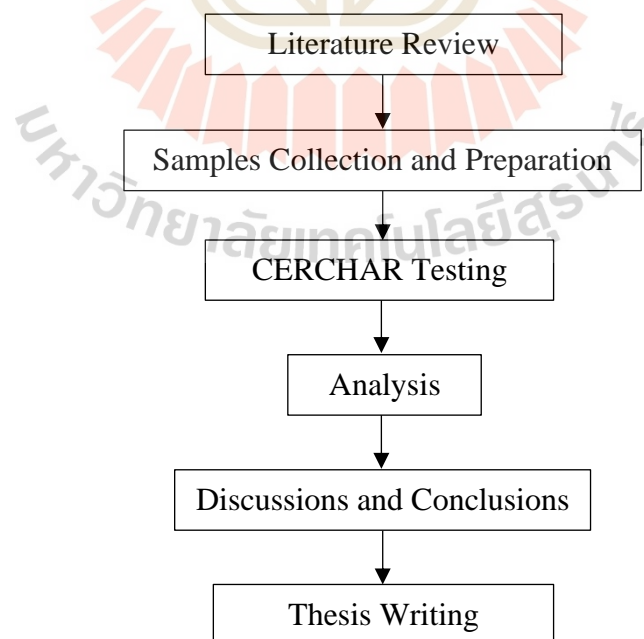


Figure 1.1 Research methodology.



Figure 1.2 Test equipment similar to West apparatus.

1.4.4 Analysis

The pin wear after CERCHAR testing is measured to predict the CAI values by using microscope. The scratching groove profile is obtained by laser scanner to determine vertical displacement. The results are analyzed to study the relationship between CAI and rock strength parameters.

1.4.5 Discussions and Conclusions

The reliability and suitability of the methods are identified. The thesis is including research activities, methods, and results.

1.4.6 Thesis writing

All research activities, methods, and results are documented and complied in the thesis. This study can be applied to reduce maintenance costs and prediction of

abrasivity/wear resistance of devices, such as chisel bit, drill bit and disc cutter etc. The findings are published in the conference proceedings.

1.5 Thesis Contents

This first chapter introduces the thesis by briefly describing the rationale and background. The second section identifying the research objectives. The third section identifies the research methodology. The fourth section describes scope and limitations. The fifth section gives a chapter-by-chapter overview of the contents of this thesis.

The second chapter summarizes results of the literature review. Chapter three describes samples preparation. The laboratory apparatus tests method are described in chapter four. The results of all tests are presented in chapter five. Analyzed of the result and energy calculation described in chapter six. The last chapter is seven which include the conclusion and recommendations for future research studies.



CHAPTER II

LITERATURE REVIEW

2.1 Introduction

This chapter describes the results of literature review performed to improve an understanding of rock abrasiveness, CERCHAR testing, factors affecting CERCHAR abrasiveness index, mechanical properties of rocks under dry and saturated conditions, and relationships between CERCHAR index and rock properties performed elsewhere.

2.2 Rock Abrasiveness

The abrasiveness of rock can be used as a factor for predicting tool wear for rock excavation on surface and underground. Abrasiveness and hardness of rocks are ones of the factors controlling excavation machinery performance. The wear of cutting tools due to rock/pick interaction is important as the cost and delays due to the replacement of the worn-out parts which reflects on the machine performance (Atkinson et al., 1986). Three methods are proposed by Thuro and Käsling (2009), as follows:

1. Investigation of the mineralogical compositions of the rock material.

The most commonly used parameter is the Equivalent Quartz Content (EQC).

2. Determination of the abrasiveness of a rock material using the CERCHAR test.

The CAI is a measurement of the wear on a steel pin scratched five times over a rough rock surface.

3. Determination of the abrasiveness of a rock sample using the Laboratoire Central des Ponts et Chaussées or LCPC test.

The CAI measurement is the most popular technique. This study is concentrated on the CAI technique, and hence only CAI is reviewed in detail.

2.3 CERCHAR Testing

The CERCHAR abrasiveness index (CAI) has long been used in tunneling excavation. The CAI has become popular due to its simplicity, speed and low cost (Prieto, 2012). The CERCHAR abrasiveness test has been widely used in the French coal industry. It is introduced in the British coal mining industry and is also a tool for determining the abrasiveness of rocks for tunneling (West, 1989).

2.3.1 Test apparatus

Generally, the CERCHAR test devices have two types (Plinninger et al., 2003) which are in use today and are divided by mechanism of stylus movement on rock surface, including original and West CERCHAR, as shown in Figure 2.1. They use a vice to clamp the specimen and a constant force of 70 N acting axially on a stylus tip when placed against the test surface. The original apparatus employs a manually operated hand lever to displace the stylus tip on the stationary rock surface held fixed in place by a vice. The West apparatus displaces the vice holding the rock by using a hand crank and driving screw under a stationary stylus.

2.3.2 Procedure

CERCHAR test procedure can be described step-by-step, as follows:

- 1) Orient and securely clamp the test specimen in the vice such that the test

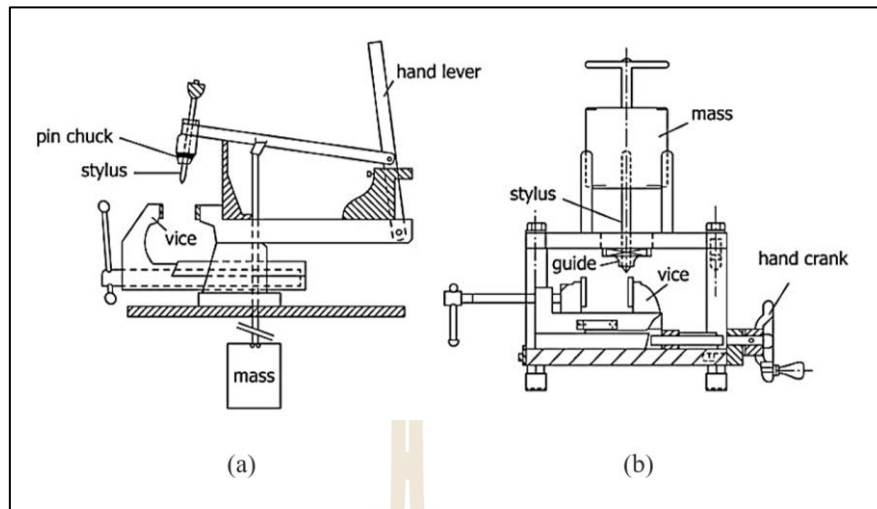


Figure 2.1 Two devices of CERCHAR testing (a) original CERCHAR and (b) West CERCHAR apparatuses (ASTM D7625-10).

Surface is horizontal and parallel to the direction of displacement with the stylus. If necessary, use wood or other suitable materials between the vice and specimen surface to assist clamping and orienting the specimen.

2) The stylus and associated components are lowered with care to bear on the specimen test surface so that the stylus tip is not damaged before testing.

3) The static mass and any associated components are positioned and checked for functionality ensuring that there are no frictional impediments to the specified 70 N total force.

4) Two scratching velocities are used, depending on which device is available. A scratching distance of 10 mm is used for both devices.

(4.1) The articulated hand lever is pulled over the test surface with a stylus scratching speed (Plininger et al., 2003) of approximately 10 mm/s.

(4.2) The hand crank is turned at a rate consistent with the number of threads on the screw-feed for moving the specimen surface under the stylus with a scratching speed of approximately 1 mm/s.

5) Carefully lift the stylus, with its associated components, off the test surface and secure in the at rest position.

6) The tested stylus is taken off the apparatus and two perpendicular diameters of the abraded flat area of the stylus are measured under a microscope in 0.1 mm increments and recorded based on the observations and suggested action

7) The test is repeated 5 times, each time with a new refurbished stylus on a new scratch location of the rock surface.

8) When the results are sensitive to water content, it may be necessary to determine the actual water content of the specimen at the time of testing. Water content may be determined in accordance with ASTM (D2216) standard practice.

2.4 Factors Affecting CERCHAR Abrasiveness Index

Several factors have been studied to determine their impact on the CAI. These include, but not limit to, pin hardness, pin speed, testing length, moisture content and varies applied load. Summarized below are the results from various researchers who study these factors.

2.4.1 Pin hardness

One of the main parameters in CERCHAR testing is pin hardness. The stylus is made of steel, heat-treated to Rockwell hardness HRC 54/56. However, the type of steel may be different depending on the type used.

Michalakopoulos et al. (2006) determine the effect of steel hardness on the CAI. Various rock types are tested with HRC 55 and 40. The two CAI values have

linear relation (Figure 2.2). The results agree well with those of Jacobs and Hagan (2009) who study the effect of nine stylus hardness (HRC 15, 24, 29, 35, 40, 45, 50, 55 and 60) on CAI for sandstone, granite, hematite, coal and shale, which have different physical and mechanical properties. It has been found that CAI linearly decreases with steel hardness. The reduction rate of CAI tends to be independent of rock type.

Stanford and Hagan (2009) study the effect of steel type and hardness on CAI. They find that selection of stylus for CERCHAR based on steel type alone has no significant effect on CAI. The values of CAI decrease with steel hardness. The results are similar to those of Rostami et al. (2014) who conclude that the CAI values with HRC 41/43 pins is higher than that with HRC 54/56 pins for both smooth and rough surfaces. Gharahbagh et al. (2011) experimentally find that the variability of the test results is minimal if the diameter of wear flat is measured from the pins taken from the side by a microscope.

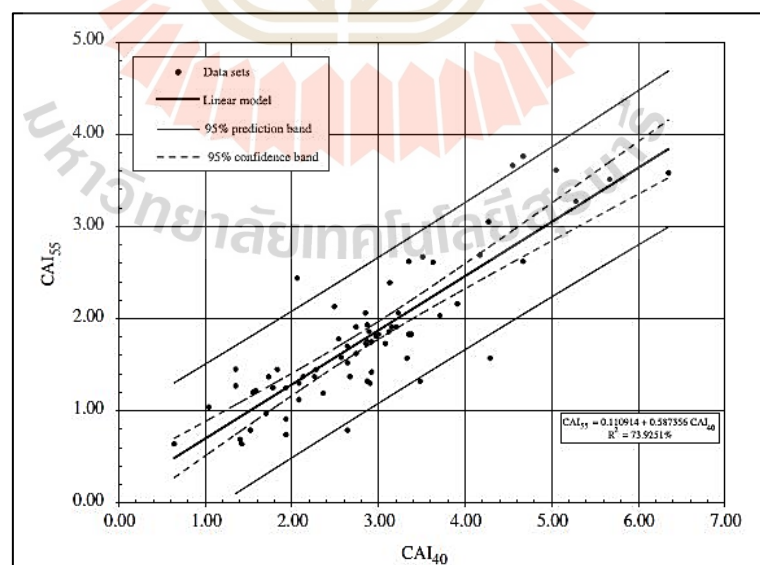


Figure 2.2 Relationship of HRC 40 (CAI₄₀) and HRC 55 (CAI₅₅) hardness values (Michalakopoulos et al., 2006).

2.4.2 Pin speed

Rostami et al. (2014) study the relationship between CAI and test duration, as shown in Figure 2.3. The diagram shows no significant trend. The speed of the tests shows no effect on the results. Hamzaban et al. (2019) study CERCHAR tests performed on seven monomineralic samples. The test result points out that variation of the pin speed affects the destruction of pin tip wear which also depends on the hardness of pin and rock specimens. The variation of pin speed in sliding was able to change through drilling into the rock specimen surface by that harder pin hardness will scratch on rock surface become deeper groove. The effects of various pin hardness decrease when the increase pin speed in scratch. It hardly affects in hard rock. Harder pins can increase the optimum velocity.

2.4.3 Testing length

Based on French standard recommendations, the testing length on the rock sample should be 10 mm, as reported by Plinninger et al. (2003) and West (1989). Tests have been carried out on same rock samples with different lengths: about 70% of the pin wear occurs during the first millimeter, about 85% of the CAI is observed after 2 mm, and only 15% of the change in CAI are obtained on the last 8 mm, and tending to be constant after 10 millimeters, as shown in Figure 2.4. The result is similar to those of Balani et al. (2017).

Yaral and Duru (2016) study the effect of scratch length on CAI by using the West apparatus with 6 different steel styluses. The tests are performed on 15 rock samples with rough and smooth surfaces with scratch lengths varying from 2 to 20 mm. Results show that about 60–70% of the final CAI (at a 20 mm sliding) is observed at

the first 2 mm, and continues to increase up to 16 mm, and levels off. About 85–90% of the final, CAI is achieved at 10 mm and about 99% of the CAI is shown at 15 mm.

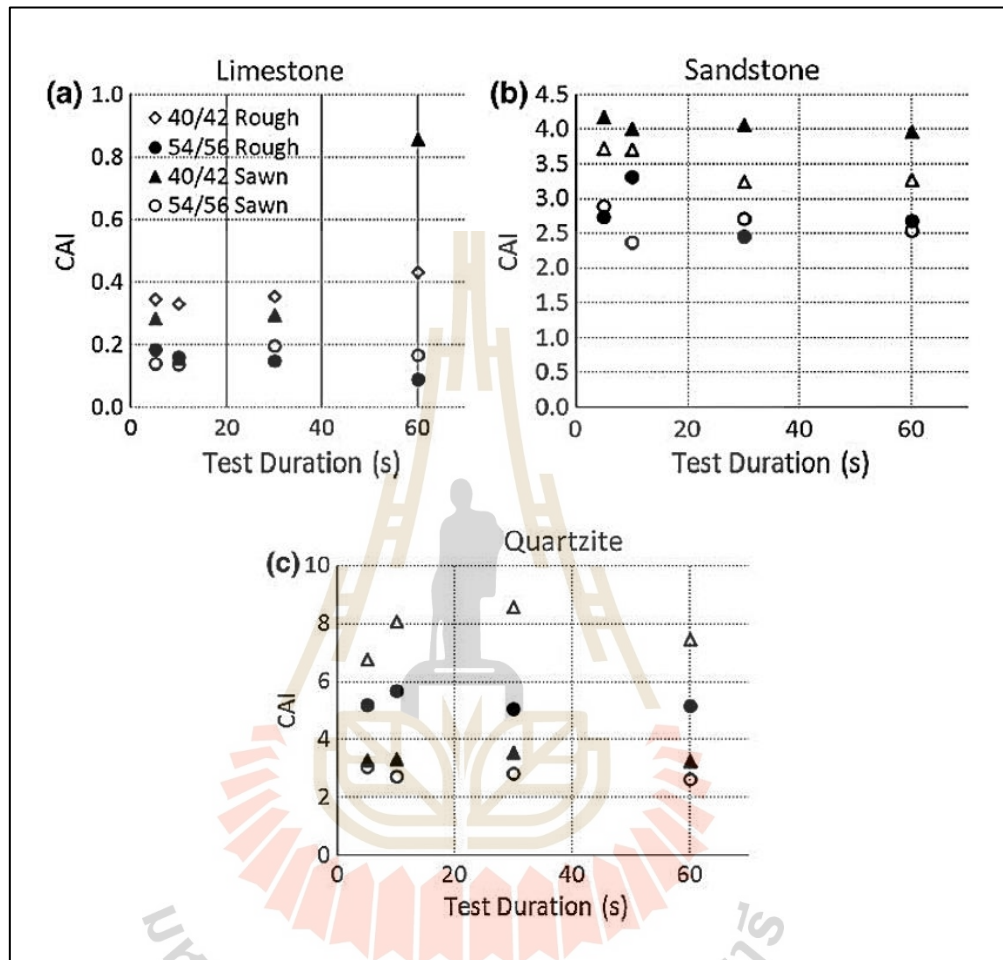


Figure 2.3 CAI values under different pin speeds (a) limestone, (b) sandstone and (c) quartzite (Rostami et al., 2014).

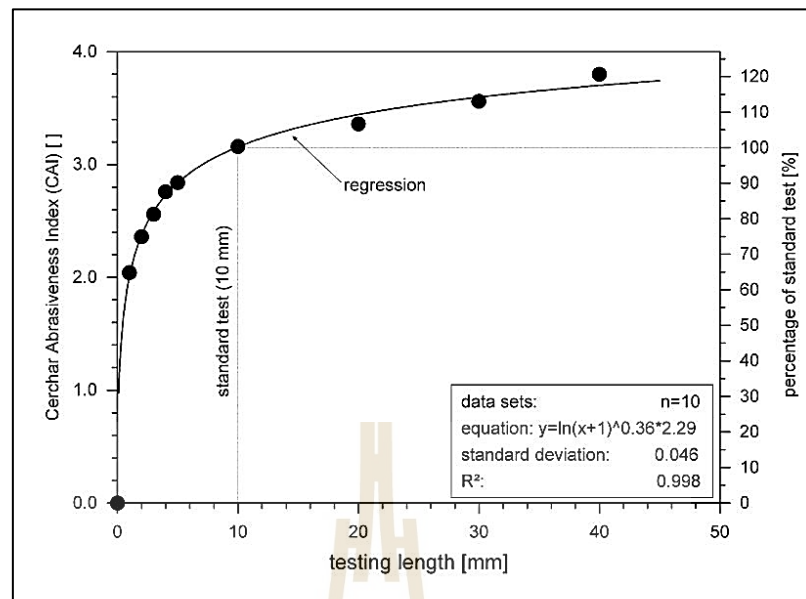


Figure 2.4 Relationship between CAI and testing length of rock specimen surface (Plinninger et al., 2003).

2.4.4 Surface conditions

Rostami et al. (2014) state that CAI obtained from rough surface are greater than on saw-cut surfaces (Figure 2.5), which confirms the conclusion drawn by Plinninger et al. (2004) and Rostami et al. (2005). This is due to the fact that the pin was easily able to slide in rock with low hardness. In such condition, the roughness of the surface has no effect on soft rock. The pins are normally used to slide on the smooth surface in hard rock. For rough surfaces, the pin has to follow an irregular path that results in a higher CAI values. Aydin et al. (2016) investigate the effects of these factors on CAI by performing two different test apparatus both on rough and on smooth specimen surfaces. It is found that rough surface CAI values are generally greater than the smooth surface CAI by about 15%.

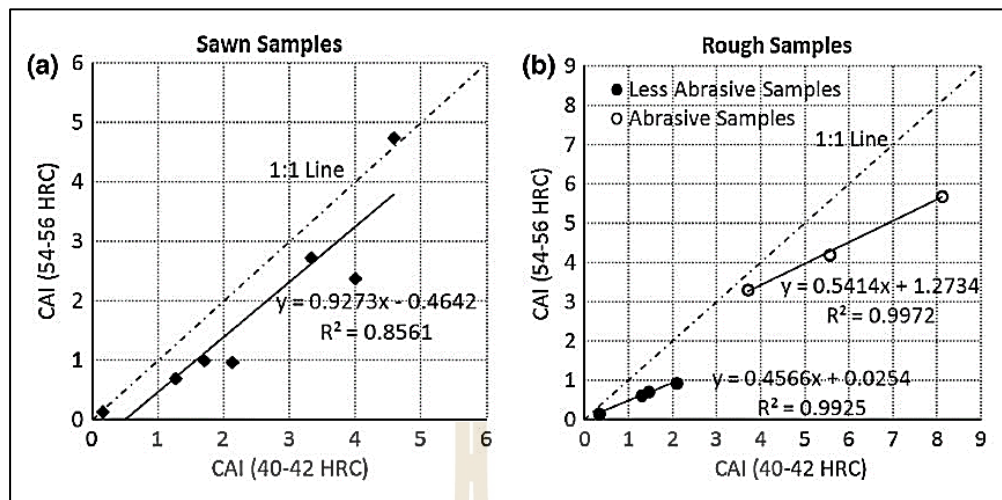


Figure 2.5 CERCHAR test results for (a) saw-cut surface and (b) rough surface

(Rostami et al., 2014).

2.4.5 Rock moisture content

Jacobs and Hagan (2009) conduct CERCHAR test by repeating at 3 levels of moisture content: 0% (oven dried sample), 2.6% (ambient condition) and 6.6% (fully saturated condition). The test was repeated ten times at each level of moisture content. The results are shown in Figure 2.6. Moisture has a significant impact on rock cutting performance with reductions of up to 40% and 49% for cutting and normal forces respectively, 38% for specific energy and 80% for impact wear of the cutting tool as reported by Mammen et al. (2009).

2.4.6 Varying applied load

Rostami et al. (2014) perform the CAI test by using 2 different steel hardness and varying applied loads. They perform on a smooth quartzite. The results are shown in Figure 2.7. A linear relationship between the applied load and tip loss is obtained.

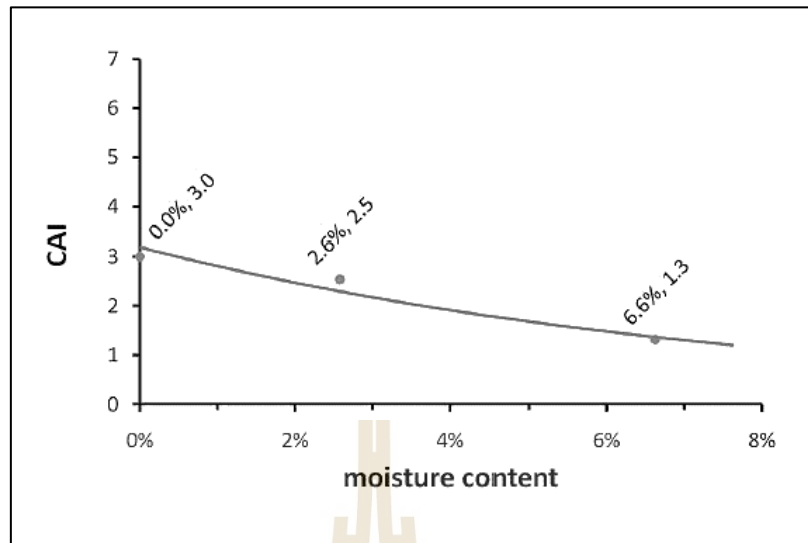


Figure 2.6 Effect of moisture contents on CAI (Jacobs and Hagan, 2009).

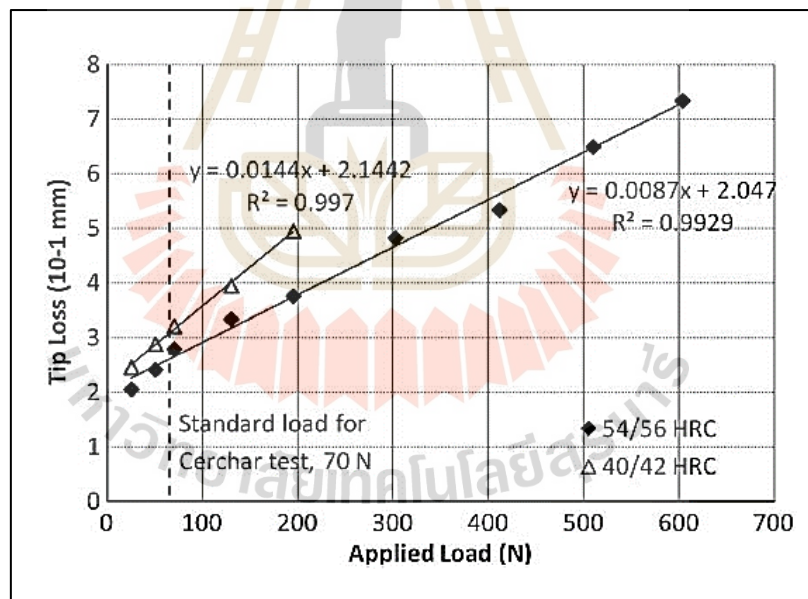


Figure 2.7 CAI as a function of force on the stylus (Rostami et al., 2014).

2.5 Factors Affecting Mechanical Properties of Rock

There are several factors affecting mechanical properties of rocks (Jaeger et al., 2007). Only those that are relevant to this resource are reviewed here, including loading rate and pore pressure.

2.5.1 Loading rate

Effect of loading rate on mechanical properties of rock specimen (e.g. the compressive strength and Young's Modulus) depends on time-dependent deformation and failure of rock. All rocks are time-dependent especially for weak rocks. Laboratory tests confirm that the mechanical response of rocks is brittle under high compression load and loading rate. This shows higher strength and Young's modulus. Compression load under low velocity or low loading rate shows that the rocks are ductile and give lower compressive strength and Young's modulus (Li and Xia, 2000; Kohmura and Inada, 2006).

The effect of loading rate can be observed on very weak rocks, such as shale, claystone, mudstone, siltstone and rock salt. It can be observed from high erosion igneous and metamorphic rocks. The effects of loading rates can be observed on time-dependent soft rocks, such as rock salt. This can also occur in harder rocks, such as sandstone as well.

Ray et al. (1999) shows the effect of cyclic loading and strain rate on the mechanical behavior of sandstone. The decrease of uniaxial compressive strength enhances with the increase in stress level. Fuenkajorn and Kenkhunthod (2010) show the effect of loading rate on deformability and compressive strength of three Thai sandstones. The rock strengths and elastic moduli increase exponentially with the loading rates. The average Poisson's ratios are independent of loading rates, as

shown in Figure 2.8. Fuenkajorn et al. (2012) also find that the salt elasticity and strength increase with the loading rates, as shown in Figure 2.9. Khamrat et al. (2016) who find that the compressive shear failure is observed in specimens under slow loading rate while extension failure is found in specimens under high loading rate.

2.5.2 Pore pressure

Vasarhelyi (2003) and Vasarhelyi and Van (2006) analyze the results of Hawkins and McConnell (1992) to study the influence of water content on the uniaxial compressive strength and Young's modulus (both tangent and secant) of 35 sandstones tested under dry and saturated conditions, as show in Figure 2.10. It is possible to say that the compressive strength decreases by about 20% due to saturation. The tangent and secant moduli are shown in Figure 2.11. The slopes of the lines are close to each other thus, it can be assumed that the influence of the degree of saturation are the same for the different petrophysical constants. The relationship between these constants was also examined. In every case, the slopes of the lines were independent of the water content such as the relationship between uniaxial compressive strength as a function of E_{tan} and E_{sec} , respectively (Figures 2.12 and 2.13). Vasarhelyi and Van (2006) study the rock strengths under dry and saturated conditions to show a method for estimating the sensitivity of sandstone rocks to water content. They find that the relationship between water content and uniaxial compressive strength could be described by an exponential curve, as shown in Figure 2.14. It shows the best-fit lines plotted for the 15 different rock types for water content values up to 5%. It is apparent that water content can remarkably reduce the rock strength after only 1% water saturation (Figure 2.15). The result is similar to those of Dyke and Dobereiner (1991).

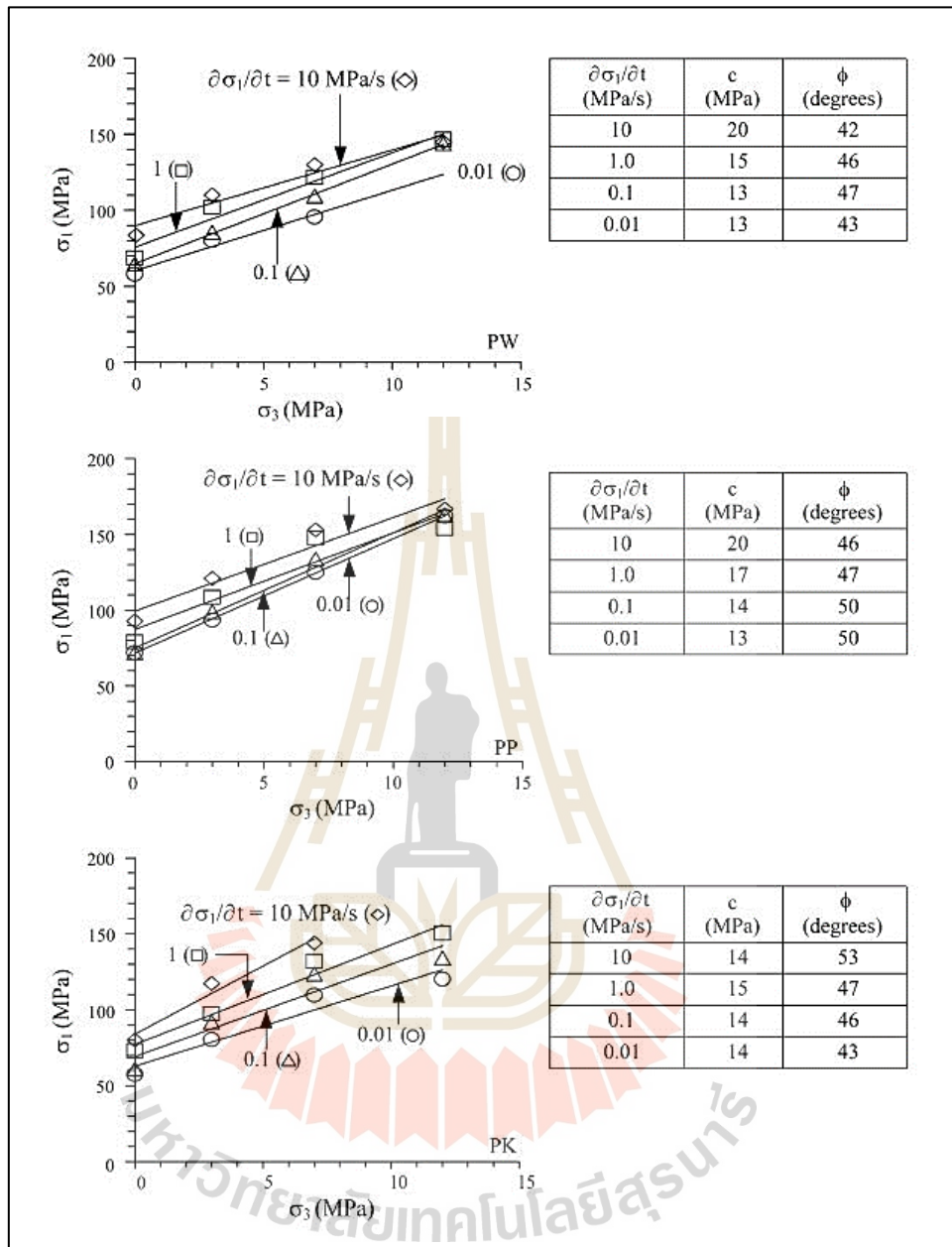


Figure 2.8 Rock strengths as a function of confining pressure at different loading rates for Phra Wihan, Phu Phan and Phu Kradung sandstones (Fuenkajorn and Kenkhunthod, 2010).

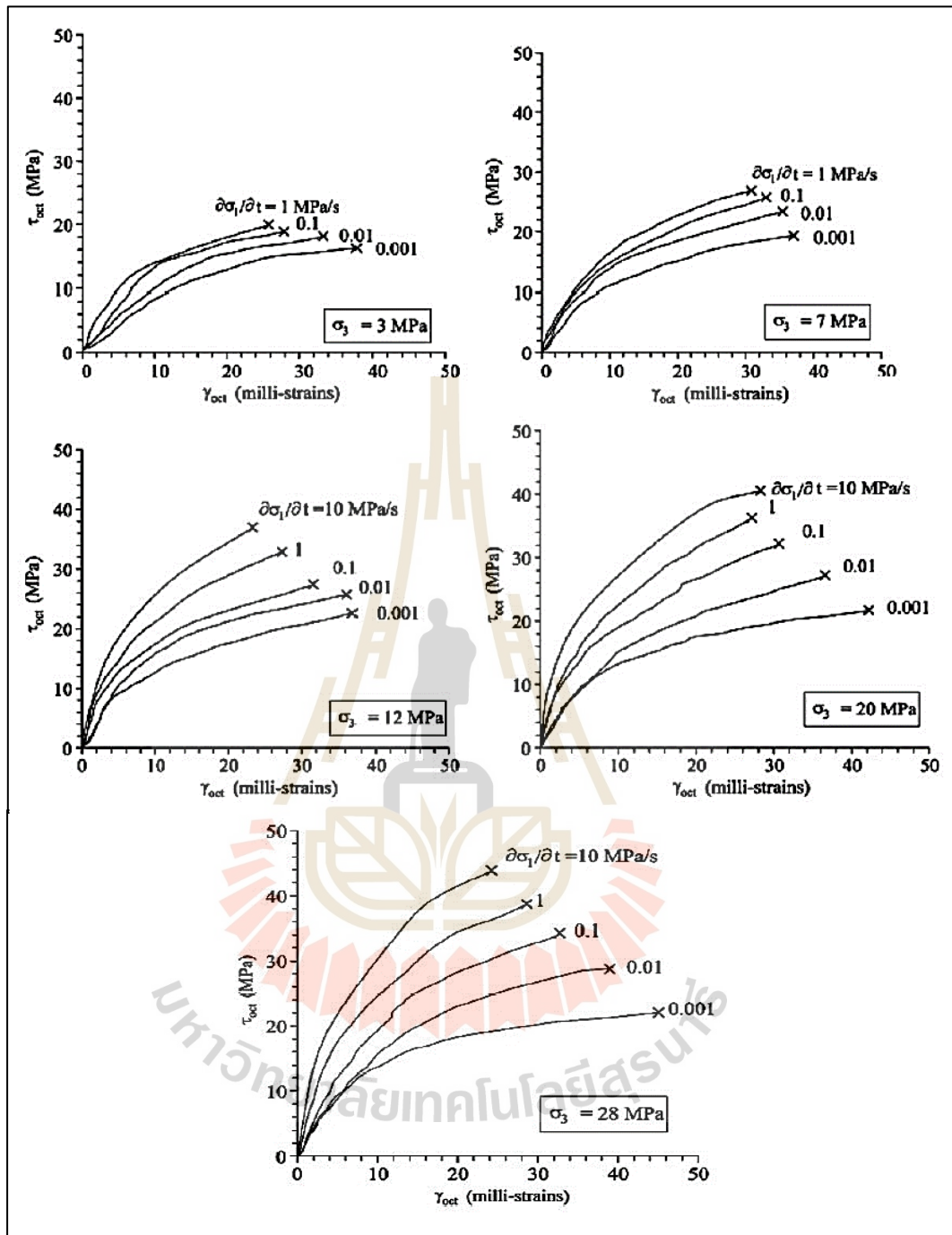


Figure 2.9 Shear stresses as a function of shear strain at different loading rates

(Fuenkajorn et al., 2012).

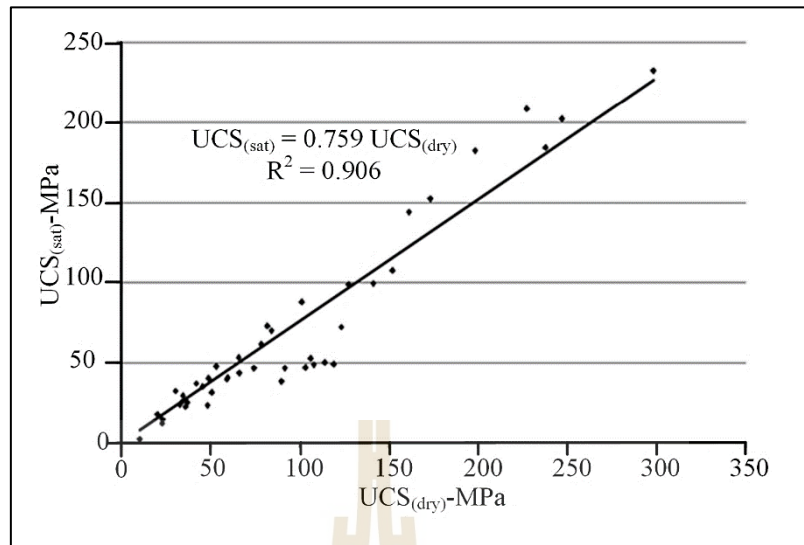


Figure 2.10 Relationships between dry and saturated UCS for 35 British sandstones (Vasarhelyi, 2003).

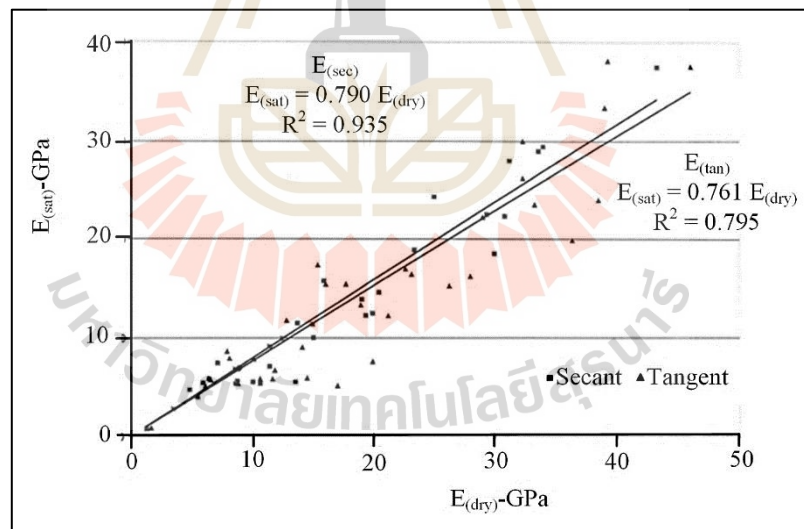


Figure 2.11 Relationships between dry and saturated Young's modulus for 35 British sandstones (Vasarhelyi, 2003).

Khamrat et al. (2016) study the influence of water content under triaxial compressive strength testing in 6 rock types: granite, marl, marble Phu Phan sandstone,

Phra Wihan sandstone, and Phu Kradung siltstone under loading rates of 0.001-1 MPa/s. Testing is made under both dry and wet conditions. The physical properties of rock specimens are shown in Table 2.1. The specimens that are under high loading rate and high confining give strength higher than the specimens when under low loading rate and low confining both dry and wet conditions (Figure 2.16). The strength of the dry specimens was always greater than that of the wet ones. as has been found for Denizli travertinel, homogeneous Indian granite, sandstone, and limestone. The differences in strengths between the wet and dry specimens increase with confining pressures. The rocks with higher porosity (Phra Wihan sandstone) yielded larger strength difference than those with lower porosity (granite, marl, marble, Phu Phan and Phu Kradung sandstones).

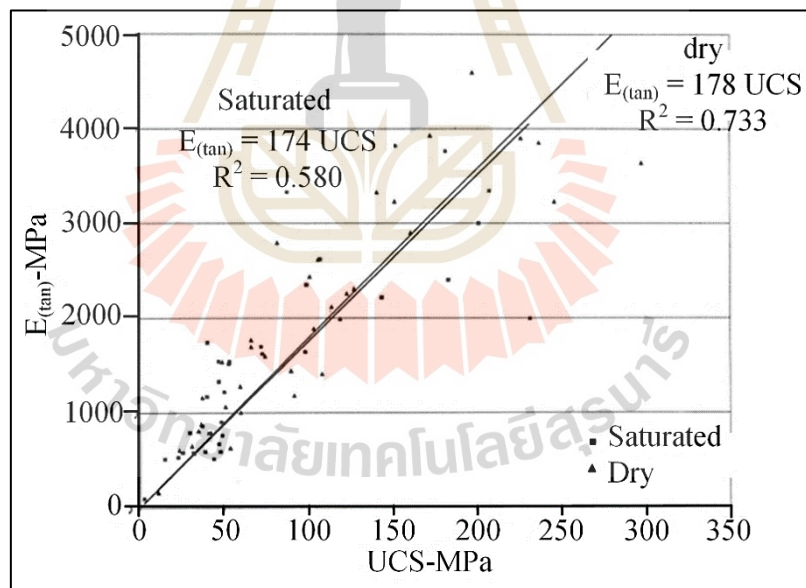


Figure 2.12 Relationships between unconfined compressive strength (UCS) and the tangent Young's modulus (E_{tan}) under dry and saturated conditions (Vasarhelyi, 2003).

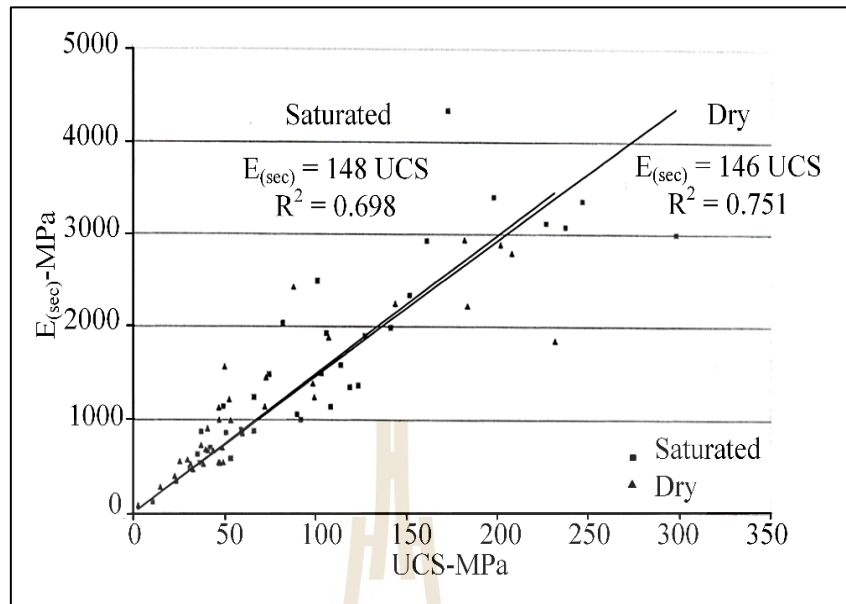


Figure 2.13 Relationships between unconfined compressive strength (UCS) and the secant Young's modulus (E_{sec}) under dry and saturated conditions (Vasarhelyi, 2003).

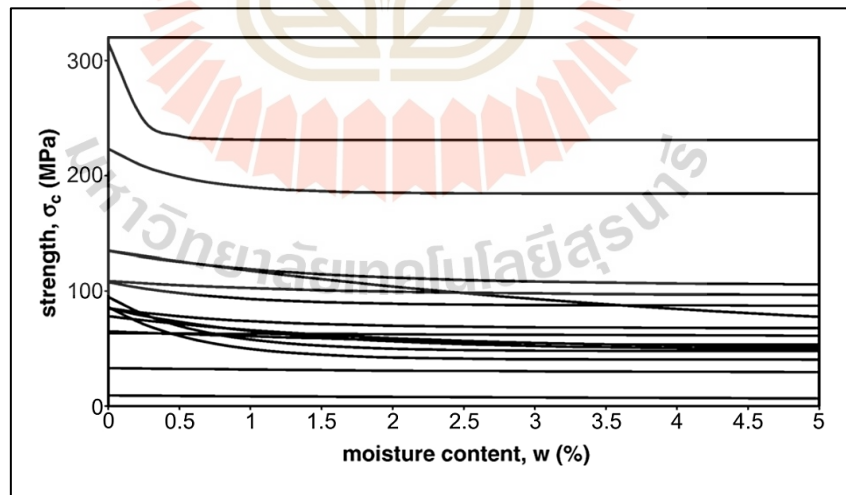


Figure 2.14 Relationship between strength (σ_c) as function of water content (w) values up to 5% (Vasarhelyi and Van, 2006).

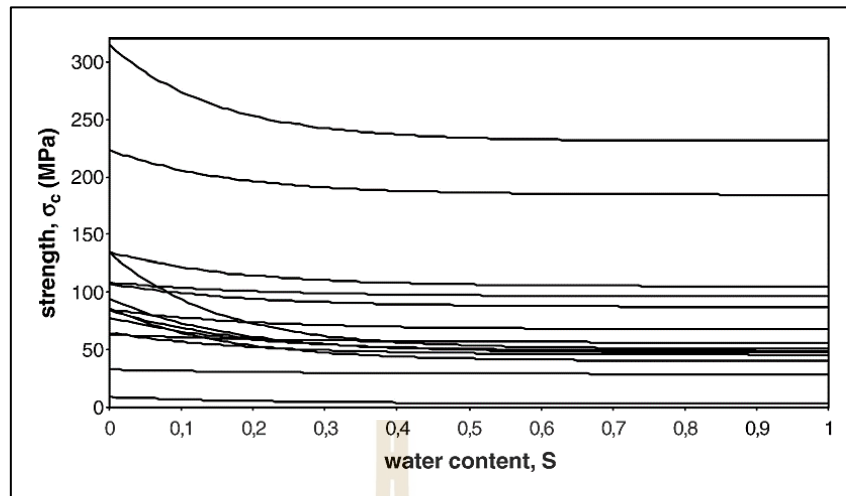


Figure 2.15 Relationships between strength (σ_c) as function of water content in only 1% (Vasarhelyi and Van, 2006).

Table 2.1 Physical properties of rock specimens (Khamrat et al., 2016).

Rock Types	Granite	Marl	Marble	Phu Phan	Phra Wihan	Phu Kradung
Dry density (g/cm ³)	2.64 ± 0.04	2.49 ± 0.05	2.74 ± 0.04	2.42 ± 0.05	2.25 ± 0.06	2.53 ± 0.03
Wet density (g/cm ³)	2.65 ± 0.06	2.55 ± 0.05	2.74 ± 0.04	2.47 ± 0.04	2.36 ± 0.04	2.57 ± 0.02
Water content, w (%)	0.14 ± 0.03	2.71 ± 0.62	0.09 ± 0.03	2.05 ± 0.22	4.91 ± 0.38	1.53 ± 0.38
Effective porosity, η (%)	0.37 ± 0.06	6.70 ± 1.40	0.26 ± 0.07	4.97 ± 0.51	11.00 ± 0.97	3.88 ± 0.98

2.6 Relation between CERCHAR and Rock Properties

Many researchers study on the factors affecting CAI on rock properties including physical properties, porosity and grain size (Ho et al., 2016; Lassnig et al., 2008; Majeed and Abu Bakar, 2016), uniaxial compressive strength, Brazilian tensile

strength, point load strength and Shore and Schmidt hardness values and mineral compositions (Capik and Yilmaz, 2017; Er and Tuğrul, 2016).

2.6.1 Physical properties

The porosity of rock may affect the CAI as indicated by the data of many researchers. Ozdogan et al. (2018) use the statistical analysis to determine the relationship between the CAI and porosity (%). There is no relation between the CAI and porosity ($R^2 = 0.05$) which confirms the earlier data from Majeed and Abu Bakar (2016). They study the effect of these parameters examined on the results of CERCHAR abrasivity test to validate the earlier research investigations and found that the relationship between CAI and porosity (%) is non-linear ($R^2 = 0.38$). Alber (2008) find that the increase in CAI per MPa confinement seems to be a function of the stiffness of rock. A rock with high porosity may be strained significantly under confinement and the porosity is therefore reduced, and hence the abrasiveness increases.

The grain size of the rock has an impact on the CAI which is a positive correlation (Er and Tuğrul, 2016; Yaralı et al., 2008). The larger the grain size, the larger the grain boundary, and then the less energy needed to keep crack growing (Whittaker et al., 1992). The grain size will have no influence on the CAI as long as the grain size ranges between 50 micron and 1000 micron (Suana and Peters, 1982). Beste et al. (2004) find that the quartz grains up to the 1 mm cause the highest tip wear rate, probably due to scratching through the rough edges formed along the grain boundaries.

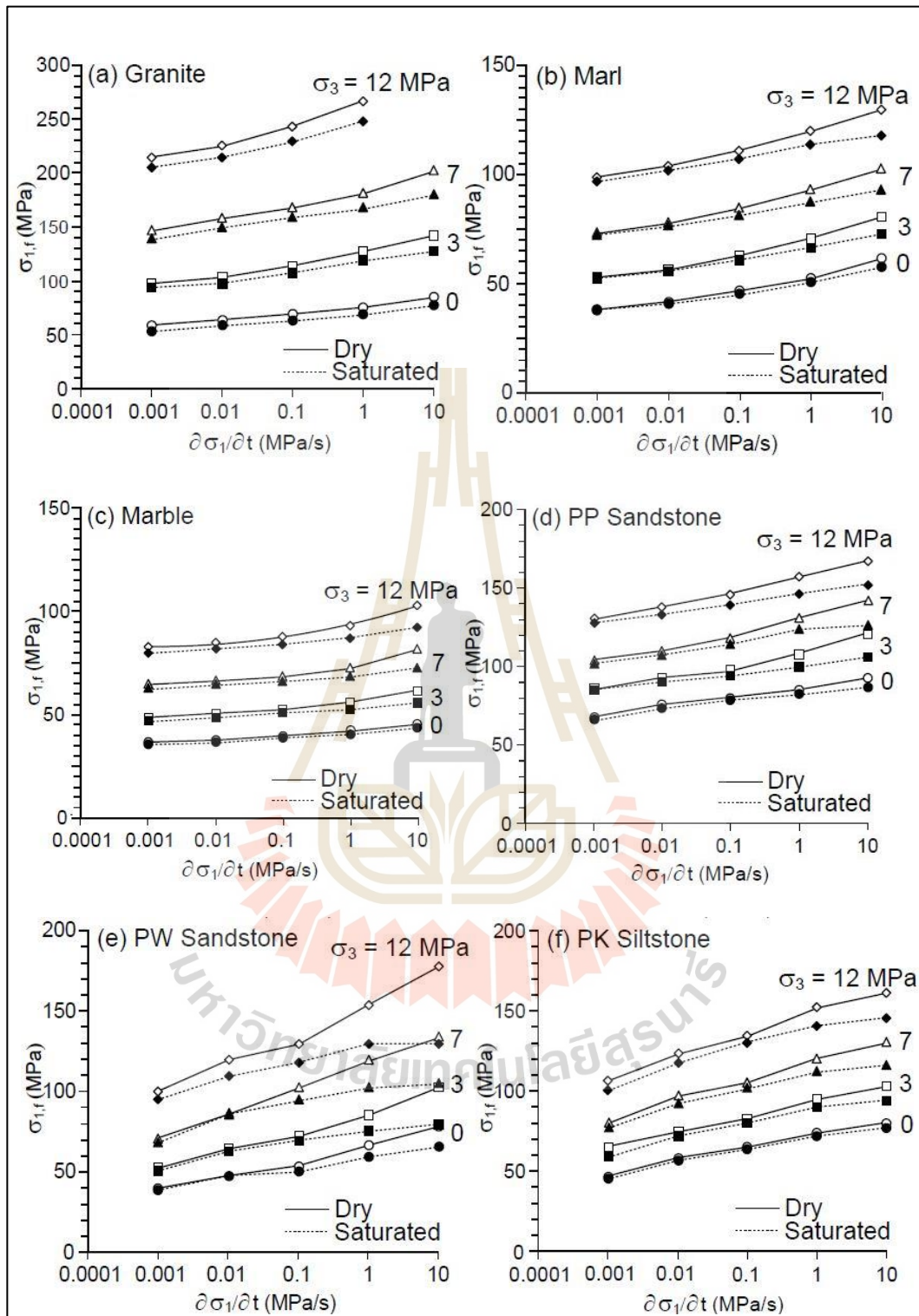


Figure 2.16 Major principal stress ($\sigma_{1,f}$) as a function of loading rate ($\partial\sigma_1/\partial t$)

(Khamrat et al., 2016).

2.6.2 Mechanical properties

The relationship between CAI and mechanical properties has been studied more than decades by many researchers. They found a positive linear relationship that the CAI increases with the increase of the mechanical properties. These include uniaxial compressive strength, Brazilian tensile strength (Capik and Yilmaz, 2017; Er and Tuğrul, 2016; Ko et al., 2016), direct shear strength (Deliormanlı, 2012), point load strength (Capik and Yilmaz, 2017) and Shore and Schmidt hardness (Ozdogan et al., 2018; Capik and Yilmaz, 2017; Er and Tuğrul, 2016; Khandelwal and Ranjith, 2010).

The mechanical properties are related to CAI by statistical analysis, including single and multiple regression analysis. Ko et al. (2016) study the single regression analysis relationships between CAI and uniaxial compressive strength, Brazilian tensile strength and brittleness index for different rock types. For igneous rocks, CAI increases with increasing uniaxial compressive strength. For metamorphic rocks, CAI also increases with increasing uniaxial compressive strength, Brazilian tensile strength and brittleness index. Uniaxial compressive strength is the common geomechanically property influencing CAI value for both rock types.

Al-Ameen and Waller (1994) find a nonlinear correlation between the uniaxial compressive strength of rocks containing abrasive minerals and rocks containing non-abrasive minerals using 1 mm sliding distance CAI, as shown in Figure 2.17. The initial wear flat diameter on the stylus tip cannot be attributed to the abrasive mineral content due to the small sliding distance. It is most likely due to a combination of the balance between rock and stylus strength and depth of tip indentation into the specimens.

2.6.3 Mineral compositions

Equivalent quartz content (EQC) is one of the most commonly used parameters to correlate CAI with the mineral compositions of rock. This is mainly due to the fact that quartz is hard and abrasive mineral. Equivalent quartz content (EQC) of rock samples can be calculated as proposed by Thuro (1997)

$$EQC = \sum_{i=1}^n A_i \times R_i \quad (\%) \quad (2.1)$$

where A is mineral compositions (%)

R is Rosiwal abrasiveness (%)

n is number of minerals

Linear correlations are found between CAI and EQC for igneous, sedimentary and metamorphic rocks (Moradizadeh et al., 2016). CAI increases with the increase of EQC (Capik and Yilmaz, 2017). He et al. (2015) find that the correlation of EQC can be described by logarithmic relation. The quartz content has an impact on the CAI. Quartz content and quartz size of rocks lead to an increase in CAI. No relationship was found between CAI and other minerals (Er and Tuğrul, 2016). Similar correlations presented for the CAI and the Abrasive Mineral Content by Al-Ameen and Waller (1994) could not be confirmed. This is in conflict with Torrijo et al. (2019) who found that the relation between CAI and EQC is no clear.

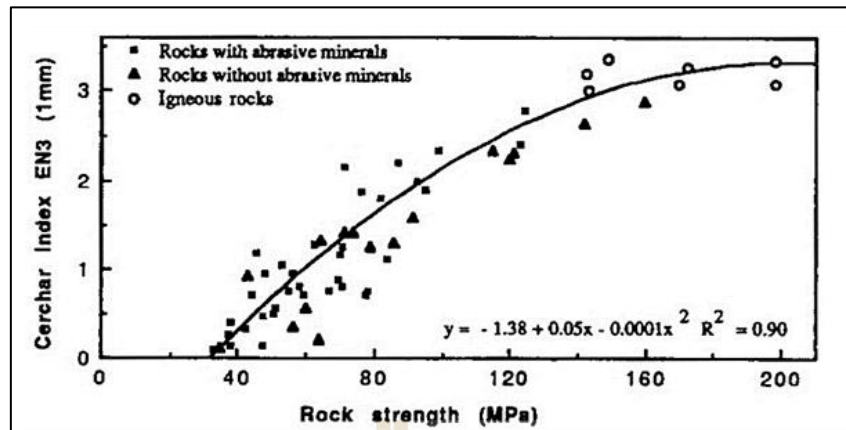


Figure 2.17 CERCHAR index (1 mm) versus rock strength (Al-Ameen and Waller, 1994).

CHAPTER III

SAMPLE PREPARATION

3.1 Introduction

Described in this chapter is the sample preparation for CERCHAR testing on saw-cut surfaces under dry and wet conditions and equivalent quartz content calculated here. The rock samples prepared in this study are Phu Phan, Phra Wihan and Phu Kradung sandstones. The physical and mechanical properties of the tested rocks obtained from related studies are provided in Table 3.1 and 3.2, respectively.

3.2 Sample Preparation for CERCHAR Test

The sandstones belong to the Khorat member and widely expose in the northeast of Thailand. For each rock type, four specimens are prepared to obtain rectangular blocks with nominal dimensions of $100 \times 100 \times 50 \text{ mm}^3$ for CERCHAR testing. Two specimens are for dry testing, the other two for saturated testing. The specimens are cut and ground to obtain saw-cut surface to comply with the ASTM D7625-10 standard

Table 3.1 Physical properties of sandstones (Khamrat et al., 2016).

Rock types	Dry Density (g/cc)	Wet Density (g/cc)	Water Content, w (%)	Effective porosity, η (%)
Phra Wihan	2.25 ± 0.06	2.36 ± 0.04	4.91 ± 0.38	11.00 ± 0.97
Phu Phan	2.42 ± 0.05	2.47 ± 0.04	2.05 ± 0.22	4.97 ± 0.51
Phu Kradung	2.53 ± 0.03	2.57 ± 0.02	1.53 ± 0.38	3.88 ± 0.98

practice, as shown in Figures 3.3 and 3.4. The CERCHAR testing are performed under dry and wet conditions. Under dry condition, the specimens are dried in an oven for 24 hours before testing. For wet condition, they are submerged under water in a pressure vacuum chamber at a negative pressure of 0.1 MPa (Figure 3.5). Their weights are measured every two hours until its weight becomes unchanged, which takes about 50 hours. Figure 3.6 shows water contents as function of time. The Phra Wihan, Phu Phan and Phu Kradung sandstones specimens have average water contents ($w_{ave.}$) of 4.63%, 2.48% and 1.62%, respectively. The water contents obtained here agree well with those tested by Khamrat et al. (2016). Tables 3.3 shows physical properties and dimensions of dry sandstone specimens and Table 3.4 shows physical properties and dimensions of saturated sandstone specimens.

Table 3.2 Mechanical properties of sandstones (Khamrat et al., 2016).

Rock Types	Loading Rate (MPa/s)	Compressive Strength, σ_c (MPa)		Cohesion, c (MPa)		Friction Angle, ϕ (degrees)		Elastic Modulus, E (GPa)		Poisson's Ratio, ν	
		Dry	Sat.	Dry	Sat.	Dry	Sat.	Dry	Sat.	Dry	Sat.
Phra Wihan	0.001	41	39	9.1	8.7	42	40	6.8	6.8	0.22	0.28
	0.01	48	48	10.1	10.5	46	43	8.2	7.8	0.24	0.28
	0.1	54	51	11.2	11.1	47	44	9.9	9.0	0.26	0.27
	1	67	60	12.3	12.3	47	45	12.0	10.3	0.28	0.27
Phu Phan	0.001	68	67	15.1	15.4	42	41	7.5	7.3	0.22	0.32
	0.01	76	74	16.4	17.0	42	41	9.2	8.8	0.25	0.33
	0.1	80	79	17.6	17.7	43	42	11.1	10.5	0.29	0.33
	1	85	82	18.9	17.9	43	44	13.5	12.7	0.33	0.33
Phu Kradung	0.001	46	45	10.6	10.5	41	40	6.7	6.2	0.10	0.24
	0.01	58	57	11.8	12.7	44	42	7.9	7.2	0.13	0.22
	0.1	65	64	13.0	13.6	45	44	9.2	8.5	0.16	0.20
	1	74	72	20.1	15.3	45	44	10.8	10.1	0.19	0.19



Figure 3.1 Some rectangular block specimens of Phra Wihan, Phu Phan and Phu Kradung sandstones used in CERCHAR test on saw-cut surface.

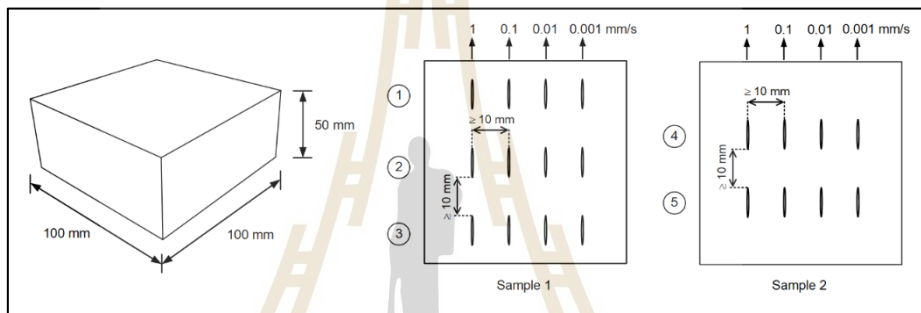


Figure 3.2 Nominal dimensions and guideline of scratching of specimens used in CERCHAR test on saw-cut surfaces.



Figure 3.3 Rock specimens saturated under water in vacuum chamber.

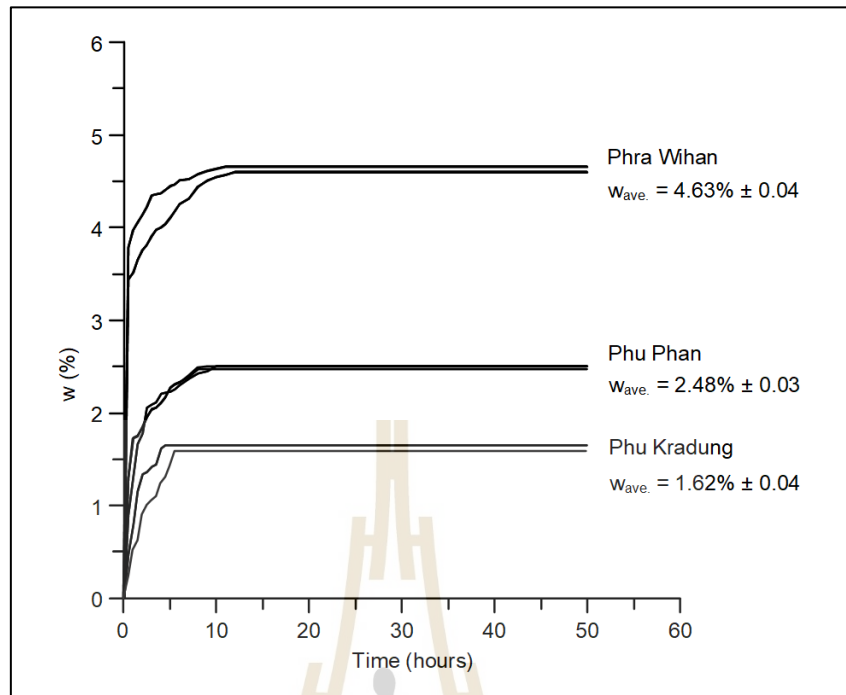


Figure 3.4 Water contents as function of time for all specimens.

Table 3.3 Dry densities of sandstone specimens.

Rock Types	Sample No.	Dimensions (mm)	Weight (g)	Dry Density (g/cc)
Phra Wihan	1	10.14×10.10×5.03	1179.89	2.29
	2	10.17×10.17×5.28	1231.39	2.26
Phu Phan	1	10.05×10.05×5.19	1270.49	2.42
	2	10.06×10.05×5.28	1287.57	2.41
Phu Kradung	1	10.10×10.07×4.99	1315.30	2.59
	2	10.11×10.12×5.16	1337.27	2.53

Table 3.4 Wet densities of sandstone specimens.

Rock Types	Sample No.	Dimensions (mm)	Weight (g)	Wet Density (g/cc)	Water Contents (%)
Phra Wihan	3	10.19×10.19×5.22	1220.65	2.36	4.60
	4	9.97×10.08×5.43	1258.20	2.41	4.66
Phu Phan	3	10.02×10.07×5.26	1272.87	2.46	2.50
	4	10.19×10.09×5.23	1268.20	2.42	2.46
Phu Kradung	3	10.12×10.08×4.71	1222.54	2.58	1.59
	4	10.23×10.11×5.09	1325.21	2.56	1.64

3.3 Equivalent Quartz Content

Based on Capik and Yilmaz (2017), the equivalent quartz content (EQC) of rocks can be calculated by:

$$EQC = \sum_{i=1}^n A_i \times R_i (\%) \quad (3.1)$$

where A is mineral compositions (%), R is Rosiwal abrasiveness (%), and n is number of minerals. For Phra Wihan, Phu Phan and Phu Kradung sandstones, EQC values are calculated (equal to 91.86, 90.06 and 48.57). The Rosiwal hardness used in this calculation as given in Table 3.5. The mineral equations of the three sandstones are given in Table 3.6.

Table 3.5 Relationship between Mohs hardness and Rosiwal hardness (Bharti et al., 2017).

Minerals	Mohs Hardness	Rosiwal Hardness
Talc	1	0.03
Gypsum	2	1.25
Calcite	3	4.5
Fluorite	4	5
Apatite	5	6.5
Orthoclase	6	37
Quartz	7	120
Topaz	8	175
Corundum	9	1000
Diamond	10	140000

Table 3.6 Mineral compositions of tested sandstones obtained from X-ray diffraction analysis.

Sandstone types	Mineral Compositions
Phra Wihan	91.50% Quartz, 4.00% Kaolinite, 3.70% Albite, 0.80% Muscovite
Phu Phan	89.90% Quartz, 5.53% Kaolinite, 3.12% Albite, 1.45 % Muscovite
Phu Kradung	47.10% Quartz, 32.00% Albite, 12.24 % Muscovite, 8.75% Kaolinite

CHAPTER IV

TEST APPARATUS AND TEST METHOD

4.1 Introduction

The objective of this chapter is to describe the apparatus and method to determine the effects of pin stylus scratching rate on CERCHAR abrasiveness index of rock specimens. The laboratory test is divided into three series; 1) CERCHAR testing, 2) ploughing force measurement, and 3) vertical displacement measurement.

4.2 CERCHAR Testing

In this study, the CERCHAR testing is performed on saw-cut surfaces of sandstone specimens under dry and saturated conditions using the apparatus similar to West apparatus of CERCHAR. The main apparatus comprises vice holding the rock specimen, a casing for the steel stylus, a vertical load of 70 N (15.7 lbs), and a hand crank with which the specimen is moved underneath the steel stylus. Figures 4.1 and Figures 4.2 show the device used in this study. The test procedures follow the ASTM D7625-10 standard practice. The scratching rates are varied from 0.001, 0.01, 0.1 to 1 mm/s. Noted that the rate of 1 mm/s is recommended by the ASTM standard. The testing is repeated 5 times for each rate.

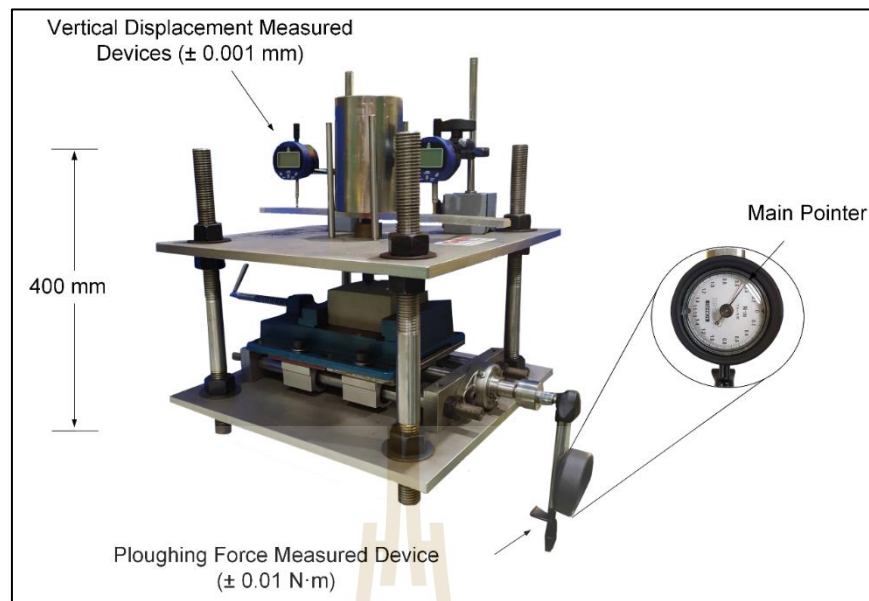


Figure 4.1 Device modified from West CERCHAR apparatus (ASTM D7625-10).

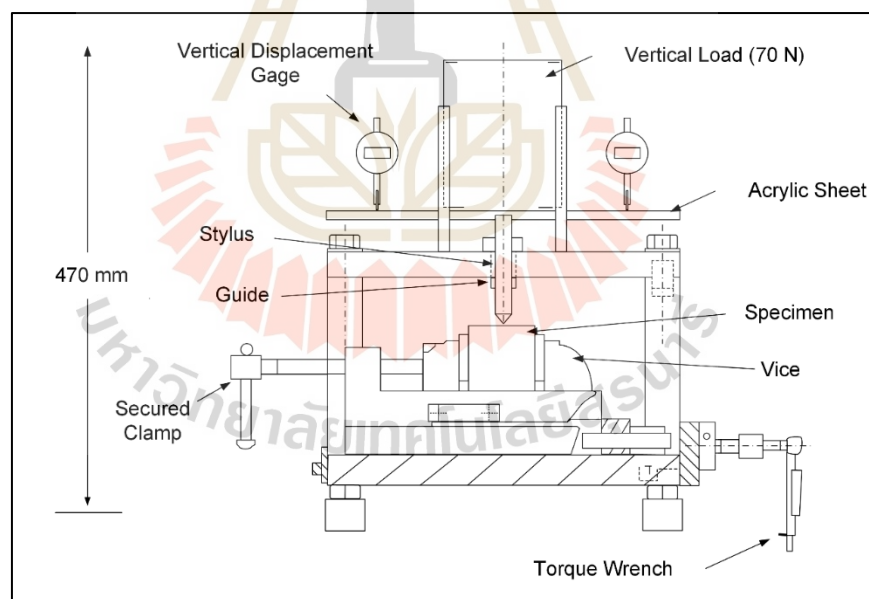


Figure 4.2 Schematic drawing of CERCHAR device used in this study.

The stylus hardened to 55 HRC is used, as suggested by the ASTM standard. The length and diameter of stylus are 100 mm and 16 mm, respectively. The sharpened profile at one end has a conical angle of 90°, with 10 mm in length (Figure 4.3). The

average width of the wear flat of the stylus tip occurred after the CERCHAR test is measured using a microscope with an accuracy of 0.001 mm. The post-test stylus is lied in a V-notch holder or jig, and four measurements are made each at 90° rotation. The measurements are taken parallel and perpendicular to the direction of scratching for each of the five styluses. The CERCHAR abrasiveness index (CAI) can be calculated by:

$$CAI \text{ or } CAI_s = \frac{1}{10} \sum_{i=1}^{10} d_i \quad (4.1)$$

where CAI or CAI_s is CERCHAR abrasiveness index for rough or saw-cut surfaces respectively. d_i is average diameter of the scratched flat area of the stylus tip measured to the nearest of 0.001 mm. If saw-cut specimen is tested, then the calculated CAI_s of Eq. (4.1), it is normalized using:

$$CAI = 0.99CAI_s + 0.48 \quad (4.2)$$

where CAI is CERCHAR abrasiveness index for rough surface and CAI_s is CERCHAR index for saw-cut surface from Eq. (4.1). The CAI classification is determined from Table 4.1, based on the stylus tip Rockwell hardness (ASTM D7625-10).

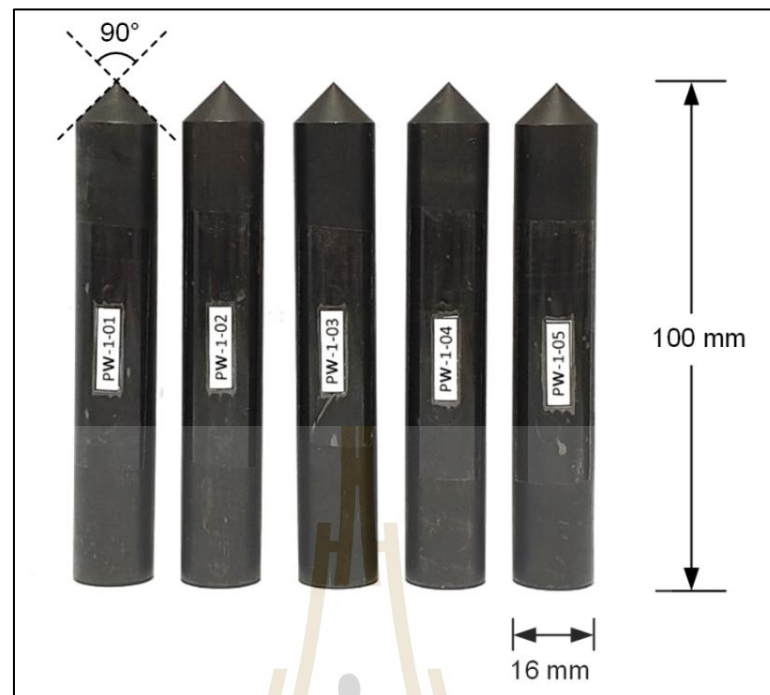


Figure 4.3 Examples of stylus-55 HRC for CERCHAR testing.

Table 4.1 CAI classification (ASTM D7625-10).

Classification	Average CAI (HRC = 55)
Very low abrasiveness	0.30–0.50
Low abrasiveness	0.50–1.00
Medium abrasiveness	1.00–2.00
High abrasiveness	2.00–4.00
Extreme abrasiveness	4.00–6.00
Quartzitic	6.0–7.0

4.3 Lateral Force Measurement

In this study the horizontal force applying on the stylus pin is measured during scratching. This can be made by monitoring the torque applying during the test. Figure 4.4

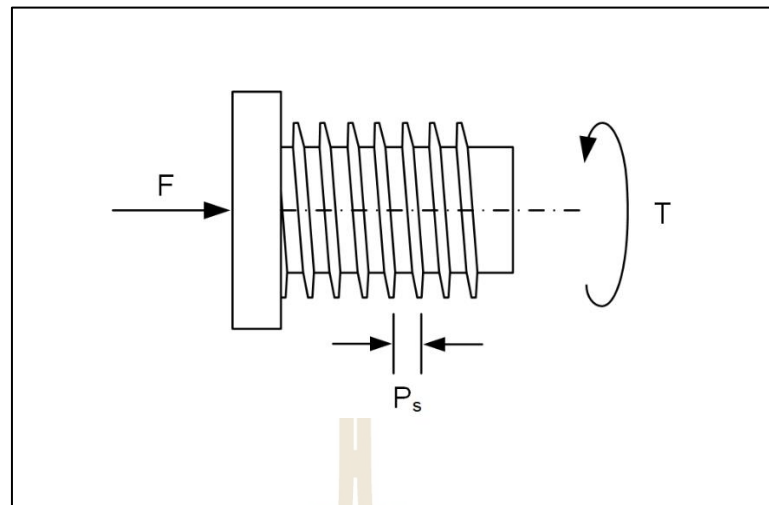


Figure 4.4 Freebody diagram of lead screw.

shows the freebody diagram of lead screw. During the test, the ploughing force is controlled by the scratching rate and torque. It can be calculated by:

$$F = 2\pi T/P_s \quad (4.3)$$

where F is lateral force (N), T is torque (N·m), and P_s is screw pitch (0.001 m). The torque is measured by a torque meter, as shown in Figure 4.1. The measurement results are used to analyze the mechanism of scratching as affected by different rates applying on the stylus.

4.4 Vertical Displacement Measurement

Another parameter that is added into the test procedure, beyond those recommended by the ASTM standard, is the vertical displacement induced on the specimen surfaces as affected by different scratching rates. Figure 4.5 shows the variables used in this study. One of the variables is vertical displacement which can be

obtained by using two displacement gages. Figure 4.2 shows the positions of the two displacement gages which are placed on opposite side of the stylus. The gages have a precision of ± 0.001 mm. The average of the two gages is used in the analysis presented in the following chapter. The initial vertical displacement is measured after applying the vertical force of 70 N. After starting the test, the vertical displacement measurement is recorded until the horizontal displacement reaches 10 mm.

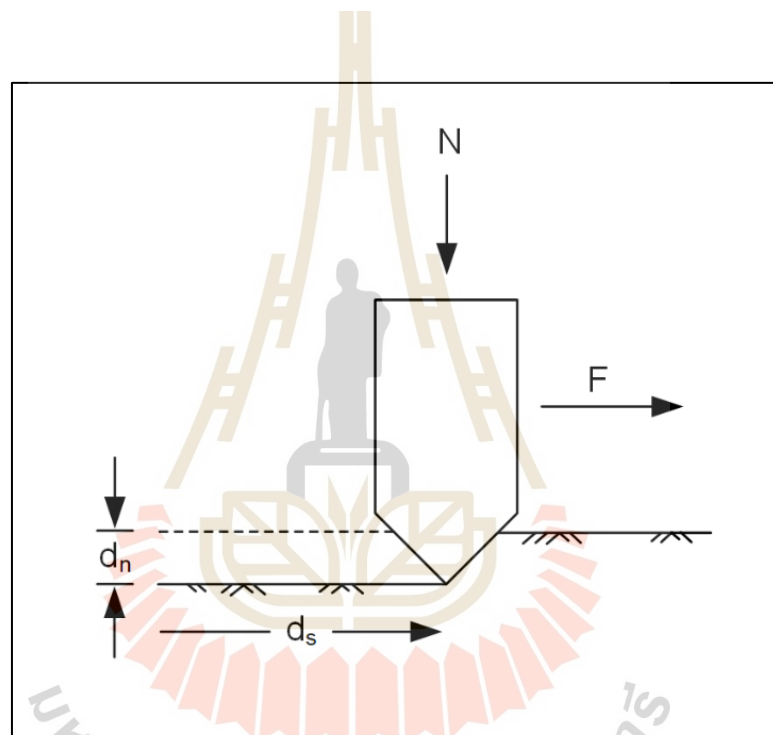


Figure 4.5 Variables used in this study.

CHAPTER V

TEST RESULTS

5.1 Introduction

This chapter describes the results of CERCHAR testing under different scratching rates and under dry and saturated conditions for the three sandstones. Also provided are the results obtained from the test parameters imposed beyond those of the standard practice (ASTM D7625-10). These include the scratching forces measured along the test length and the groove volume on the specimen surfaces under different scratching rates.

5.2 CAI Results

Figure 5.1 gives examples images of pin wear from Phra Wihan specimens tested under scratching rate of 1 mm/s and saturated condition. The d_i value is used to calculate the CAI values. All results are given in Tables 5.1 through 5.3 for Phra Wihan, Phu Phan and Phu Kradung sandstones. For all scratching rates and sandstone types, CAI values under saturated conditions are slight lower than those under dry condition. CAI values increase with increasing scratching rates (Figure 5.2). Phra Wihan sandstone tends to yield the largest CAI, as compared to the other two sandstone types. The variation of the five CAI values (testing is repeated 5 times using 5 pins) under the same conditions is about 10% or less.

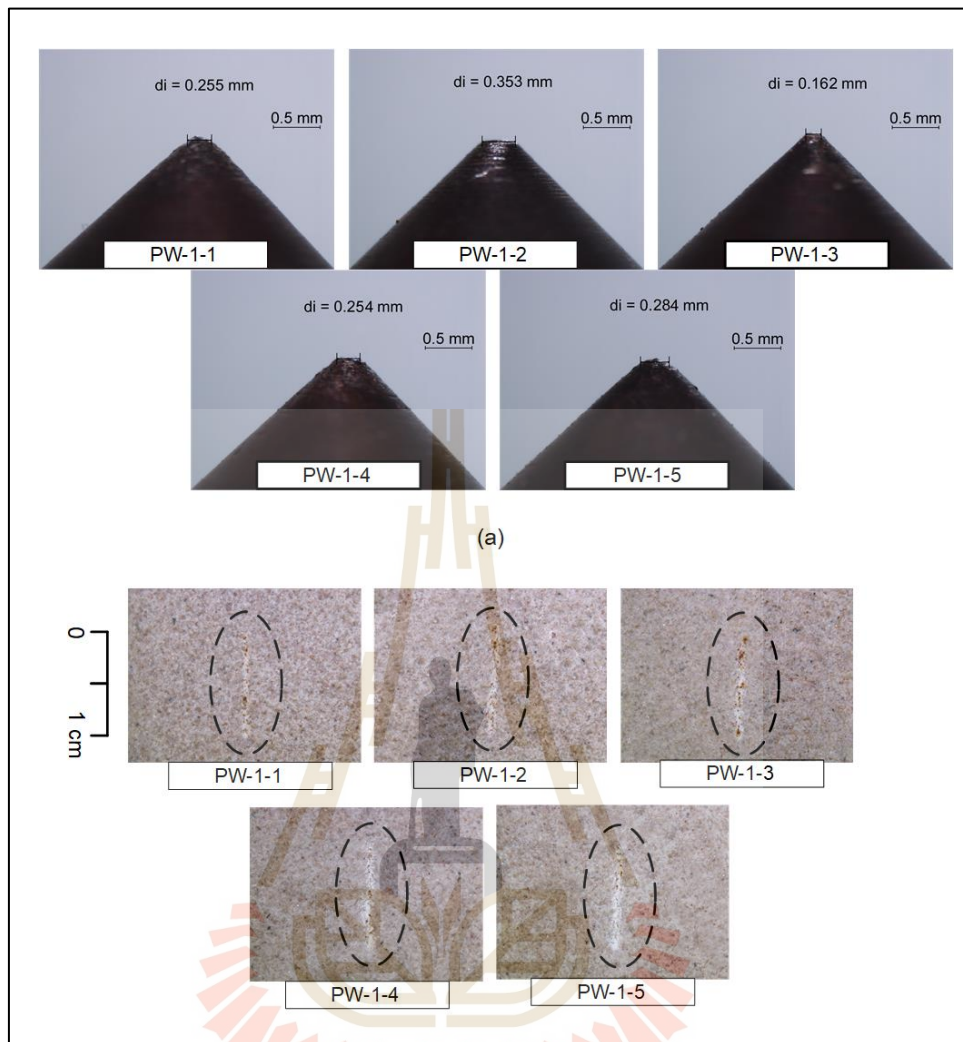


Figure 5.1 CERCHAR stylus pins after testing on Phra Wihan sandstone specimens (a) and their corresponding groove images (b) under scratching rate of 1 mm/s and saturated conditions.

Table 5.1 CAI values under different scratching rates for Phra Wihan sandstones.

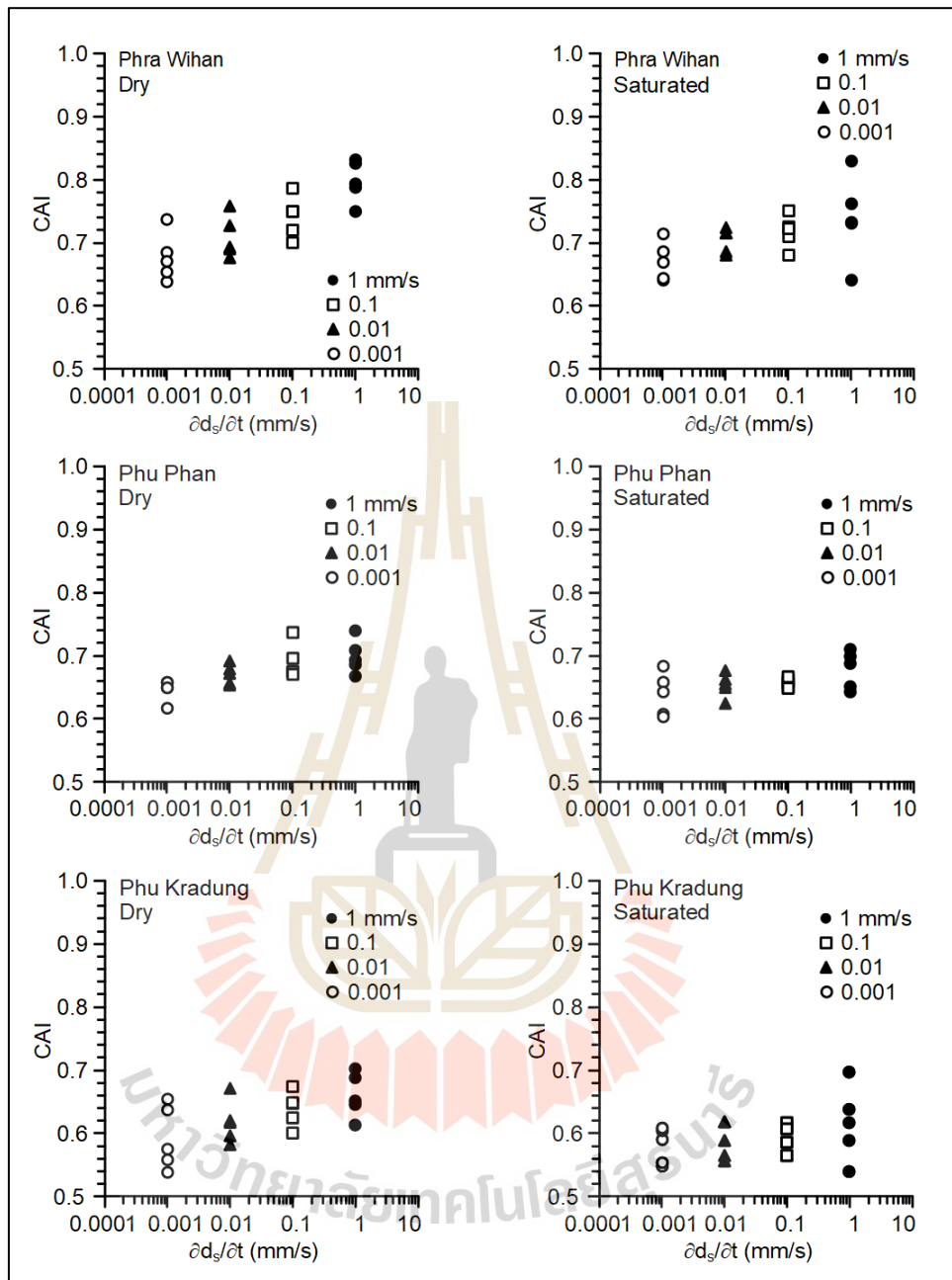
$\partial d_s/\partial t$ (mm/s)	Pin No.	Phra Wihan sandstone			
		d_i (mm)		CAI	
		Dry	Sat.	Dry	Sat.
0.001	1	0.260	0.237	0.74	0.71
	2	0.207	0.192	0.68	0.67
	3	0.160	0.208	0.64	0.69
	4	0.193	0.163	0.67	0.64
	5	0.176	0.165	0.65	0.64
	avg. \pm SD	0.199 \pm 0.04	0.193 \pm 0.03	0.68 \pm 0.04	0.67 \pm 0.03
0.01	1	0.282	0.202	0.76	0.68
	2	0.250	0.208	0.73	0.69
	3	0.217	0.238	0.69	0.72
	4	0.213	0.246	0.69	0.72
	5	0.199	0.239	0.68	0.72
	avg. \pm SD	0.232 \pm 0.03	0.227 \pm 0.02	0.71 \pm 0.03	0.70 \pm 0.02
0.1	1	0.272	0.274	0.75	0.75
	2	0.310	0.232	0.79	0.71
	3	0.243	0.249	0.72	0.73
	4	0.272	0.202	0.75	0.68
	5	0.224	0.245	0.70	0.72
	avg. \pm SD	0.264 \pm 0.03	0.240 \pm 0.03	0.74 \pm 0.03	0.72 \pm 0.03
1	1	0.355	0.255	0.83	0.73
	2	0.350	0.353	0.83	0.83
	3	0.273	0.162	0.75	0.64
	4	0.317	0.254	0.79	0.73
	5	0.311	0.284	0.79	0.76
	avg. \pm SD	0.321 \pm 0.03	0.262 \pm 0.07	0.80 \pm 0.03	0.74 \pm 0.07

Table 5.2 CAI values under different scratching rates for Phu Phan sandstones.

$\partial d_s/\partial t$ (mm/s)	Pin No.	Phu Phan sandstone			
		d_i (mm)		CAI	
		Dry	Sat.	Dry	Sat.
0.001	1	0.172	0.128	0.65	0.61
	2	0.180	0.180	0.66	0.66
	3	0.181	0.123	0.66	0.60
	4	0.172	0.205	0.65	0.68
	5	0.139	0.163	0.62	0.64
	avg. \pm SD	0.169 \pm 0.02	0.160 \pm 0.04	0.65 \pm 0.02	0.64 \pm 0.03
0.01	1	0.202	0.146	0.68	0.62
	2	0.215	0.197	0.69	0.68
	3	0.195	0.171	0.67	0.65
	4	0.176	0.183	0.65	0.66
	5	0.179	0.176	0.66	0.65
	avg. \pm SD	0.193 \pm 0.02	0.175 \pm 0.02	0.67 \pm 0.02	0.65 \pm 0.02
0.1	1	0.218	0.178	0.70	0.66
	2	0.261	0.182	0.74	0.66
	3	0.198	0.171	0.68	0.65
	4	0.197	0.188	0.67	0.67
	5	0.193	0.169	0.67	0.65
	avg. \pm SD	0.213 \pm 0.03	0.177 \pm 0.01	0.69 \pm 0.03	0.66 \pm 0.01
1	1	0.190	0.209	0.67	0.69
	2	0.263	0.163	0.74	0.64
	3	0.216	0.221	0.69	0.70
	4	0.208	0.231	0.69	0.71
	5	0.232	0.171	0.71	0.65
	avg. \pm SD	0.222 \pm 0.03	0.199 \pm 0.03	0.70 \pm 0.03	0.68 \pm 0.03

Table 5.3 CAI values under different scratching rates for Phu Kradung sandstones.

$\partial d_s/\partial t$ (mm/s)	Pin No.	Phu Kradung sandstone			
		d_i (mm)		CAI	
		Dry	Sat.	Dry	Sat.
0.001	1	0.060	0.110	0.54	0.59
	2	0.159	0.126	0.64	0.60
	3	0.176	0.069	0.65	0.55
	4	0.097	0.130	0.58	0.61
	5	0.080	0.074	0.56	0.55
	avg. \pm SD	0.114 \pm 0.05	0.102 \pm 0.03	0.59 \pm 0.05	0.58 \pm 0.03
0.01	1	0.139	0.077	0.62	0.56
	2	0.193	0.139	0.67	0.62
	3	0.118	0.086	0.60	0.56
	4	0.142	0.110	0.62	0.59
	5	0.103	0.140	0.58	0.62
	avg. \pm SD	0.139 \pm 0.03	0.110 \pm 0.03	0.62 \pm 0.03	0.59 \pm 0.03
0.1	1	0.122	0.107	0.60	0.59
	2	0.170	0.130	0.65	0.61
	3	0.170	0.086	0.65	0.57
	4	0.146	0.139	0.62	0.62
	5	0.197	0.128	0.67	0.61
	avg. \pm SD	0.161 \pm 0.03	0.118 \pm 0.02	0.64 \pm 0.03	0.60 \pm 0.02
1	1	0.168	0.159	0.65	0.64
	2	0.225	0.219	0.70	0.70
	3	0.210	0.060	0.69	0.54
	4	0.173	0.138	0.65	0.62
	5	0.135	0.110	0.61	0.59
	avg. \pm SD	0.182 \pm 0.04	0.137 \pm 0.06	0.66 \pm 0.04	0.62 \pm 0.06



(a)

(b)

Figure 5.2 CAI values as a function of scratching rates ($\partial d_s / \partial t$) for dry (a) and saturated (b) conditions.

5.3 Lateral Force and Vertical Displacement

During scratching, lateral force (F) exerting on the stylus pin and the vertical displacement (d_n) of the pin have been measured for all rates and test conditions. Figure 5.3 plots the force (F) and displacement (d_n) as a function of scratching distance. Noted that each line in the diagram represents average of five CAI tests (five pins). Both forces and displacements increase with increasing scratching distance. Their largest values are obtained at the end of scratching. For all sandstone types, lower lateral force is obtained under lower scratching rates. It seems also that lower scratching rates induce larger vertical displacement of the pin, suggesting that the rock surfaces are scratching deeper under the low rates. The results obtained here will be used to calculate the energy required to scratch the rock surfaces under different rates and test conditions, in the following section.

5.4 Groove Volumes

All rock surfaces after CAI testing have been laser-scanned to observe the groove shape and to calculate the groove volume. Representative images of all rock types, scratching rates and test conditions are given in Figures 5.4 through 5.6 for Phra Wihan, Phu Phan, and Phu Kradung sandstones. Table 5.2 gives the calculated groove volumes. The volumes are calculated using SURFER software 16.6 (Golden Software, 2019) Figure 5.7 plots the mean groove volume (V_m) as a function of scratching rates. For all three sandstones, the groove volumes decrease with increasing scratching rates. Both dry and saturated test conditions show similar results. The diagrams suggest that decreasing the scratching rates by 3 orders of magnitude can increase the groove volume by about 25%.

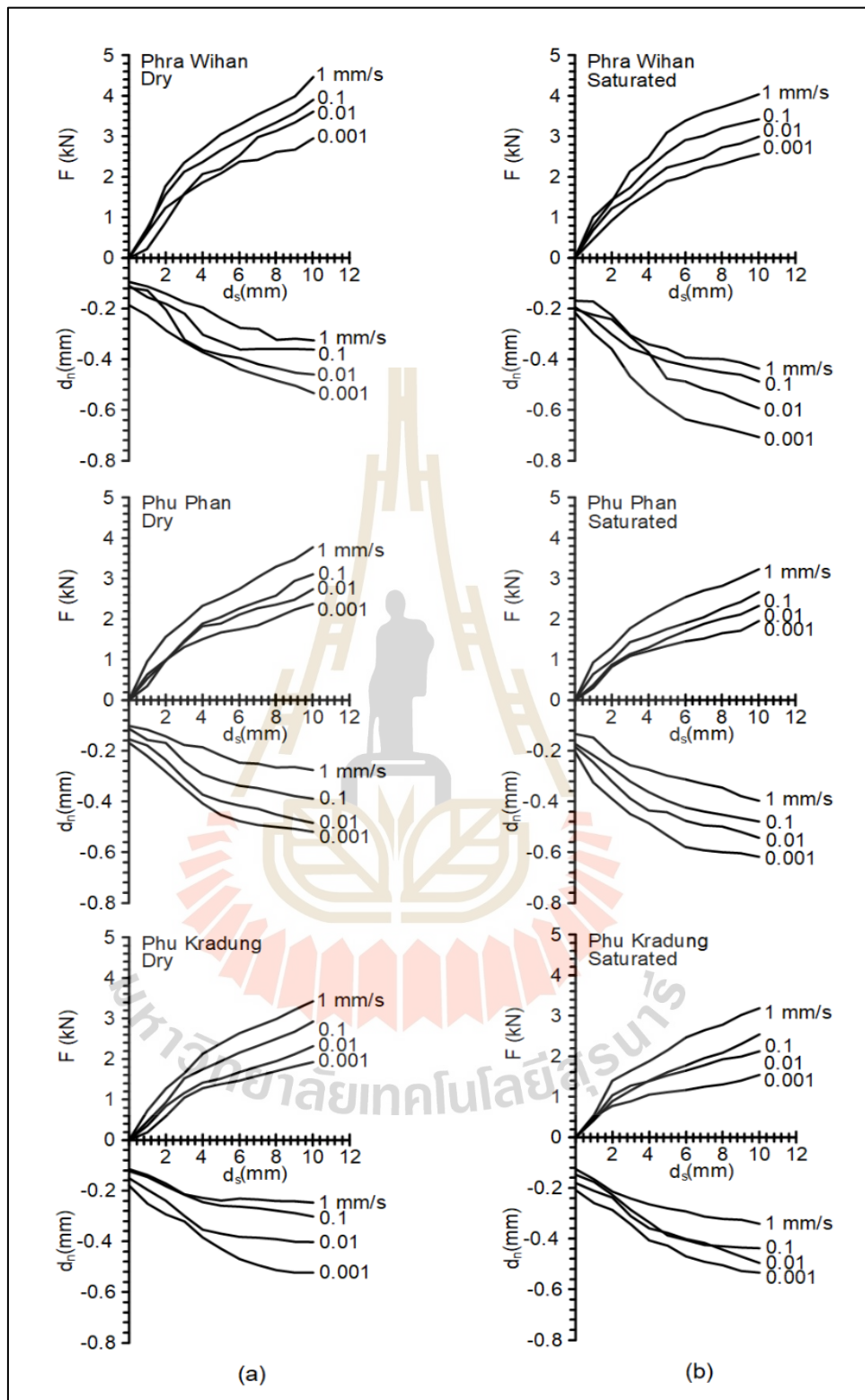


Figure 5.3 Scratching forces (F) and vertical displacement (d_n) as a function of scratching distance for dry (a) and saturated (b) conditions.

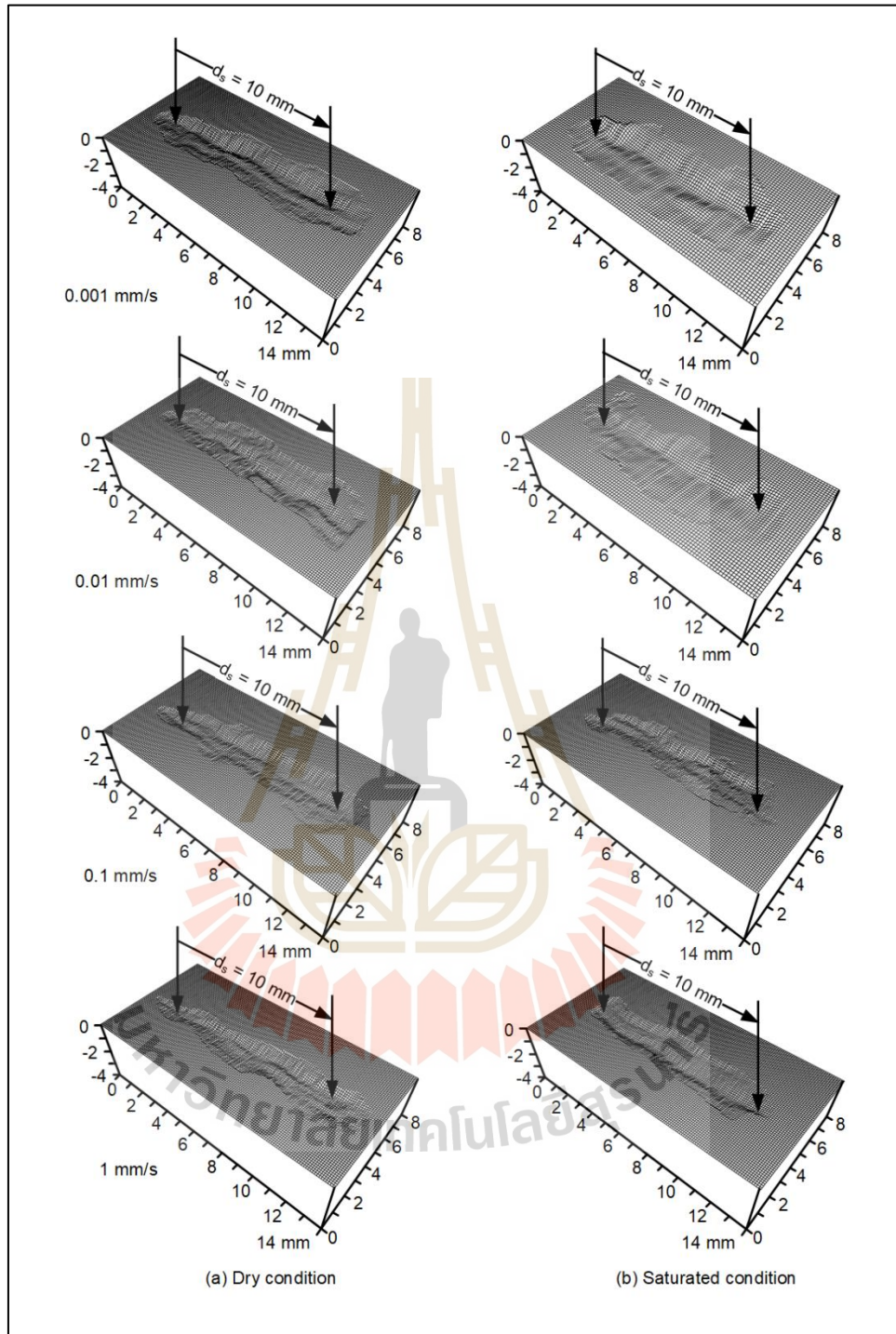


Figure 5.4 Representative laser-scanned images of grooves on rock surfaces after CAI testing under dry (a) and saturated (b) conditions for Phra Wihan sandstone.

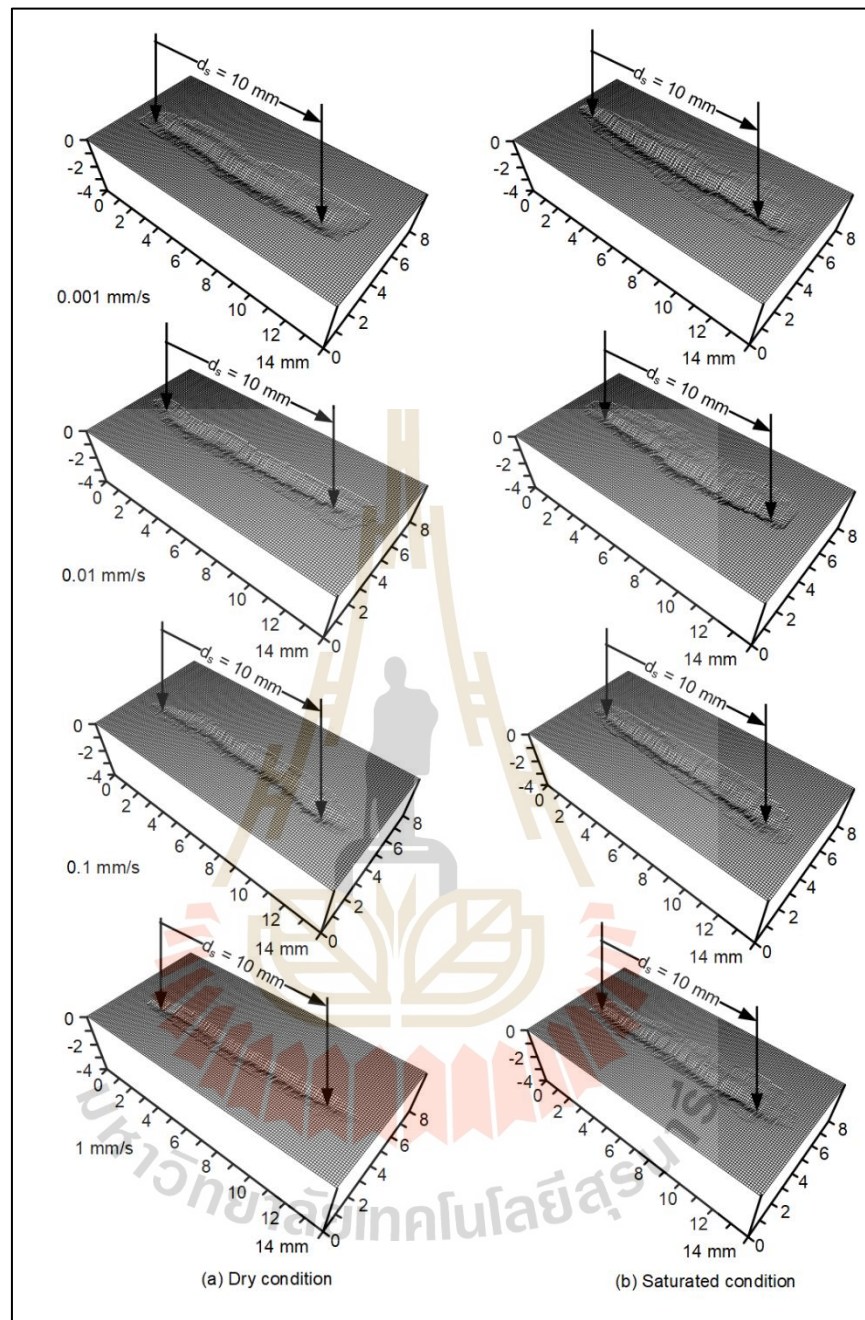


Figure 5.5 Representative laser-scanned images of grooves on rock surfaces after CAI testing under dry (a) and saturated (b) conditions for Phu Phan sandstone.

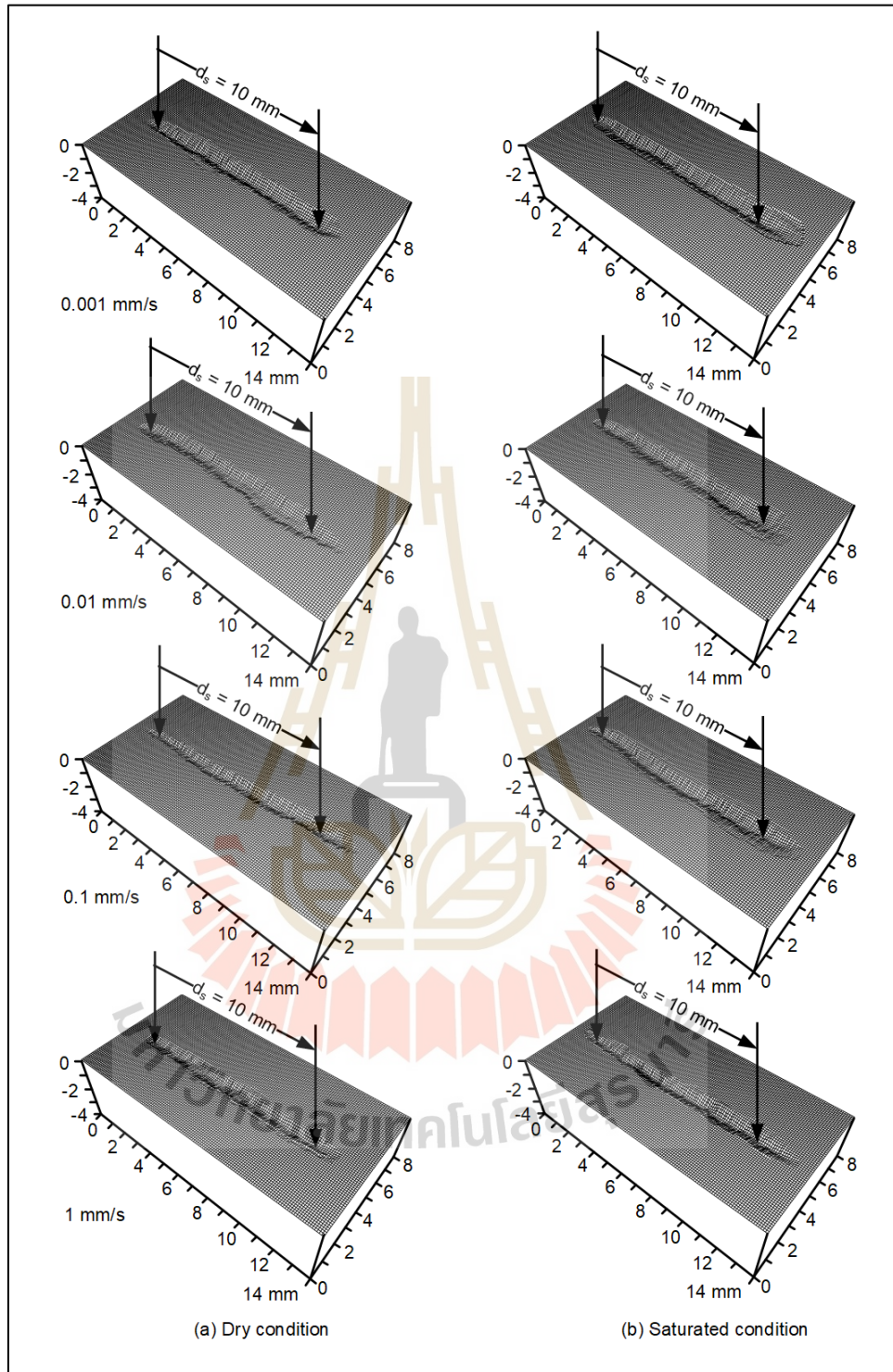


Figure 5.6 Representative laser-scanned images of grooves on rock surfaces after CAI testing under dry (a) and saturated (b) conditions for Phu Kradung sandstone.

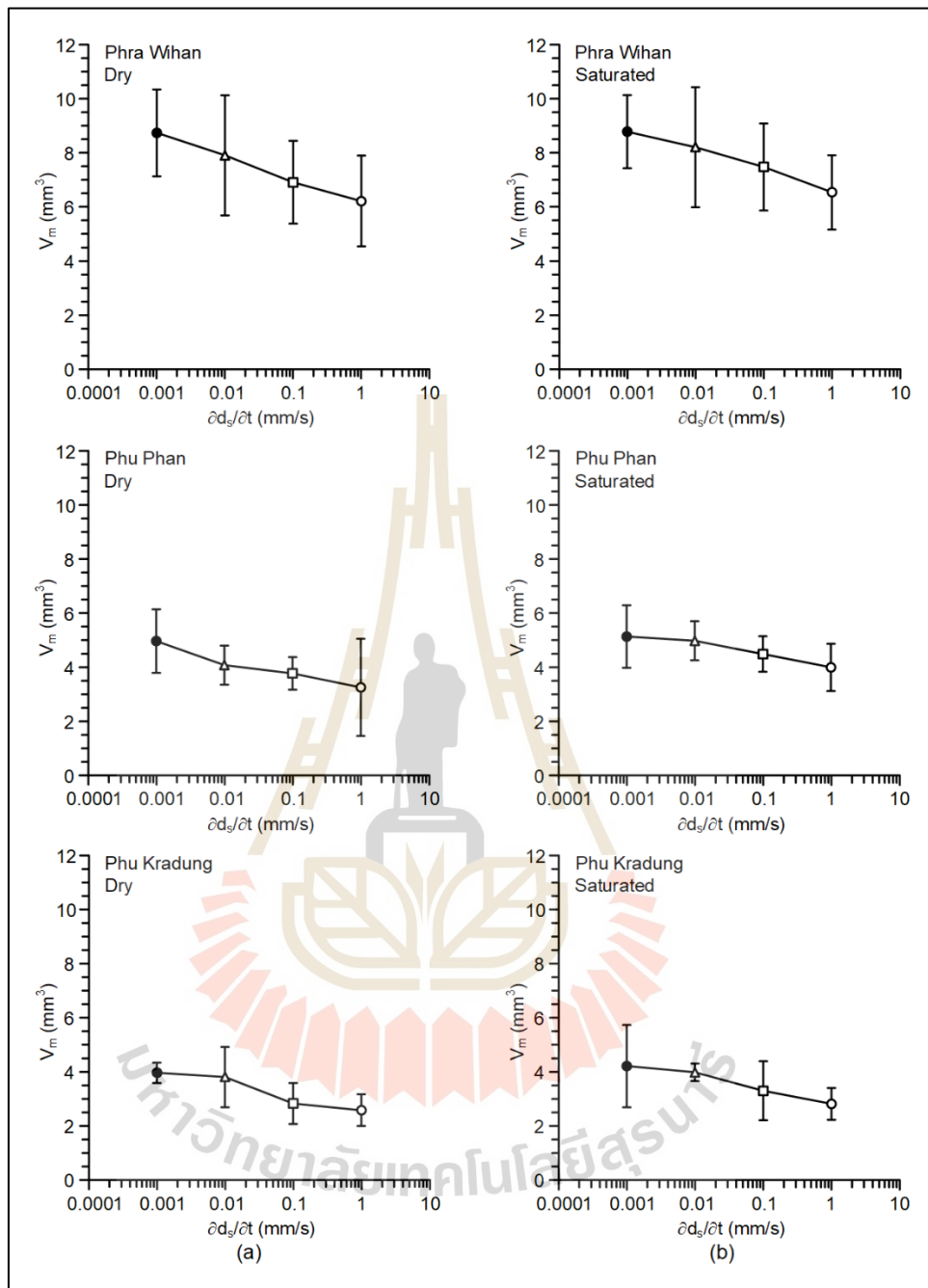


Figure 5.7 Mean groove volume (V_m) as a function of scratching rates under dry (a) and saturated (b) conditions.

Table 5.4 Groove volumes.

Rock Type	$\partial d_s/\partial t$ (mm/s)	Mean groove volumes, V_m (mm ³)	
		Dry	Sat.
Phra Wihan	0.001	8.72 ± 1.79	8.94 ± 1.51
	0.01	7.89 ± 2.48	8.19 ± 2.48
	0.1	6.90 ± 1.71	7.06 ± 1.80
	1	6.20 ± 1.87	6.52 ± 1.54
Phu Phan	0.001	4.96 ± 1.32	5.12 ± 1.29
	0.01	4.07 ± 0.81	4.97 ± 0.81
	0.1	3.77 ± 0.67	4.48 ± 0.73
	1	3.25 ± 2.01	3.98 ± 0.98
Phu Kradung	0.001	3.95 ± 0.42	4.21 ± 1.70
	0.01	3.79 ± 1.25	3.98 ± 0.36
	0.1	2.82 ± 0.84	3.29 ± 1.22
	1	2.57 ± 0.66	2.81 ± 0.66



CHAPTER VI

ANALYSIS OF RESULTS

6.1 Introduction

This chapter attempts to correlate the CAI values with the mechanical properties of sandstones under different rates and test conditions. Also presented are the correlations between CAI values and groove volumes. The mechanical properties of the same sandstones, used in the analysis here, are from those by Khamrat et al. (2016).

6.2 Mathematical Relationships

Figure 6.1 shows the relationship between CAI values and compressive strengths under dry and saturated conditions. The results show that CAI linearly increases with the rock compressive strength for all sandstone types and under both test conditions. Good correlation has been obtained ($R^2 > 0.9$). Under saturated conditions, both CAI values and compressive strengths tend to be lower than those under dry condition. Phra Wihan sandstone gives larger CAI and compressive strength than other two sandstones. The results suggest that after the rocks have been isolated from other factors (variations of quartz contents, porosity, EQC, etc.). It's clear that CAI values linearly depend on the unconfined compressive strength of the rocks.

Figure 6.2 plots CAI as a function of rock cohesion obtained from Khamrat et al. (2016). Good correlations have also been obtained ($R^2 > 0.7$). This is primarily because the rock cohesion is largely related to the unconfined compressive strength of

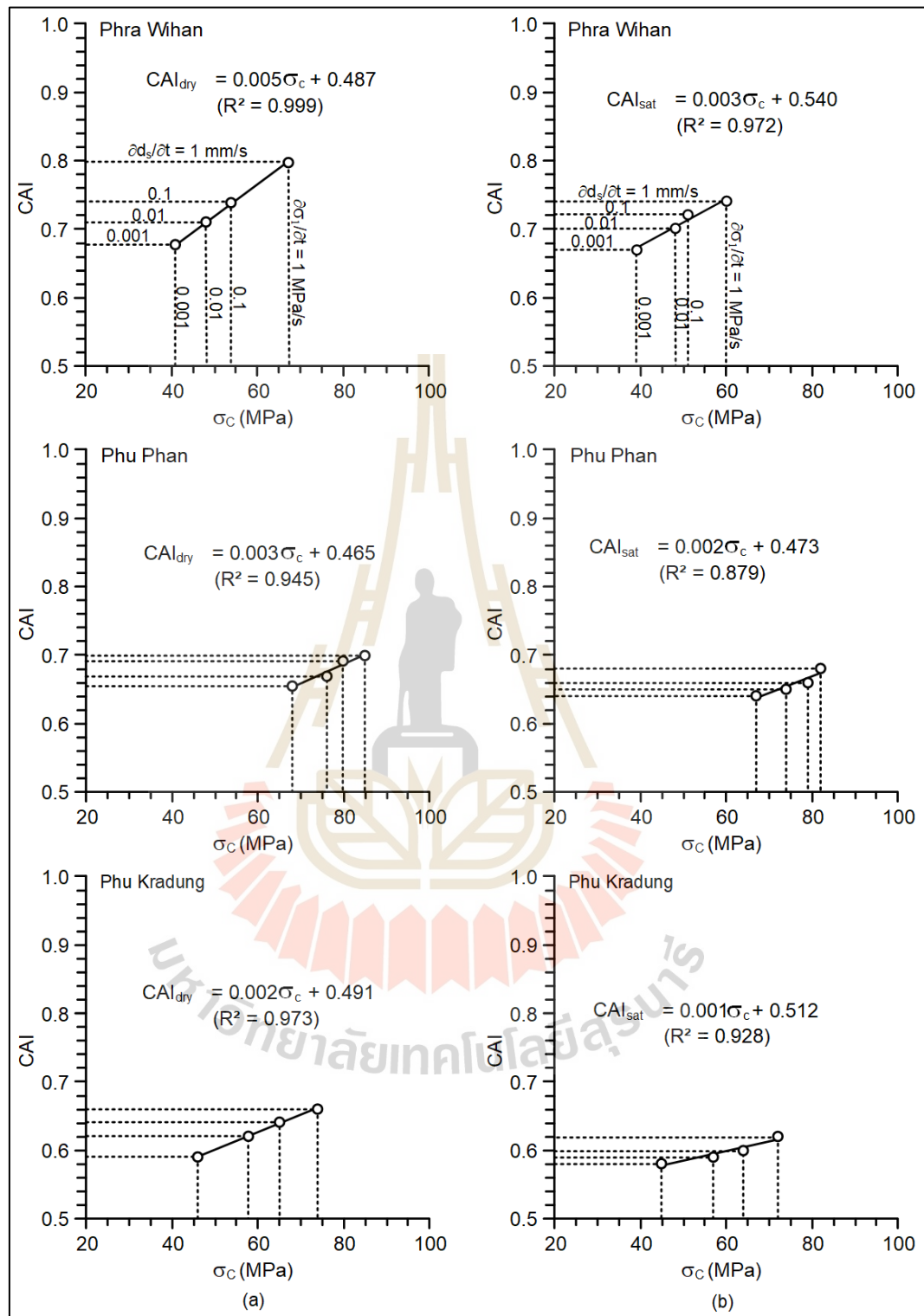


Figure 6.1 Relationship between CAI value and compressive strength under dry (a) and saturated (b) conditions.

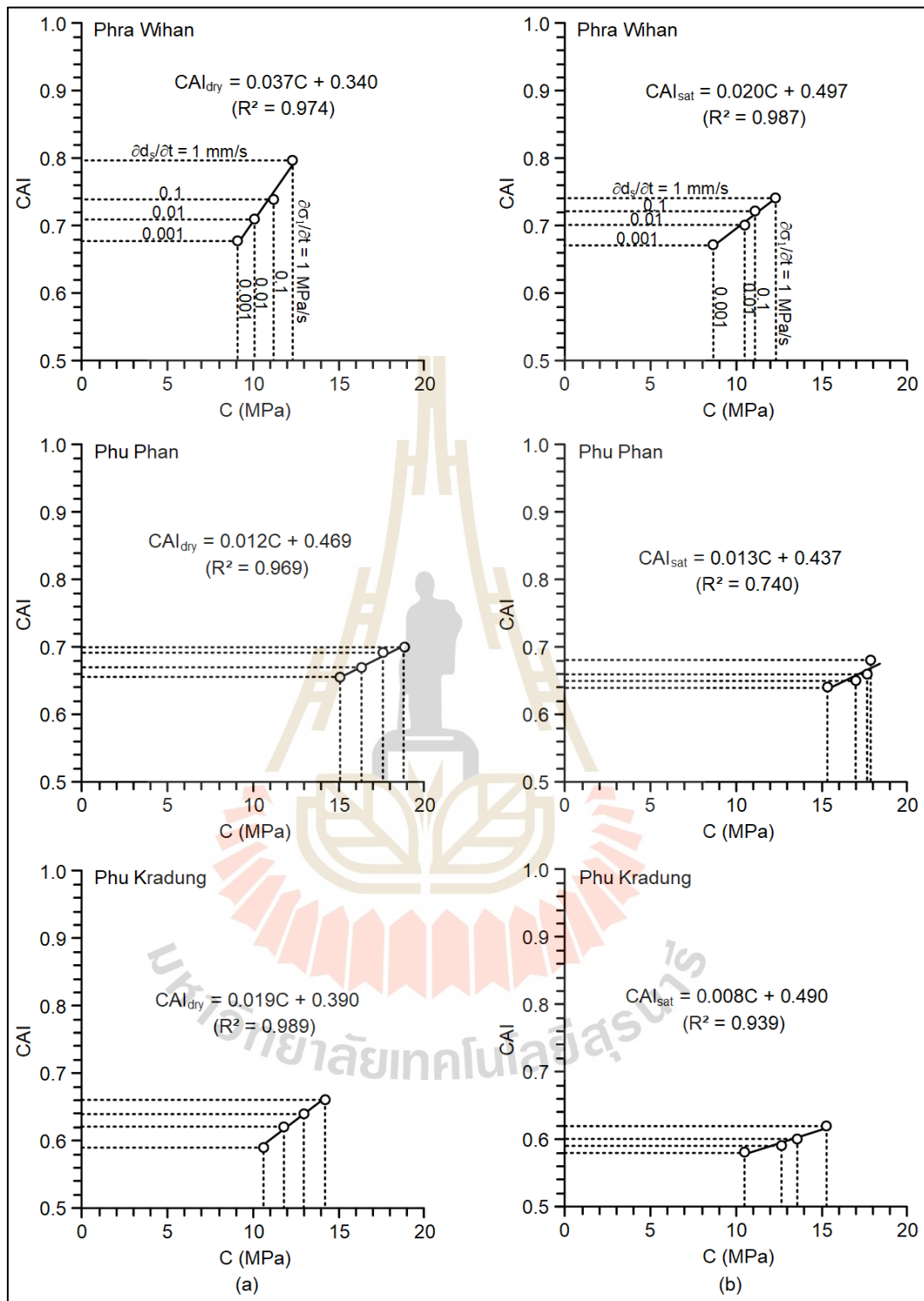


Figure 6.2 Relationship between CAI and cohesion under dry (a) and saturated (b) conditions.

the rock. Again, positive linear relationship has been obtained for all rock types under both conditions

Poor correlation is however obtained between CAI value and internal friction angle (ϕ) of the rocks, as shown in Figure 6.3. This is primarily due to the fact that the rock friction is related to confined compressive strength while the scratching mechanism of CERCHAR pin is under unconfined conditions.

The CAI values are plotted as a function of groove volume in Figure 6.4. Linear correlations are proposed to describe the decrease of CAI as the groove volume increases. All rock types under both test conditions give good correlations ($R^2 > 0.9$). The results suggest that under lower scratching rate not only the CAI decreases but also the groove volume increases. There is no significant difference between scratching the rock surface under dry and saturated conditions in this case.

6.3 Work and Energy

An attempt is made here to determine the work and energy required to scratch the rock surfaces under different rates and test conditions. First, mathematical relationships are determined to define the increase of lateral force (F) as a function of the increase of the scratching distance (d_s). Such relationships are used to calculate the work done through the process of scratching using a polynomial equation as follows:

$$F = \alpha(d_s^2) + \beta(d_s) \quad (6.1)$$

where α and β are empirical counts.

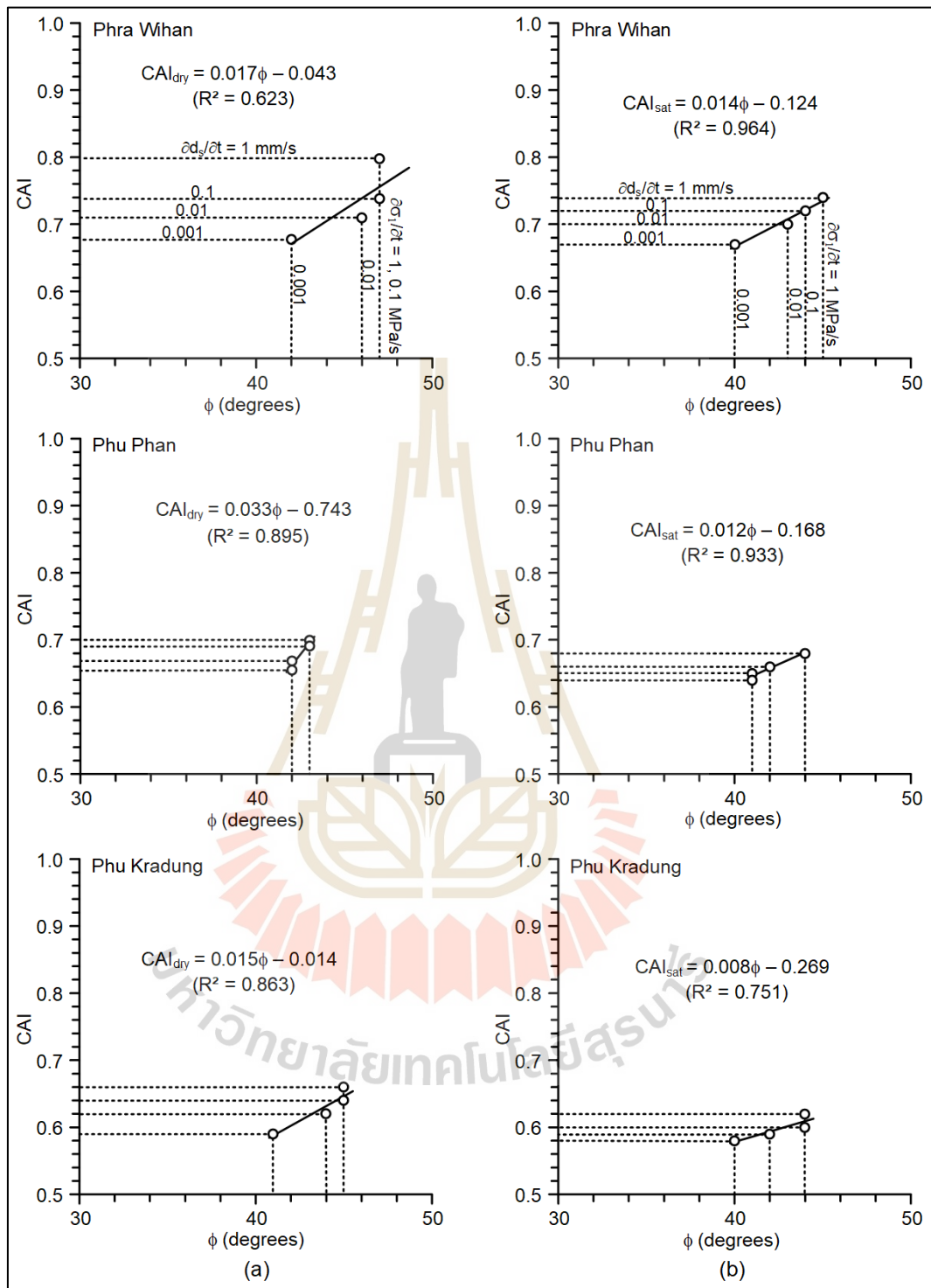


Figure 6.3 Relationship between CAI value and internal friction under dry (a) and saturated (b) conditions.

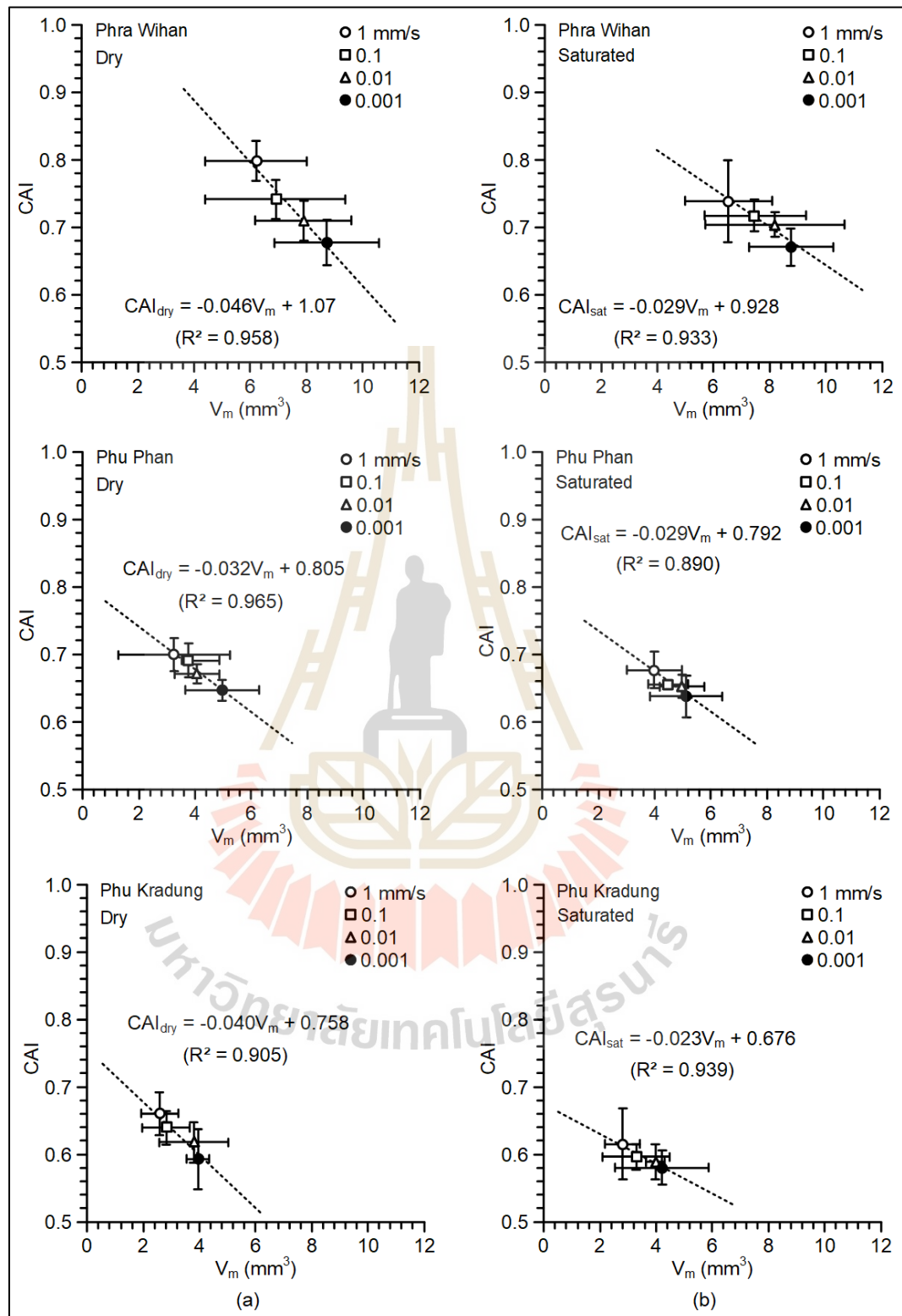


Figure 6.4 Relationship between CAI value and groove volume under dry (a) and saturated (b) conditions.

Figures 6.5 through 6.7 show the relationship between the two values. The numerical values of the constants are given in the figures. The work done can be calculated by integration of equations (6.1), where SW is scratching work done depending on the lateral force in terms of scratching distance.

$$SW = \int_{d_s=0}^{10} F \cdot d_s \quad (6.2)$$

Figure 6.8 plots the results in terms of work done (SW) as a function of CAI value. The results suggest that lower scratching rate not only uses lower work done but also yields lower CAI value. This is true for all rock types under dry and saturated conditions. Exponential equations can best describe the relationship between the work done (SW) and the CAI values under both test conditions. The work done is also plotted as a function of scratching rate in Figure 6.9. The diagrams also confirm that lower work done is required under lower scratching rate. Their relationship can be best represented by a logarithmic equation.

Zhang et al. (2020) propose CERCHAR specific energy (CSE) to correlate with CAI. This value can be calculated by:

$$CSE = \frac{SW}{V_m} = \frac{\int_{d_s=0}^{10} F \cdot d_s}{V_m} \quad (6.3)$$

where SW is from equation (6.2) and V_m is the parameter that are calculated from Chapter 5. The CSE values are plotted as a function of mean groove volume in Figure 6.10. The diagrams suggest that the specific energy decreases with decreasing scratching rates, which results in a larger groove volume. For Phu Phan and Phu Kradung

sandstones, CSE volume obtained from dry and saturated specimens are comparable for Phra Wihan sandstone less specific energy is required for saturated specimens than for dry specimens. The effect of saturation pronounces more for Phra Wihan sandstone than the other two because it has higher porosity (Figure 3.6).



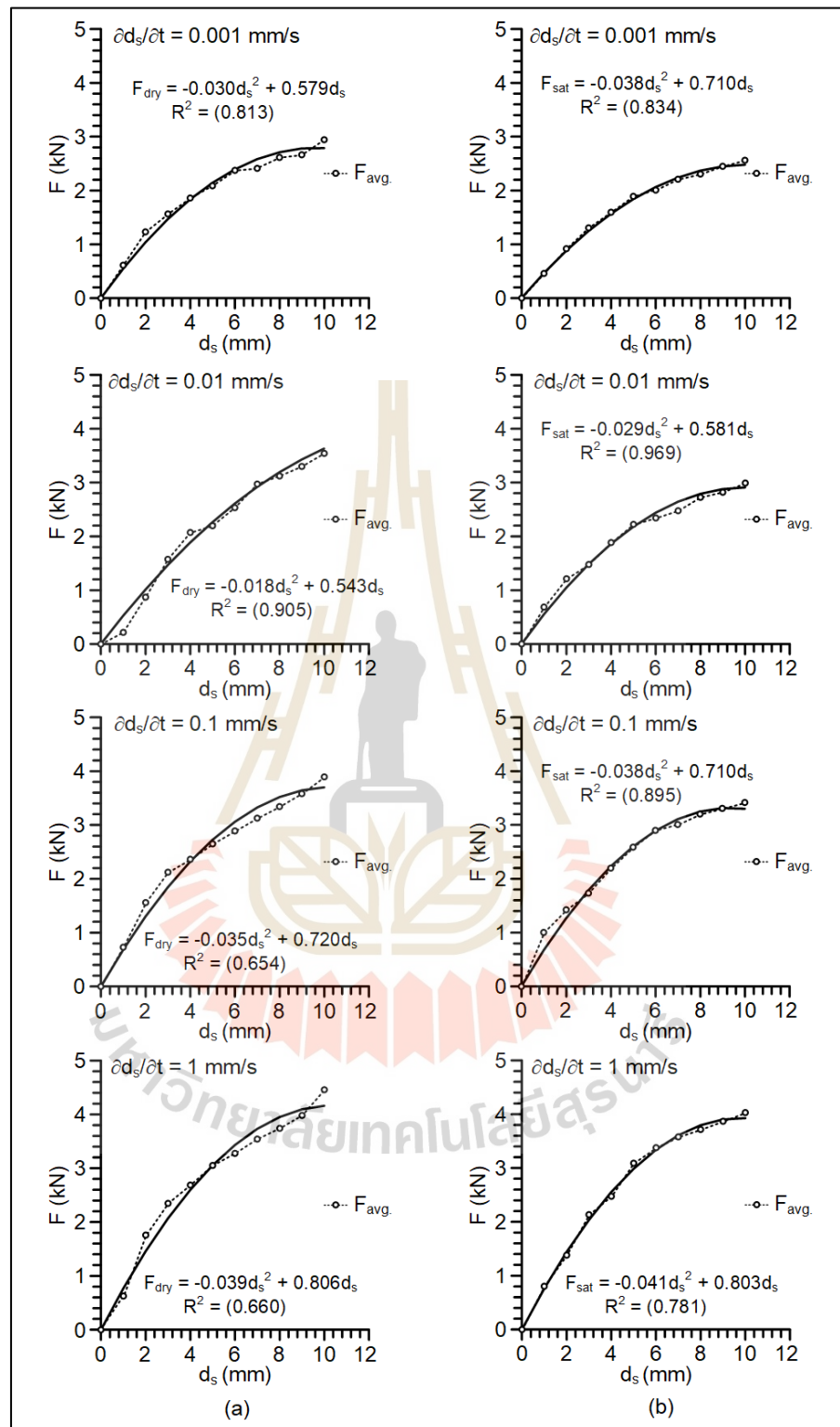


Figure 6.5 Force as a function of horizontal displacement curve fit of Phra Wihan sandstone under dry (a) and saturated (b) conditions.

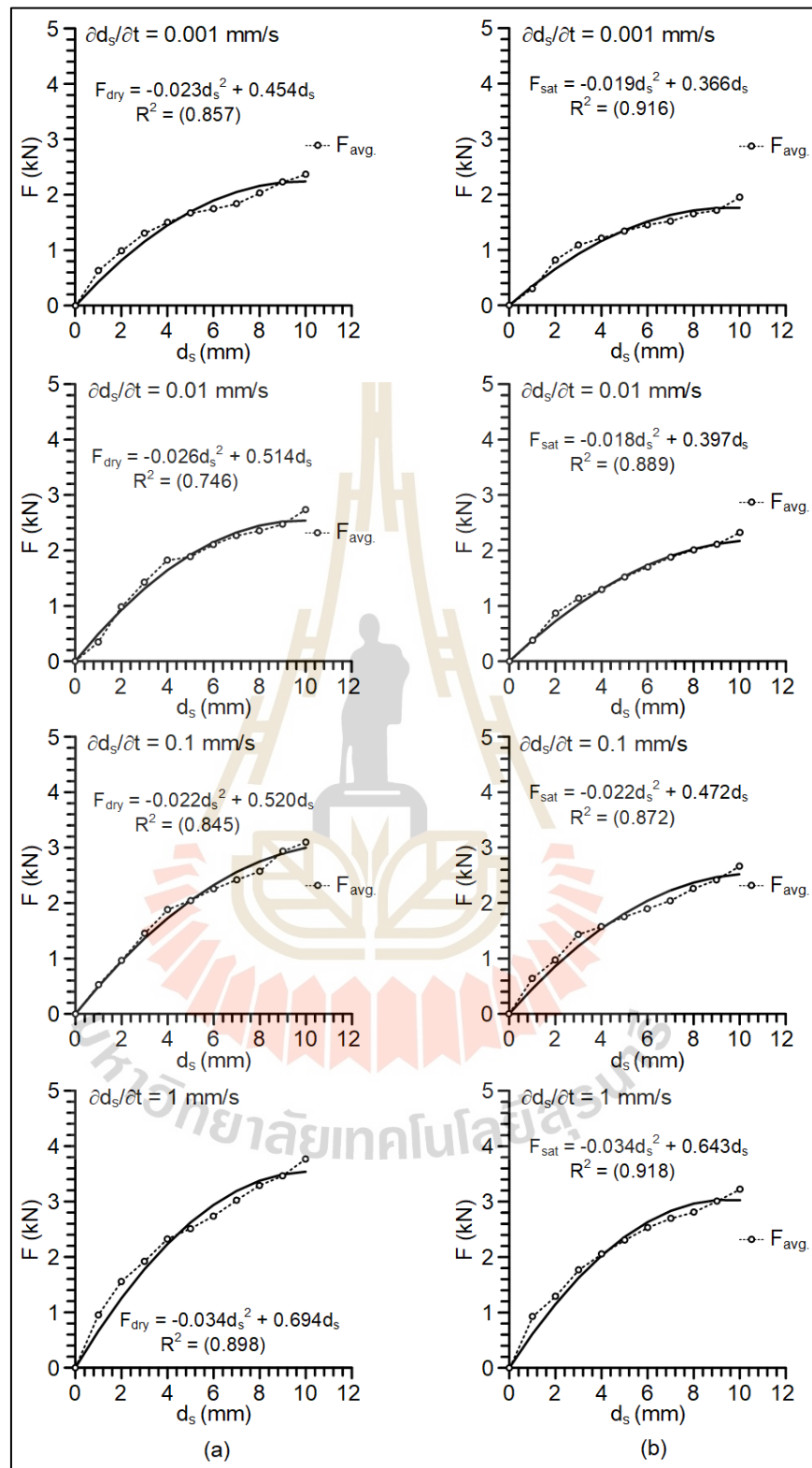


Figure 6.6 Force as a function of horizontal displacement curve fit of Phu Phan sandstone under dry (a) and saturated (b) conditions.

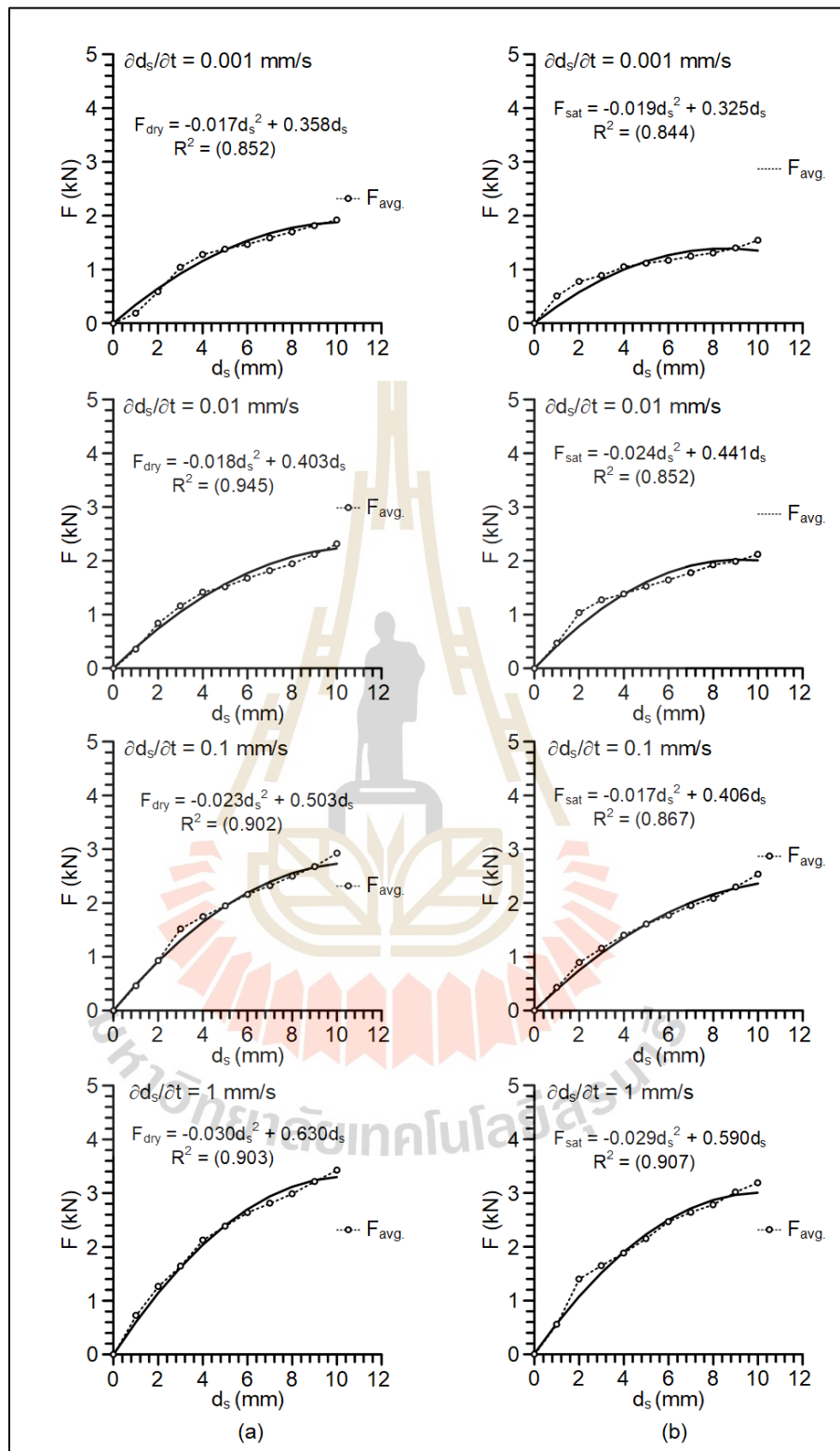


Figure 6.7 Force as a function of horizontal displacement curve fit of Phu Kradung sandstone under dry (a) and saturated (b) conditions.

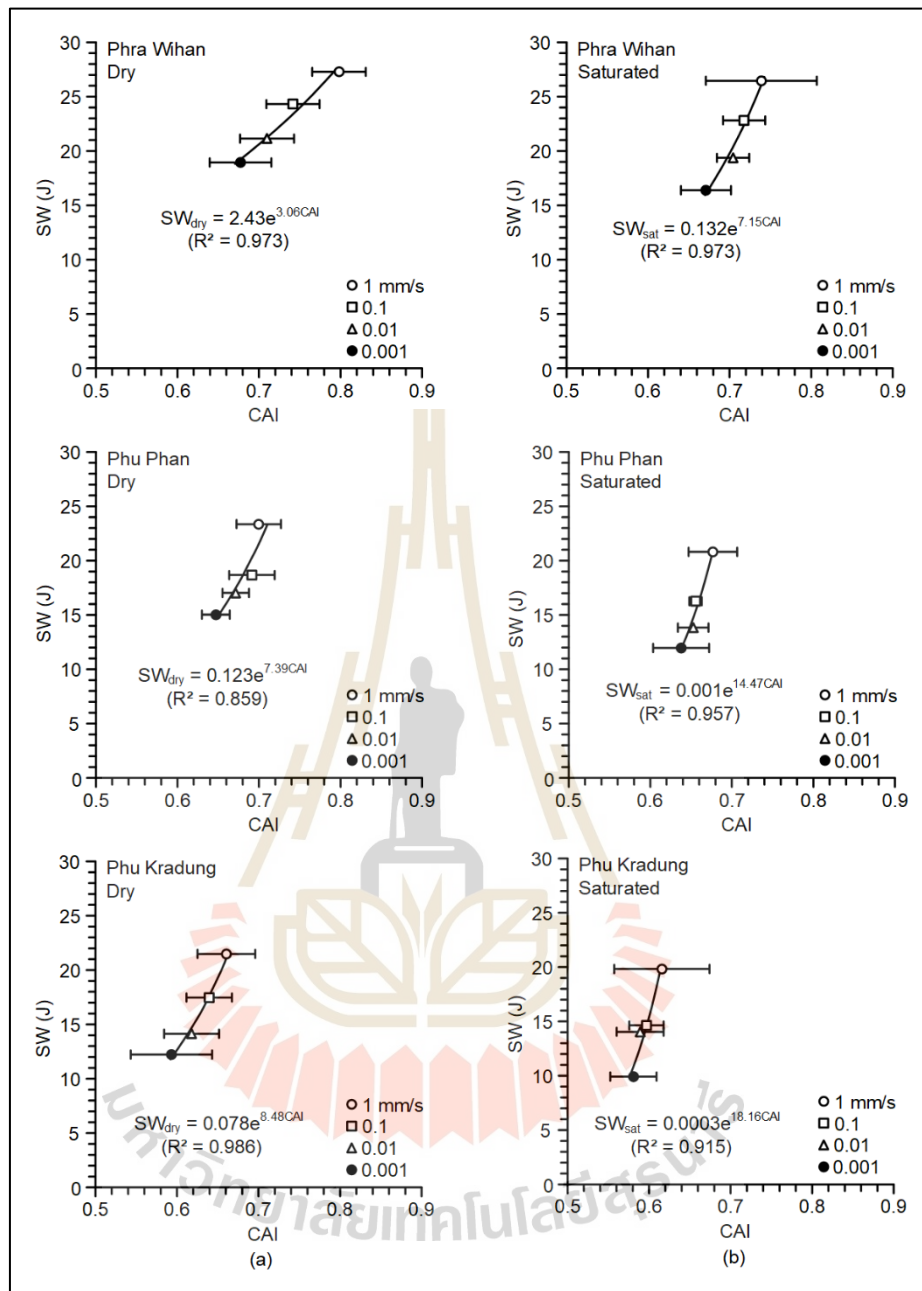


Figure 6.8 Work done and CAI under dry (a) and saturated (b) conditions.

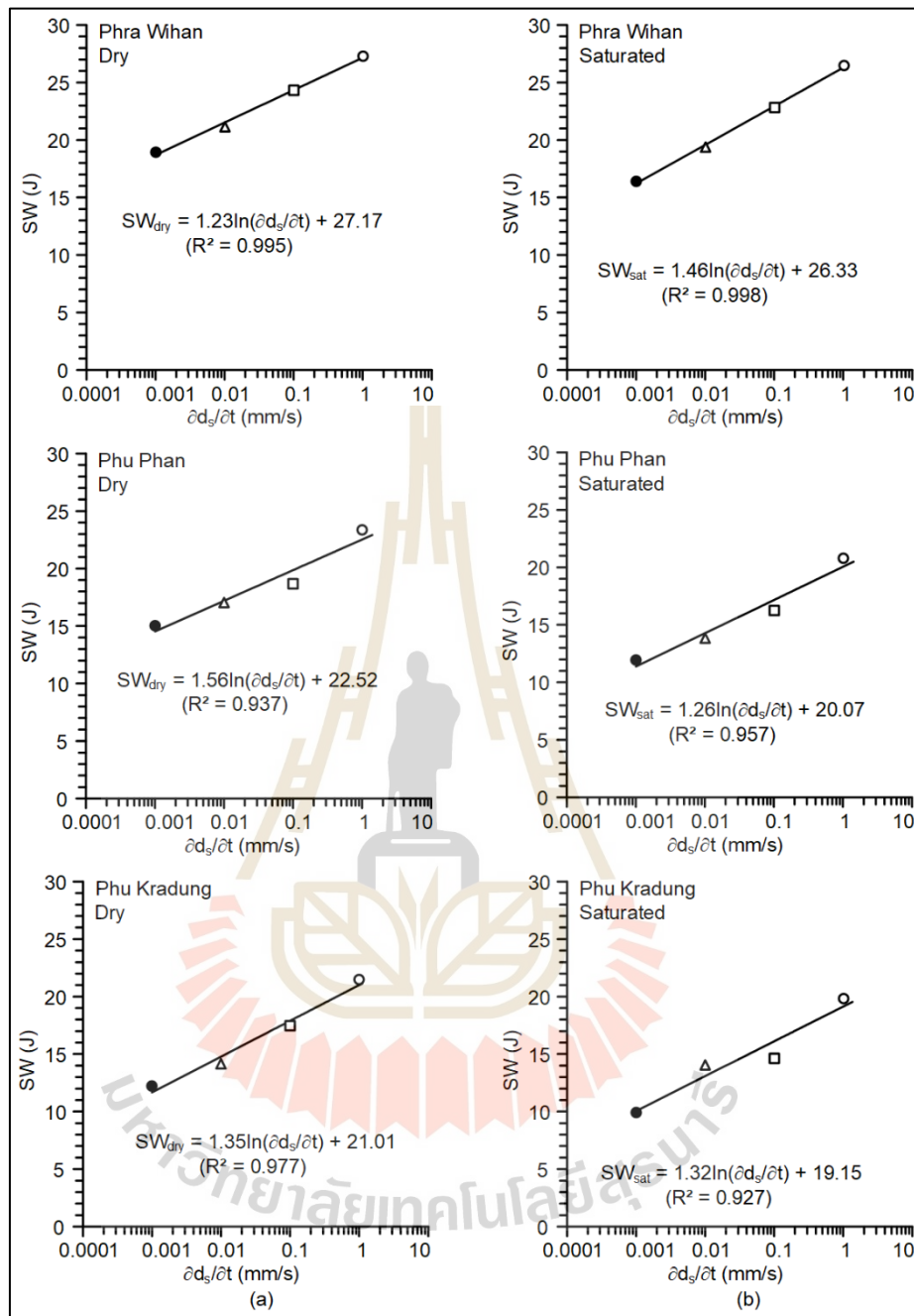


Figure 6.9 Work done as a function of scratching rates under dry (a) and saturated (b) conditions.

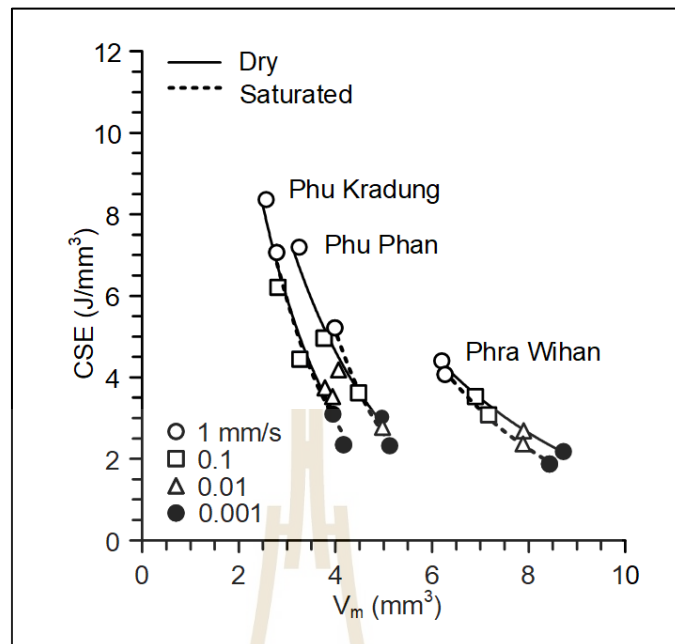


Figure 6.10 CSE and mean groove volume.

CHAPTER VII

DISCUSSIONS AND CONCLUSIONS

7.1 Discussions

Even though intrinsic variability of diameter of the scratched flat area (d_i) and CAI for each scratching rate has been observed for all tested sandstones, these parameters are found to be lower for the saturated specimens than for the dry specimens. This occurs at all scratching rates, as shown in Figure 5.2. This observation agrees with those obtained by Jacobs and Hagan (2009). This may be due to the effect of pore pressure on the rock strength. The pore pressure effect also reflects on the CAI- σ_c relations (Figure 6.1). As evidenced by that the slopes of CAI- σ_c curve under dry condition are greater those under saturated condition. This is true for all sandstone types.

The lateral forces (F) exerting on the stylus pin tends to be lower under saturated condition than those under dry condition. This discrepancy tends to be more noticeable under low scratching rates (Figure 5.3). This may be because under low scratching rates the stylus pin tends to penetrate deeper into the rock surface, and hence the effect of pore pressure can pronounce more. This is supported by the measured pin vertical movement (d_n), as shown in the same figure (Figure 5.3).

Calculation of the groove volume from the laser-scanned profiles seems sufficiently accurate (Figures 5.4 through 5.6). This is due to that the laser scanning measurements are to the nearest ± 0.001 mm (1 micro-meter). The groove volume can

be useful to determine to specific energy for different scratching conditions. Saturated specimens yield slightly larger groove volumes than dry specimens do (Table 5.2). This is true for all scratching rates. This is because the pins penetrate deeper into the saturated surfaces than the dry surfaces, as mentioned earlier.

Based on the Coulomb strength criterion, the rock cohesion is mainly related to the unconfined compressive strength of the rock (Jaeger et al., 2007). This explains why correlations between CAI and cohesion (Figure 6.2) are as good as those between CAI and unconfined compressive strength (Figure 6.1). The rock friction angle is more related to the confined compressive strength, and hence the correlation between CAI and friction angle are not as good as those of unconfined compressive and cohesion (Figure 6.3).

For the same sandstone type, lower CAI values lead to larger groove volumes (as shown in Figure 6.4). Such conclusions can be drawn because the application of different scratching rates on the same rock. The results are isolated from other geological factors, such as variations of porosity, mineral compositions, density, etc.

Polynomial equations seem adequate to describe the lateral force (F) as a function of scratching distance, as shown in Figures 6.5 to 6.7. This allows calculation of the scratching work (SW) required to scratch the rock surfaces to 10 mm. Similar approach has been used by Zhang et al. (2020). The polynomial equation used in this study is better than the exponential equation proposed by Zhang et al. (2020). This is because the polynomial equation gives $F=0$ when $ds = 0$, while the exponential equation does not.

The work done (SW) decrease with decreasing CAI values and scratching rates (Figures 6.8 and 6.9). This agrees with the conclusions drawn by Zhang et al. (2020).

The results imply that under low scratching rates, the pin wear not only reduces, but the work required to scratch the rock surface also reduces. Under the same specific energy, larger groove values will be obtained from Phra Wihan than those of Phu Phan and Phu Kradung sandstones (Figure 6.10). The diagrams in the figure suggest also that for all sandstones and test conditions lower scratching rates will require less energy and yield larger groove volumes than higher scratching rates. This agrees with the previous results of the work done.

The relationship between CAI and the Equivalent quartz content (EQC) cannot be established here. This is due to the fact that there are only three sandstone types tested here and they show comparable values of EQC (equal to 11.13, 10.92 and 6.88) for Phra Wihan, Phu Phan and Phu Kradung sandstones, respectively

7.2 Conclusions

The outcomes of the results and analysis from this study can be summarized as follows:

- CAI values increase linearly with increasing unconfined compressive strength and cohesion of the tested sandstones. Their correlation coefficients are greater 0.9.
- Under the same scratching rate, saturated sandstones give lower CAI values, rock strength and cohesion but larger groove volume than dry sandstones do.
- Lower scratching rates induce lower CAI values but larger scratched volumes.
- Work done calculated from integrating lateral force over scratching distance increase with increasing CAI values and scratching rate. Work done required for dry specimens is greater than that for saturated specimens.

- Under the same test conditions, Phra Wihan sandstone yields largest CAI values, groove volumes and work done but uses least specific energy as compared to the other two sandstones.
- Lower scratching rates tend to give lower specific energy but larger groove volume than higher rates do.

7.3 Recommendations for Future Studies

Limitations and results of this study lead to recommendations for future studies as follows:

- More CAI testing is required on a variety of rock types with different strengths and mineral compositions. The results would provide a more rigorous conclusion, in particular, the relationship between CAI and uniaxial compressive strength of rocks.
- Testing under longer scratching lengths of the pin would be desirable, particularly for the rocks that contain grain sizes larger than 10 mm. Such approach can incorporate the different responses of various rock-forming minerals on the pin wear.
- The effect of confining pressures on the specimens is needed. The results may reveal a better correlation between CAI and the triaxial compressive strengths (c and ϕ) of the rocks.
- Acoustic emission technique may be applied on the specimens during scratching. The acoustic wears generated by the interaction between the pin and rock surface might be able to correlate with the specific energy required during scratching.

REFERENCES

- Al-Ameen, S. I. and Waller, M. D. (1994). The influence of rock strength and abrasive mineral content on the CERCHAR abrasive index. **Engineering Geology**. 36(3): 293-301.
- Alber, M. (2008). Stress dependency of the CERCHAR abrasivity index (CAI) and its effects on wear of selected rock cutting tools. **Tunnelling and Underground Space Technology**. 23(4): 351-359.
- ASTM D2216-19. (2019). **Standard Test Method for Laboratory Determination of Water (Moisture) Content of Soil and Rock by Mass**. Annual Book of ASTM Standards, American Society for Testing and Materials, West Conshohocken, PA.
- ASTM D7625-10. (2010). **Standard Test Method for Laboratory Determination of Abrasiveness of Rock Using the CERCHAR Method**. Annual Book of ASTM Standards, American Society for Testing and Materials, West Conshohocken, PA.
- Atkinson, T., Cassapi, V. B., and Singh, R. N. (1986). Assessment of abrasive wear resistance potential in rock excavation machinery. **International Journal of Mining and Geological Engineering**. 4(2): 151-163.
- Aydın, H., Yaralı, O., and Duru, H. (2016). The effects of specimen surface conditions and type of test apparatus on CERCHAR abrasivity index. **Karaelmas Science and Engineering Journal**. 6(2): 293-298.

- Balani, A., Chakeri, H., Barzegari, G., and Ozcelik, Y. (2017). Investigation of various parameters effect on CERCHAR abrasivity index with PFC3D modeling. **Geotechnical and Geological Engineering**. 35(6): 2747-2762.
- Beste, U., Lundvall, A., and Jacobson, S. (2004). Micro-scratch evaluation of rock types a means to comprehend rock drill wear. **Tribology International**. 37(2): 203-210.
- Bharti, S., Deb, D., and Das, P. (2017). Abrasivity investigation by physic-mechanical parameters and microscopic analysis of rock samples. In **Proceedings of the International Conference on Deep Excavation, Energy Resources and Production** (pp. 24-26). India.
- Capik, M. and Yilmaz, A. O. (2017). Correlation between CERCHAR abrasivity index, rock properties, and drill bit lifetime. **Arabian Journal of Geosciences**. 10(15): 1-12.
- Deliormanlı, A. H. (2012). CERCHAR abrasivity index (CAI) and its relation to strength and abrasion test methods for marble stones. **Construction and Building Materials**. 30: 16-21.
- Dyke, C.G. and Dobereiner, L. (1991). Evaluating the strength and deformability of sandstones. **Quarterly Journal of Engineering Geology**. 24: 123-134.
- Er, S. and Tuğrul, A. (2016). Correlation of physico-mechanical properties of granitic rocks with CERCHAR abrasivity index in Turkey. **Measurement**. 91: 114-123.
- Fuenkajorn, K. and Kenkhunthod, N. (2010). Influence of loading rate on deformability and compressive strength of three Thai sandstones. **Geotechnical and Geological Engineering**. 28: 707–715.
- Fuenkajorn, K., Sriapai, T., and Samsri, P. (2012). Effects of loading rate on strength and deformability of Maha Sarakham salt. **Engineering Geology**. 135-136: 10-23.

- Gharahbagh, E.A, Rostami, J., Ghasemi, A. R., and Tonon, F. (2011). Review of rock abrasion testing. In **Proceedings of the 45th U.S. Rock Mechanics/Geomechanics Symposium**. San Francisco, California.
- Golden Software. (2019). **Surfer 16.6 User's Guide**. Golden Software,. LLC., Colorado, United States.
- Hamzaban, M. T., Karami, B., and Rostami, J. (2019). Effect of pin speed on CERCHAR abrasion test results. **Journal of Testing and Evaluation**. 47(1): 121-139.
- Hawkins, A.B. and McConnell, B.J. (1992). Sensitivity of sandstone strength and deformability to changes in moisture content. **Quarterly Journal of Engineering Geology**. 25: 115-130.
- He, J., Li, S., Li, X., Wang, X., and Guo, J. (2015). Study on the correlations between abrasiveness and mechanical properties of rocks combining with the microstructure characteristic. **Rock Mechanics and Rock Engineering**. 49(7): 2945-2951.
- Ho, Y. K., So, S. T. C., Lau, T. M. F., and Kwok, R. C. M. (2016). Abrasiveness of common rocks in Hong Kong. **Rock Mechanics and Rock Engineering**. 49(7): 2953-2958.
- Jacobs, N. and Hagan, P. (2009). The effect of stylus hardness and some test parameters on CERCHAR abrasivity index. In **Proceedings of the 43rd U.S. Rock Mechanics Symposium & 4th U.S. Canada Rock Mechanics Symposium**. Asheville, North Carolina.
- Jaeger, J. C., Cook, N. G. W., and Zimmerman, R. W. (2007). **Fundamentals of Rock Mechanics**. Blackweel: Oxford. 475p.

- Khamrat, S., Archeeploha, S., and Fuenkajorn, K. (2016). Pore pressure effects on strength and elasticity of ornamental stones. **Scienceasia**. 42: 121-135.
- Khandelwal, M. and Ranjith, P. G. (2010). Correlating index properties of rocks with P-wave measurements. **Journal of Applied Geophysics**. 71(1): 1-5.
- Ko, T. Y., Kim, T. K., Son, Y., and Jeon, S. (2016). Effect of geomechanical properties on CERCHAR abrasivity index (CAI) and its application to TBM tunnelling. **Tunnelling and Underground Space Technology**. 57: 99-111.
- Kohmura, Y. and Inada, Y. (2006). The effect of the loading rate on stress-strain characteristics of tuff. **Journal of the Society of Materials Science Japan**. 55(3): 323-328.
- Lassnig, K., Latal, C., and Klima, K. (2008). Impact of grain size on the Cerchar abrasiveness test. **Geomechanics and Tunnelling**. 1(1): 71-76.
- Li, Y. and Xia, C. (2000). Time-dependent tests on intact rocks in uniaxial compression. **International Journal of Rock Mechanics and Mining Sciences**. 37(3): 467-475.
- Majeed, Y. and Abu Bakar, M. Z. (2016). Statistical evaluation of CERCHAR abrasivity index (CAI) measurement methods and dependence on petrographic and mechanical properties of selected rocks of Pakistan. **Bulletin of Engineering Geology and the Environment**. 75(3): 1341-1360.
- Mammen, J., Saydam, S., and Hagan, P. (2009). A study on the effect of moisture content on rock cutting performance. In **Proceedings of the 2009 Coal Operators' Conference** (pp. 340-347). Australia.

- Michalakopoulos, T. N., Anagnostou, V. G., Bassanou, M. E., and Panagiotou, G. N. (2006). The influence of steel styli hardness on the CERCHAR abrasiveness index value. **International Journal of Rock Mechanics and Mining Sciences**. 43: 321-327.
- Moradizadeh, M., Cheshomi, A., Ghafoori, M., and TrighAzali, S. (2016). Correlation of equivalent quartz content, Slake durability index and I_{s50} with CERCHAR abrasiveness index for different types of rock. **International Journal of Rock Mechanics and Mining Sciences**. 86: 42-47.
- Ozdogan, M. V., Deliormanli, A. H., and Yenice, H. (2018). The correlations between the CERCHAR abrasivity index and the geomechanical properties of building stones. **Arabian Journal of Geosciences**. 11(604): 1-13.
- Plinninger, R. J., Kasling, H., and Thuro, K. (2004). Wear prediction in hardrock excavation using the CERCHAR abrasiveness index (CAI). In **Proceedings of the EUROCK 2004 & 53rd Geomechanics Colloquium**. Salzburg, Austria.
- Plinninger, R., Käsling, H., Thuro, K., and Spaun, G. (2003). Testing conditions and geomechanical properties influencing the CERCHAR abrasiveness index (CAI) value. **International Journal of Rock Mechanics and Mining Sciences**. 40(2): 259-263.
- Prieto, L. (2012). The CERCHAR abrasivity index's applicability to dredging rock. In **Proceedings of the Western Dredging Association (WEDA XXXII) Technical Conference and Texas A and M University (TAMU 43) Dredging Seminar** (pp.212-219). San Antonio, Texas.
- Ray, S. K., Sarkar, M., and Singh, T. N. (1999). Effect of cyclic loading and strain rate on the mechanical behavior of sandstone. **International Journal of Rock Mechanics and Mining Sciences**. 36(4): 543-549.

- Rostami, J., Ghasemi, A., Gharahbagh, E.A, Dogruoz, C., and Dahl, F. (2014). Study of dominant factors affecting CERCHAR abrasivity index. **Rock Mechanics and Rock Engineering**. 47(5): 1905-1919.
- Rostami, J., Ozdemir, L., Bruland, A., and Dahl, F. (2005). Review of issues related to CERCHAR abrasivity testing and their implications on geotechnical investigations and cutter cost estimates. In **Proceedings of the Rapid Excavation & Tunneling Conference** (pp. 738-751). Seattle, Washington.
- Stanford, J. and Hagan, P. (2009). An assessment of the impact of stylus metallurgy on CERCHAR abrasiveness index. In **Proceedings of the 2009 Coal Operators' Conference** (pp. 348-355). Australia.
- Suana, M. and Peters, T. (1982). The CERCHAR abrasivity index and its relation to rock mineralogy and petrography. **Rock Mechanics and Rock Engineering**. 15(1): 1-8.
- Thuro, K. (1997). Drillability prediction: geological influences in hard rock drill and blast tunnelling. **Geologische Rundschau**. 86(2): 426-438.
- Thuro, K. and Käsling, H. (2009). Classification of the abrasiveness of soil and rock. **Geomechanics and Tunneling**. 2(2): 179-188.
- Torrijo, F. J., Garzón-Roca, J., Company, J., and Cobos, G. (2019). Estimation of CERCHAR abrasivity index of andesitic rocks in Ecuador from chemical compounds and petrographical properties using regression analyses. **Bulletin of Engineering Geology and the Environment**. 78(4): 2331-2344.
- Vasarhelyi, B. (2003). Some observations regarding the strength and deformability of sandstones in case of dry and saturated conditions. **Bulletin of Engineering Geology and the Environment**. 62: 245-249.

- Vasarhelyi, B. and Van, P. (2006). Influence of water content on the strength of rock. **Engineering Geology**. 84: 70-74.
- West, G. (1989). Rock abrasiveness testing for tunnelling. **International Journal of Rock Mechanics and Mining Sciences & Geomechanics Abstracts**. 26(2): 151-160.
- Whittaker, A., Bott, M. H. P., and Waghorn, G. D. (1992). Stresses and plate boundary forces associated with subduction plate margins. **Journal of Geophysical Research: Solid Earth**. 97(B8): 11933-11944.
- Yaralı, O. and Duru, H. (2016). Investigation into effect of scratch length and surface condition on CERCHAR abrasivity index. **Tunnelling and Underground Space Technology**. 60: 111-120.
- Yaralı, O., Yaşar, E., Bacak, G., and Ranjith, P. G. (2008). A study of rock abrasivity and tool wear in coal measures rocks. **International Journal of Coal Geology**. 74(1): 53-66.
- Zhang, G., Konietzky, H., and Frühwirth, T. (2020). Investigation of scratching specific energy in the Cerchar abrasivity test and its application for evaluating rock-tool interaction and efficiency of rock cutting. **Wear**. vol. 448-449.



APENDIX A

CERCHAR STYLUS PINS AFTER TESTING

มหาวิทยาลัยเทคโนโลยีสุรนารี

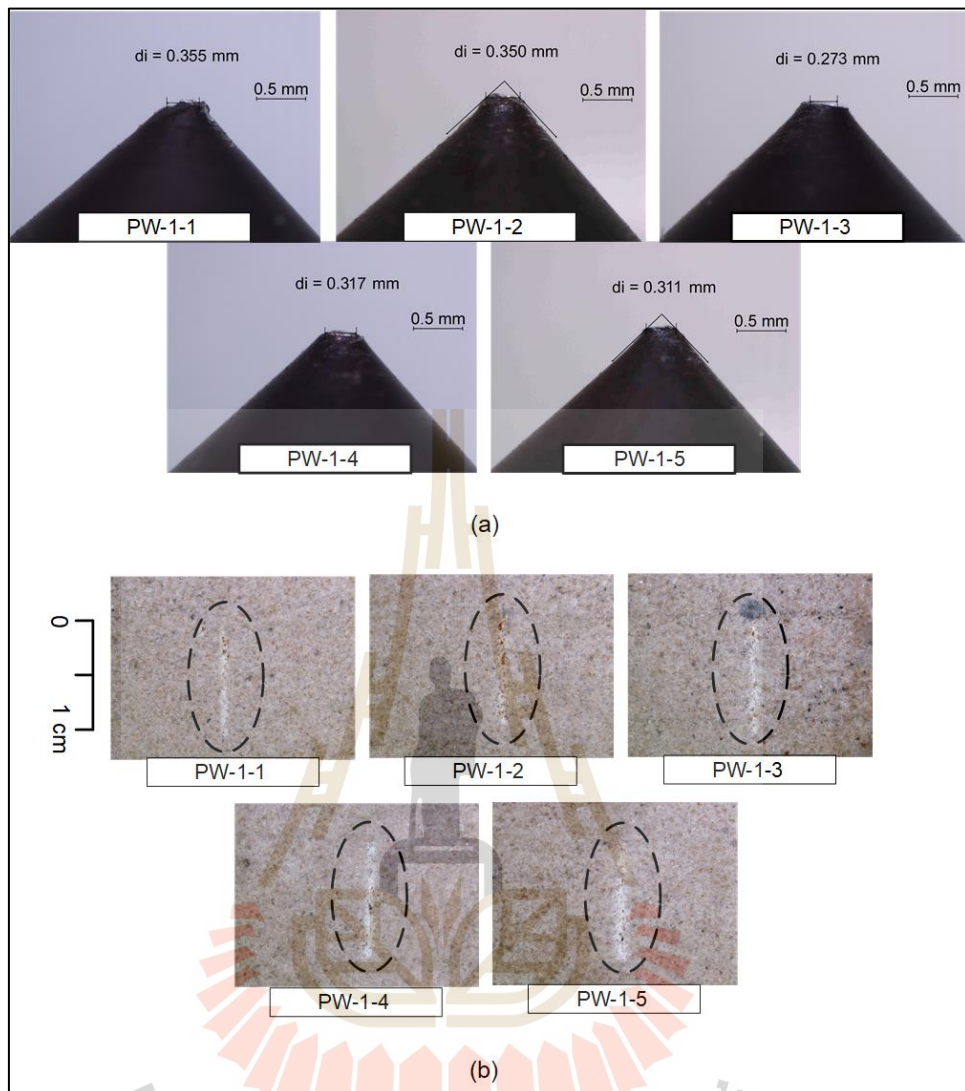


Figure A.1 CERCHAR stylus pins after testing on Phra Wihan sandstone specimens (a) and their corresponding groove images (b) under scratching rate of 1 mm/s and dry conditions.

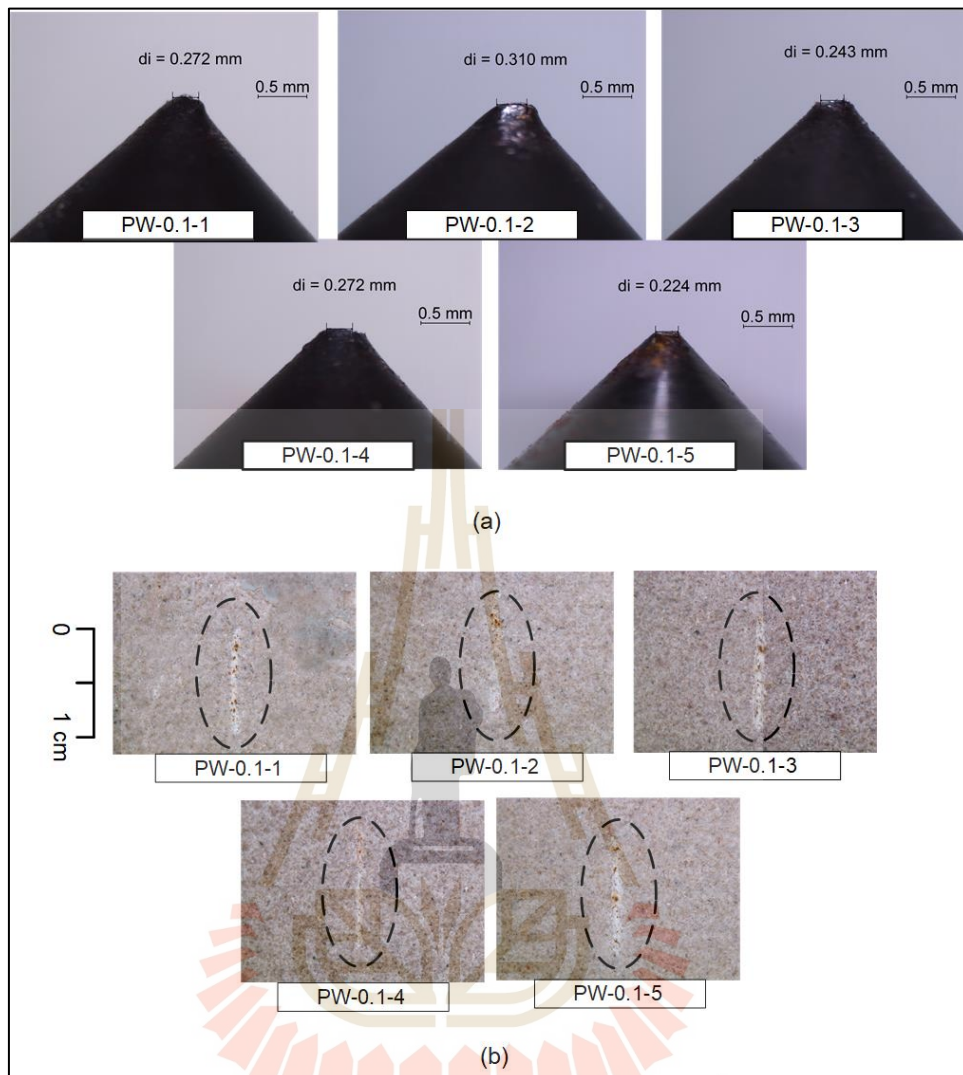


Figure A.2 CERCHAR stylus pins after testing on Phra Wihan sandstone specimens (a) and their corresponding groove images (b) under scratching rate of 0.1 mm/s and dry conditions.

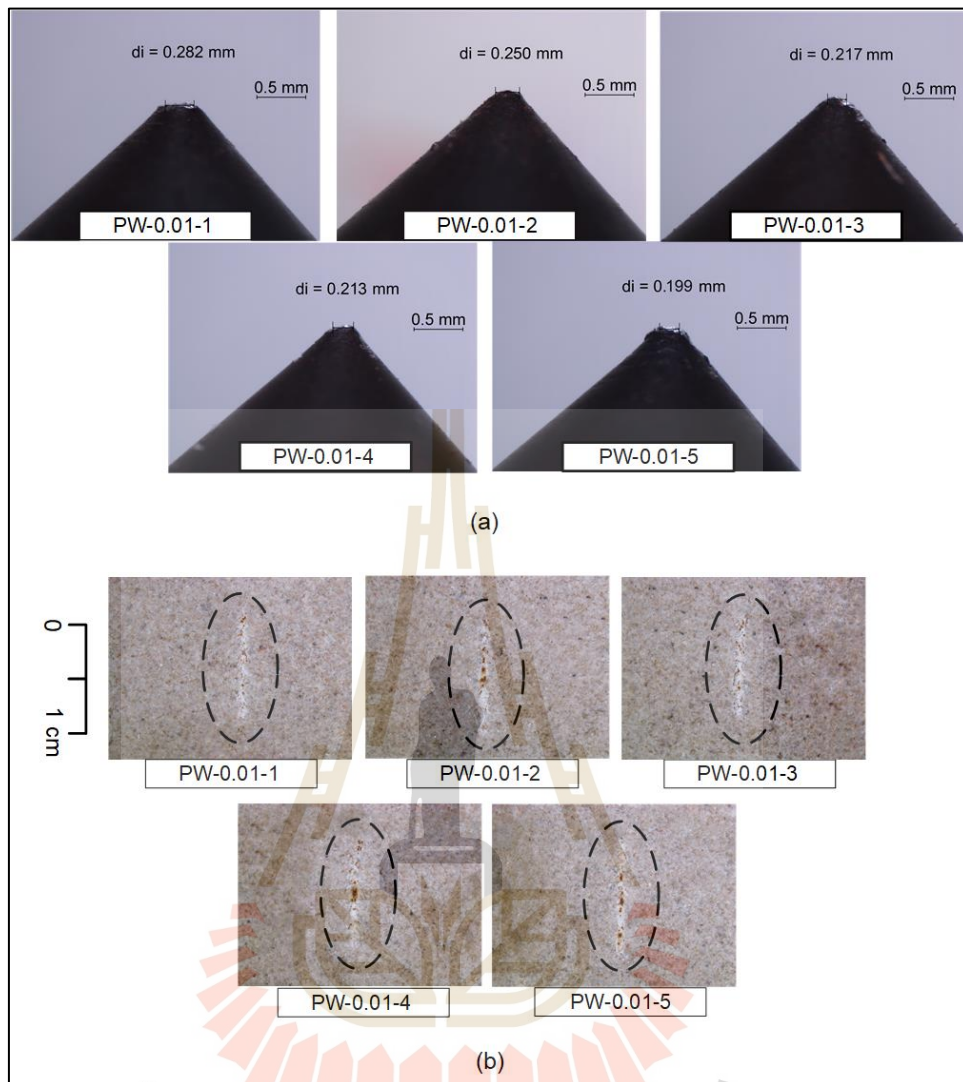


Figure A.3 CERCHAR stylus pins after testing on Phra Wihan sandstone specimens (a) and their corresponding groove images (b) under scratching rate of 0.01 mm/s and dry conditions.

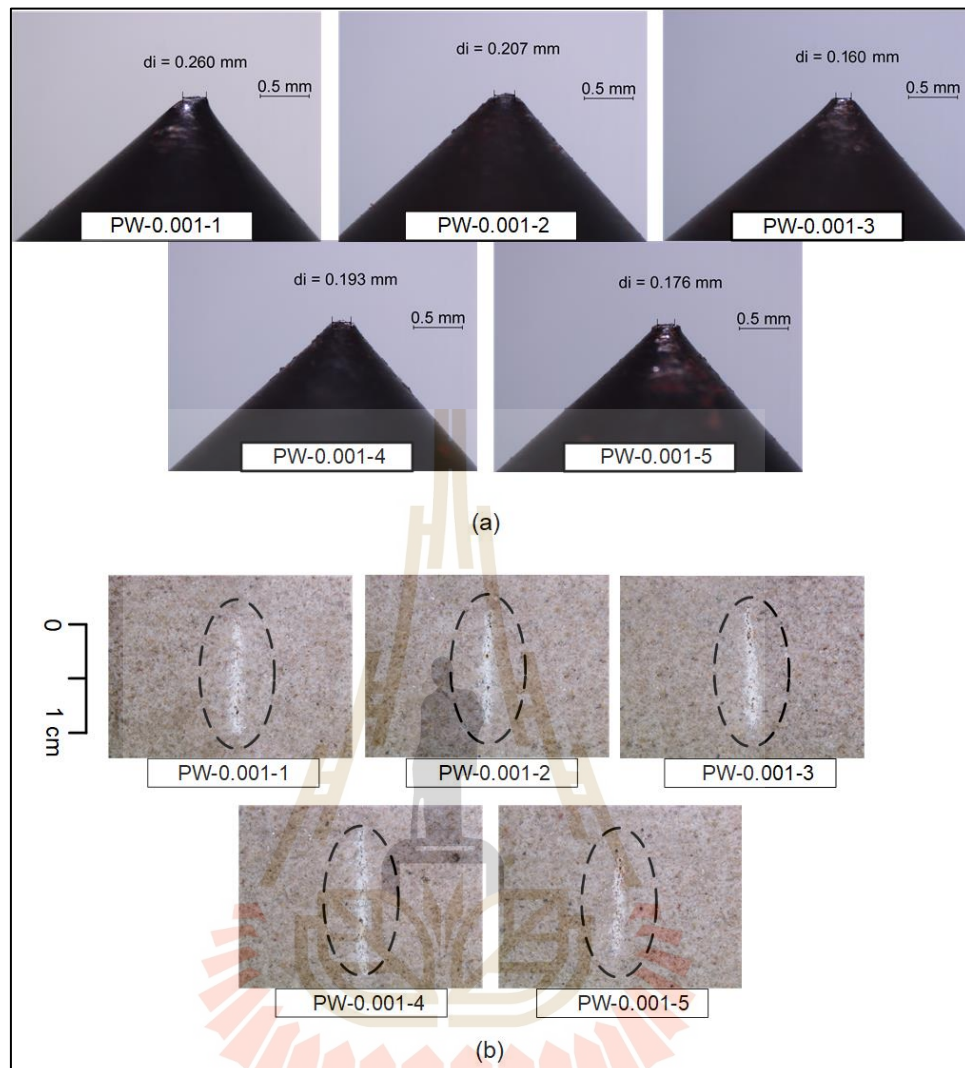


Figure A.4 CERCHAR stylus pins after testing on Phra Wihan sandstone specimens (a) and their corresponding groove images (b) under scratching rate of 0.001 mm/s and dry conditions.

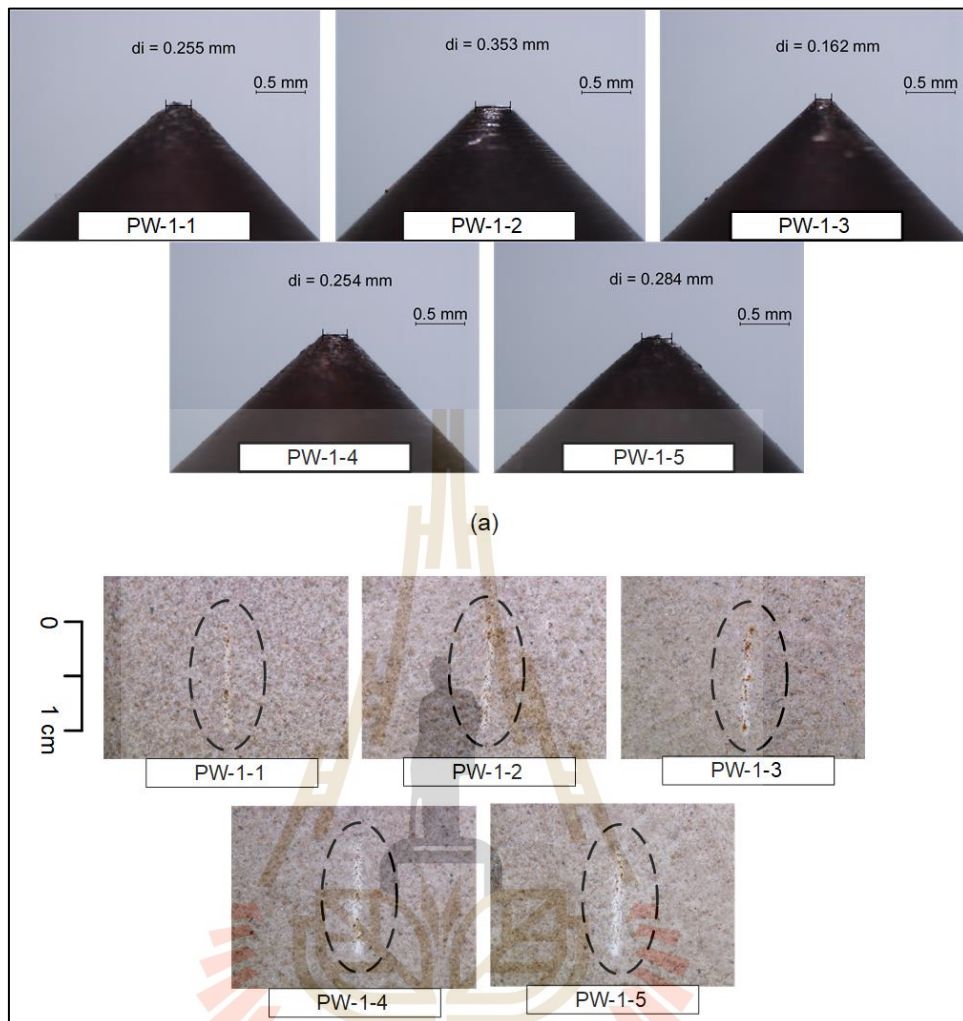


Figure A.5 CERCHAR stylus pins after testing on Phra Wihan sandstone specimens (a) and their corresponding groove images (b) under scratching rate of 1 mm/s and saturated conditions.

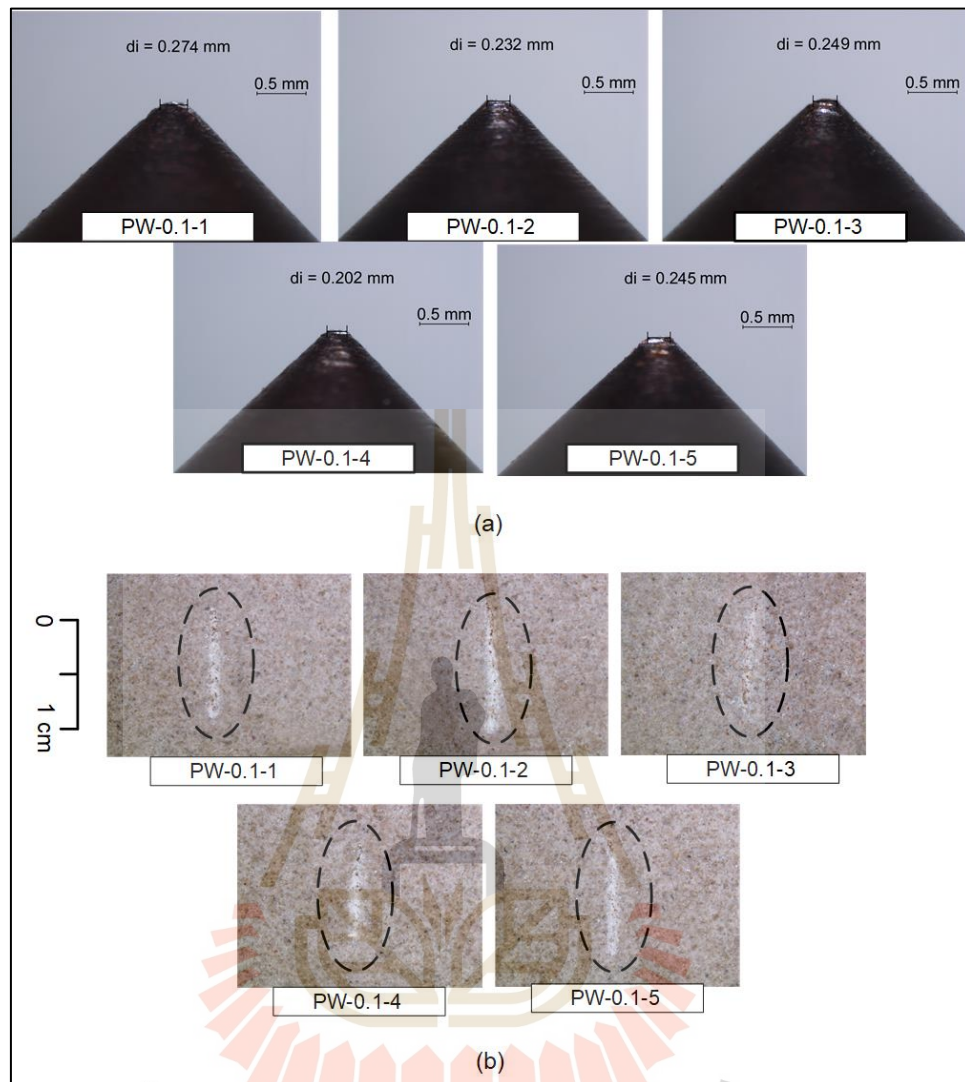


Figure A.6 CERCHAR stylus pins after testing on Phra Wihan sandstone specimens (a) and their corresponding groove images (b) under scratching rate of 0.1 mm/s and saturated conditions.

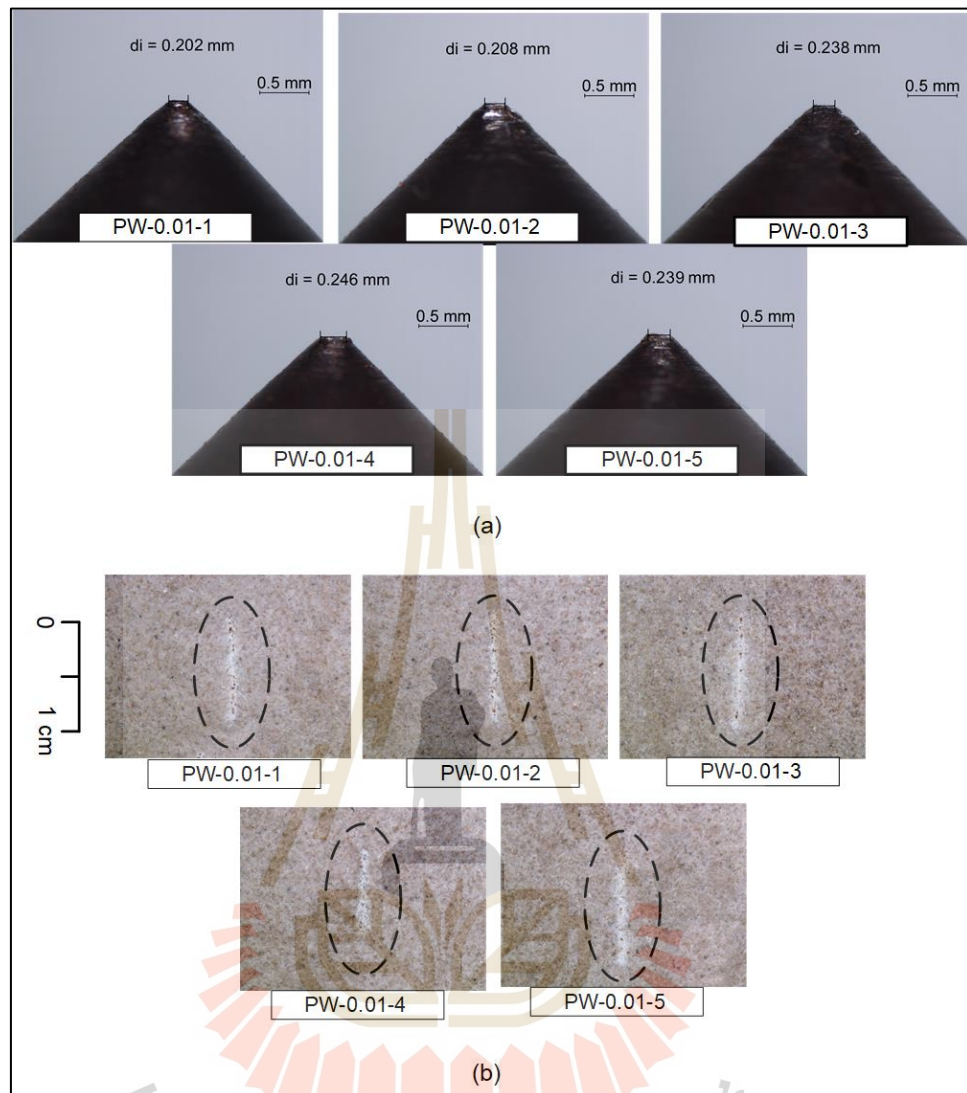


Figure A.7 CERCHAR stylus pins after testing on Phra Wihan sandstone specimens (a) and their corresponding groove images (b) under scratching rate of 0.01 mm/s and saturated conditions.

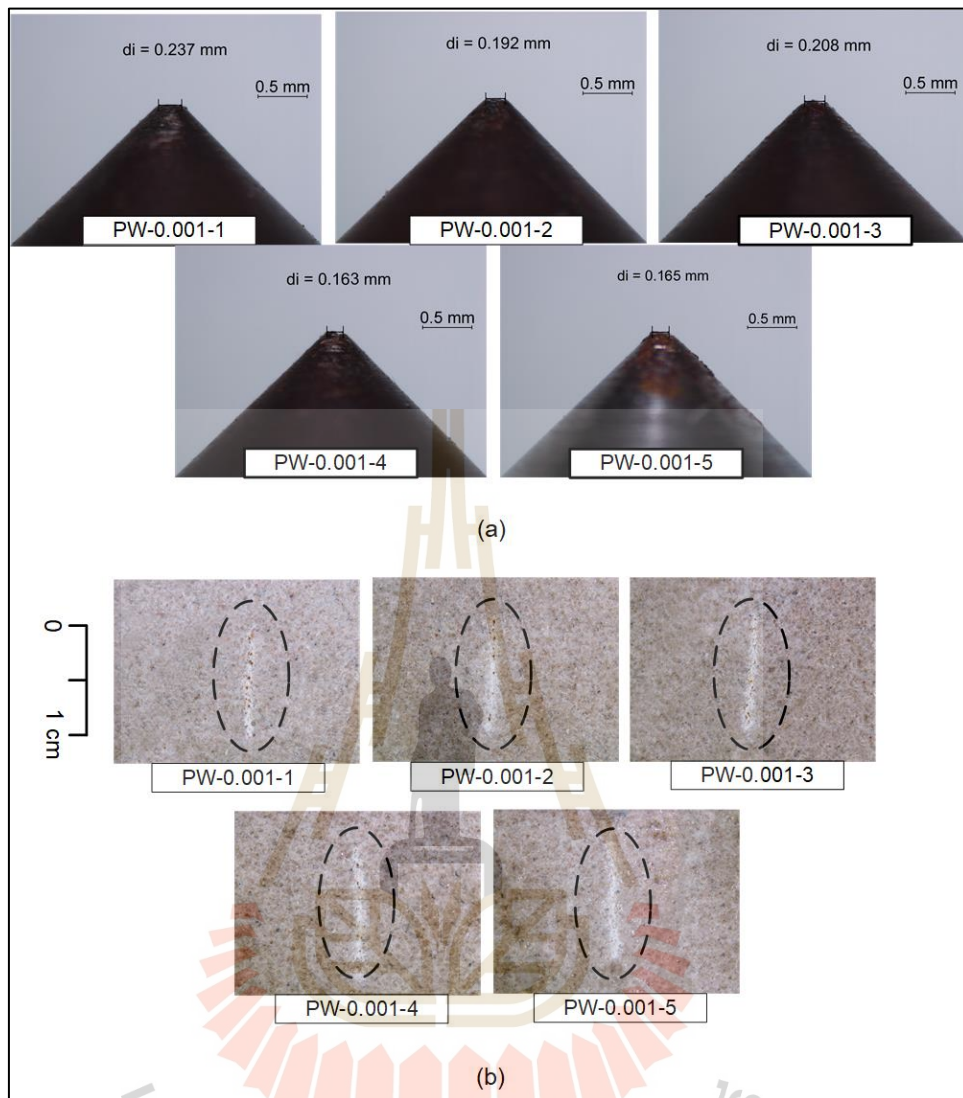


Figure A.8 CERCHAR stylus pins after testing on Phra Wihan sandstone specimens (a) and their corresponding groove images (b) under scratching rate of 0.001 mm/s and saturated conditions.

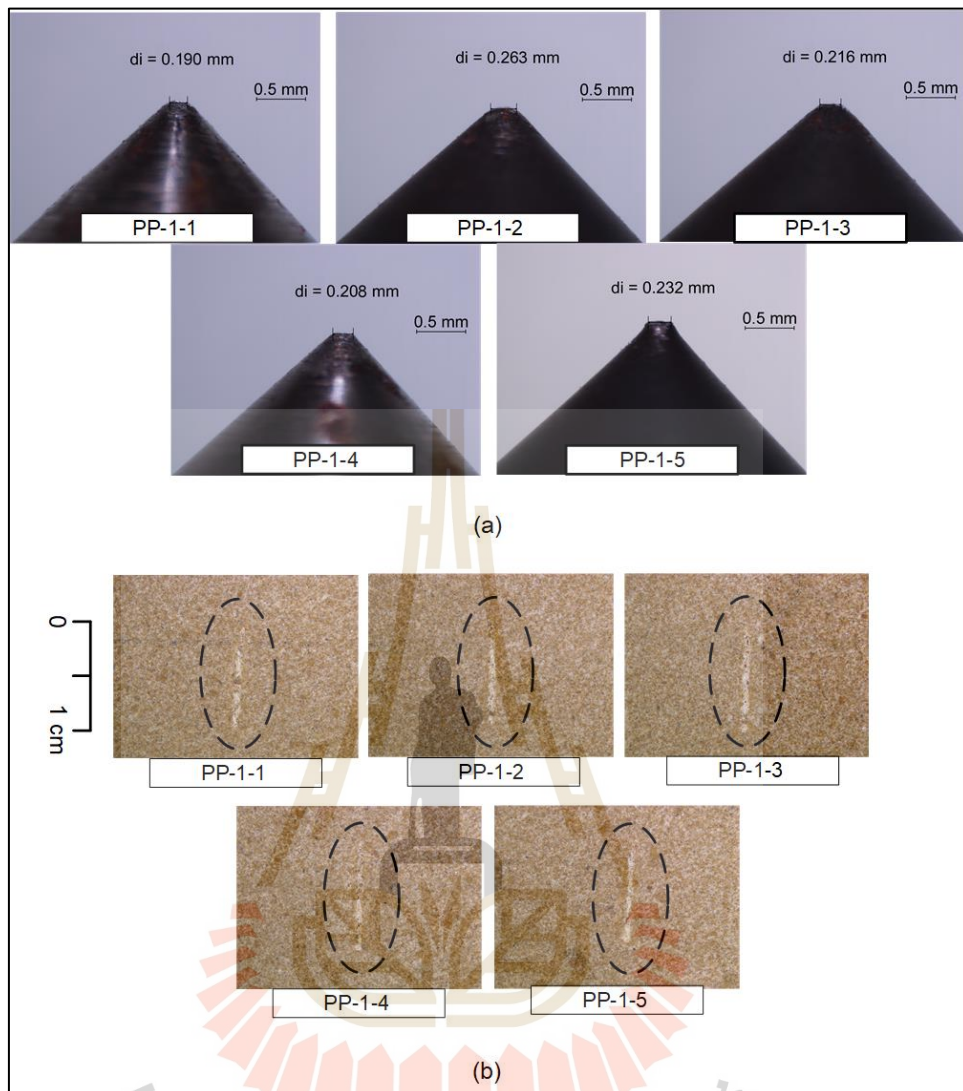


Figure A.9 CERCHAR stylus pins after testing on Phu Phan sandstone specimens (a) and their corresponding groove images (b) under scratching rate of 1 mm/s and dry conditions.

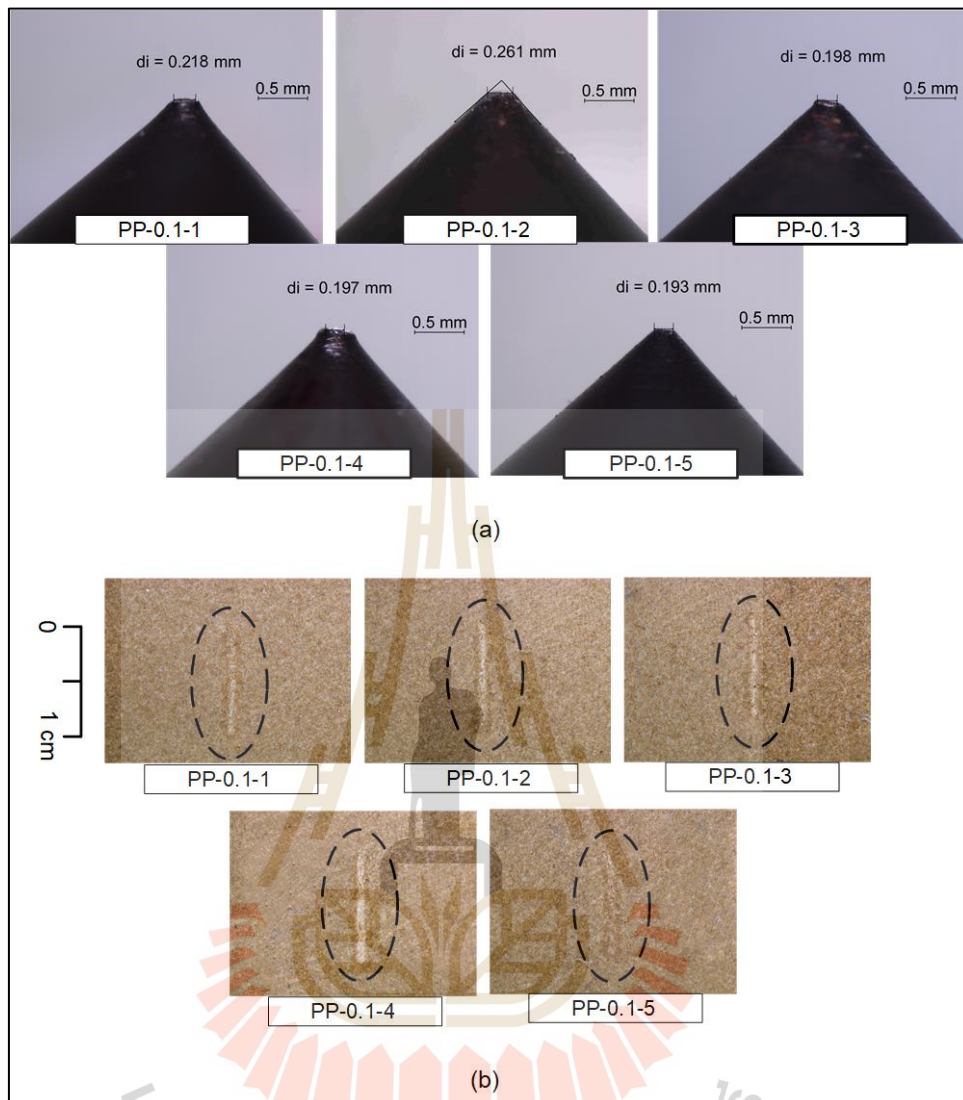


Figure A.10 CERCHAR stylus pins after testing on Phu Phan sandstone specimens (a) and their corresponding groove images (b) under scratching rate of 0.1 mm/s and dry conditions.

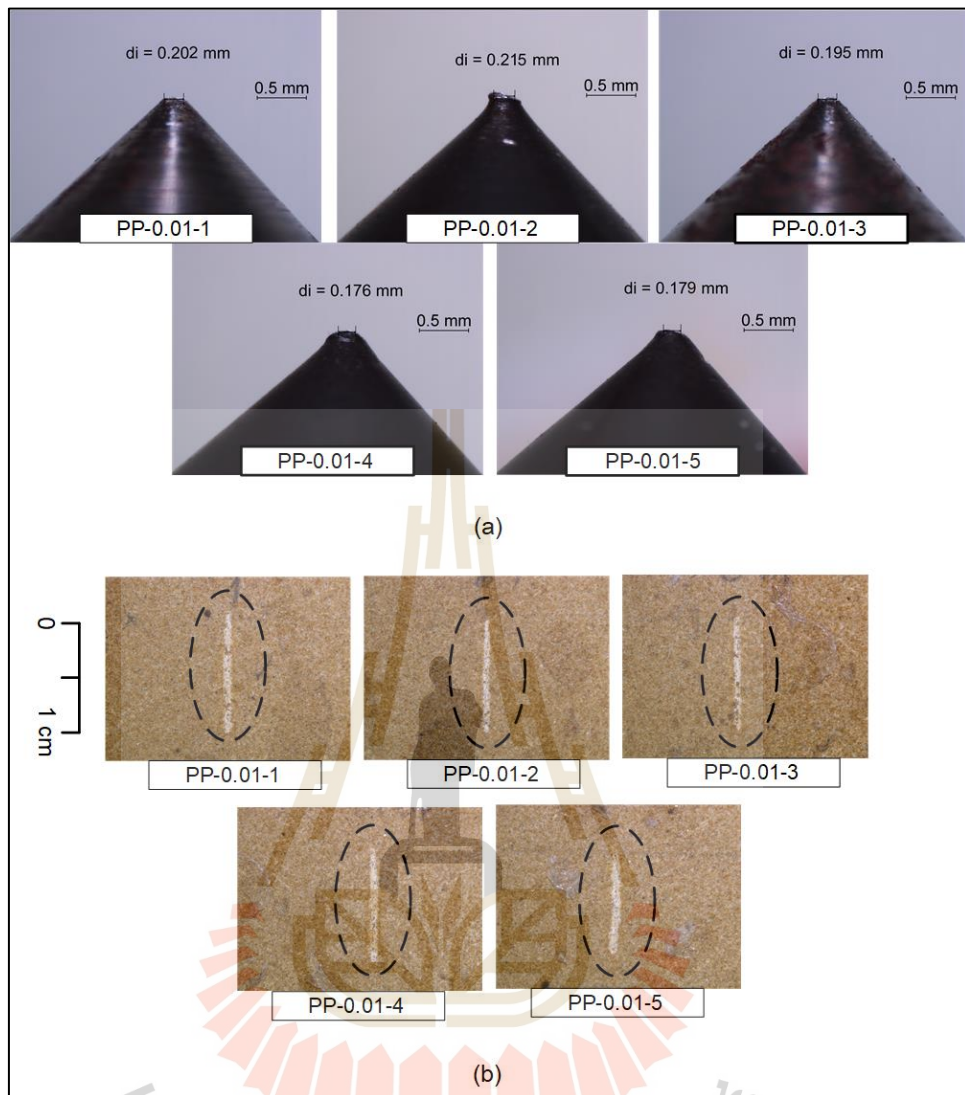


Figure A.11 CERCHAR stylus pins after testing on Phu Phan sandstone specimens (a) and their corresponding groove images (b) under scratching rate of 0.01 mm/s and dry conditions.

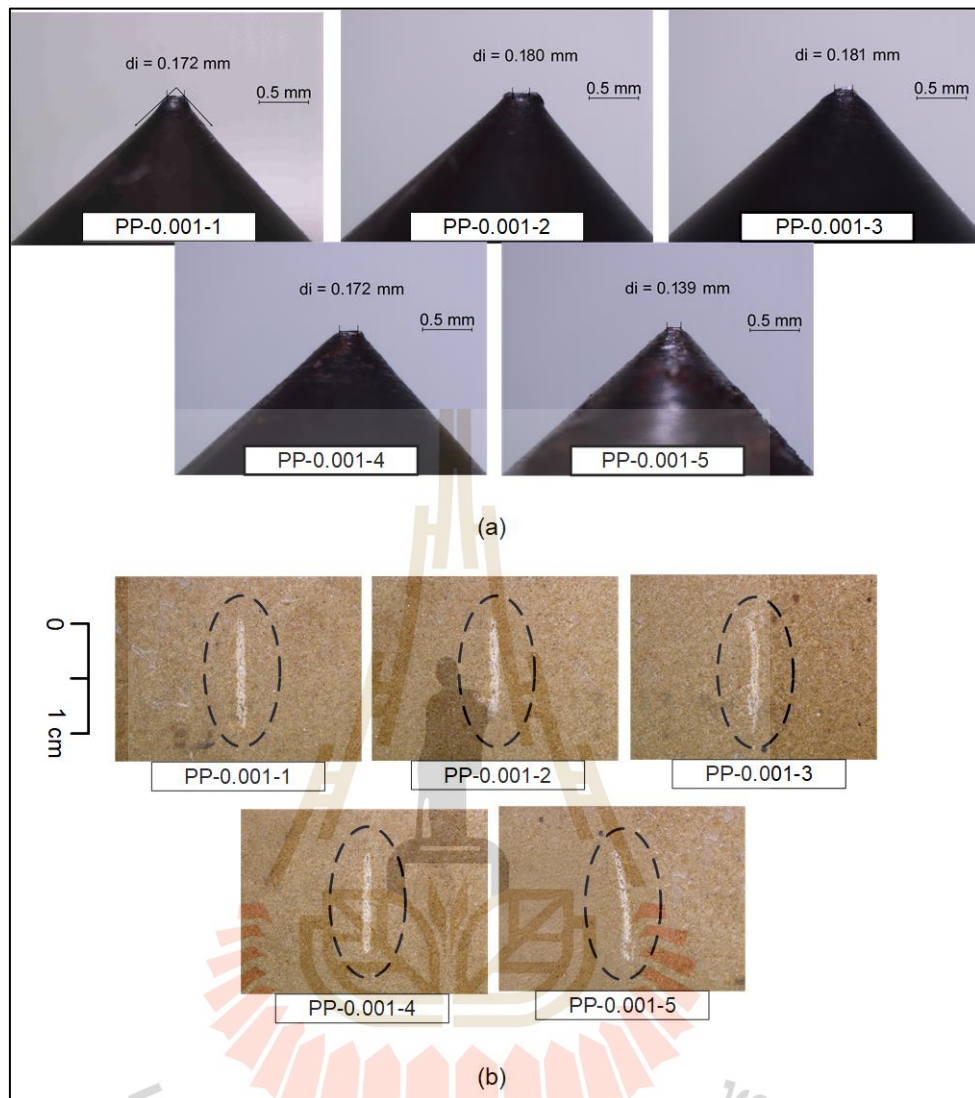


Figure A.12 CERCHAR stylus pins after testing on Phu Phan sandstone specimens (a) and their corresponding groove images (b) under scratching rate of 0.001 mm/s and dry conditions.

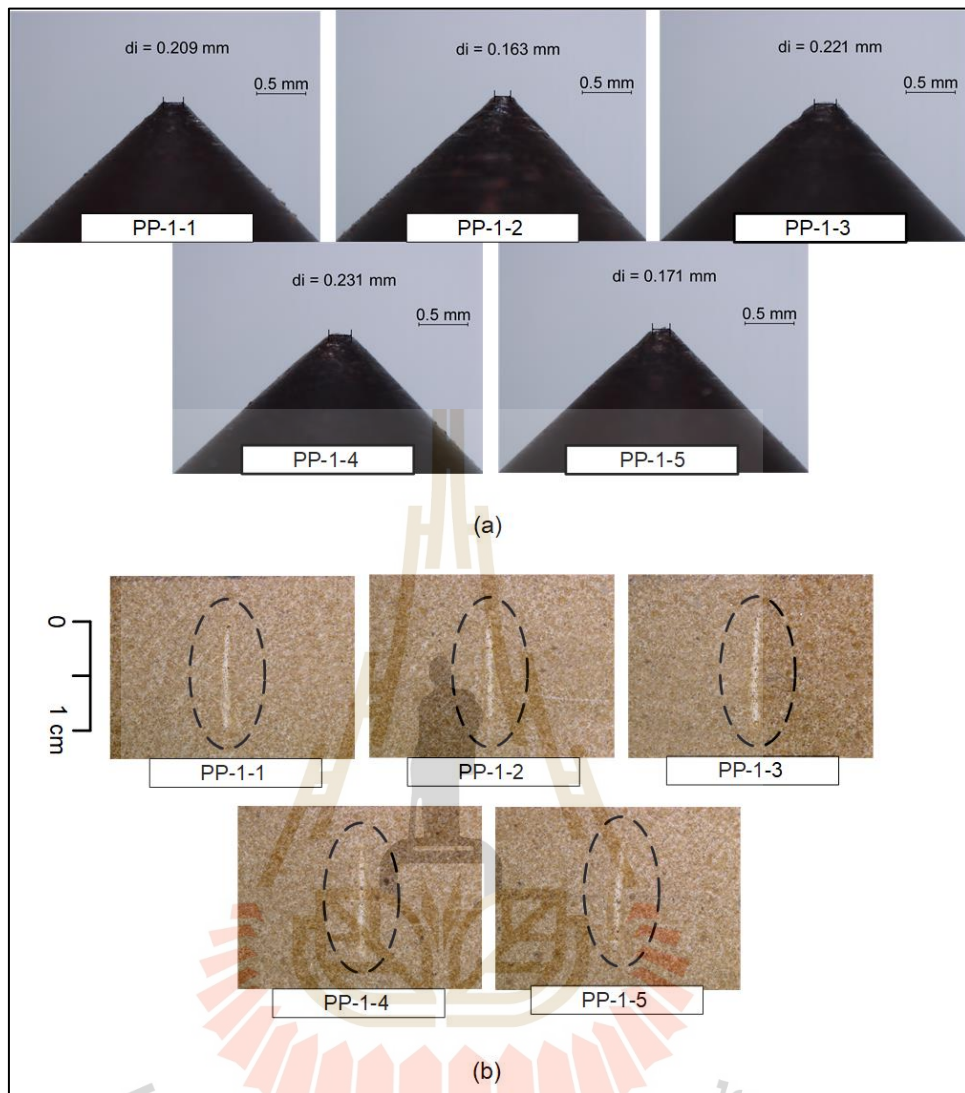


Figure A.13 CERCHAR stylus pins after testing on Phu Phan sandstone specimens (a) and their corresponding groove images (b) under scratching rate of 1 mm/s and saturated conditions.

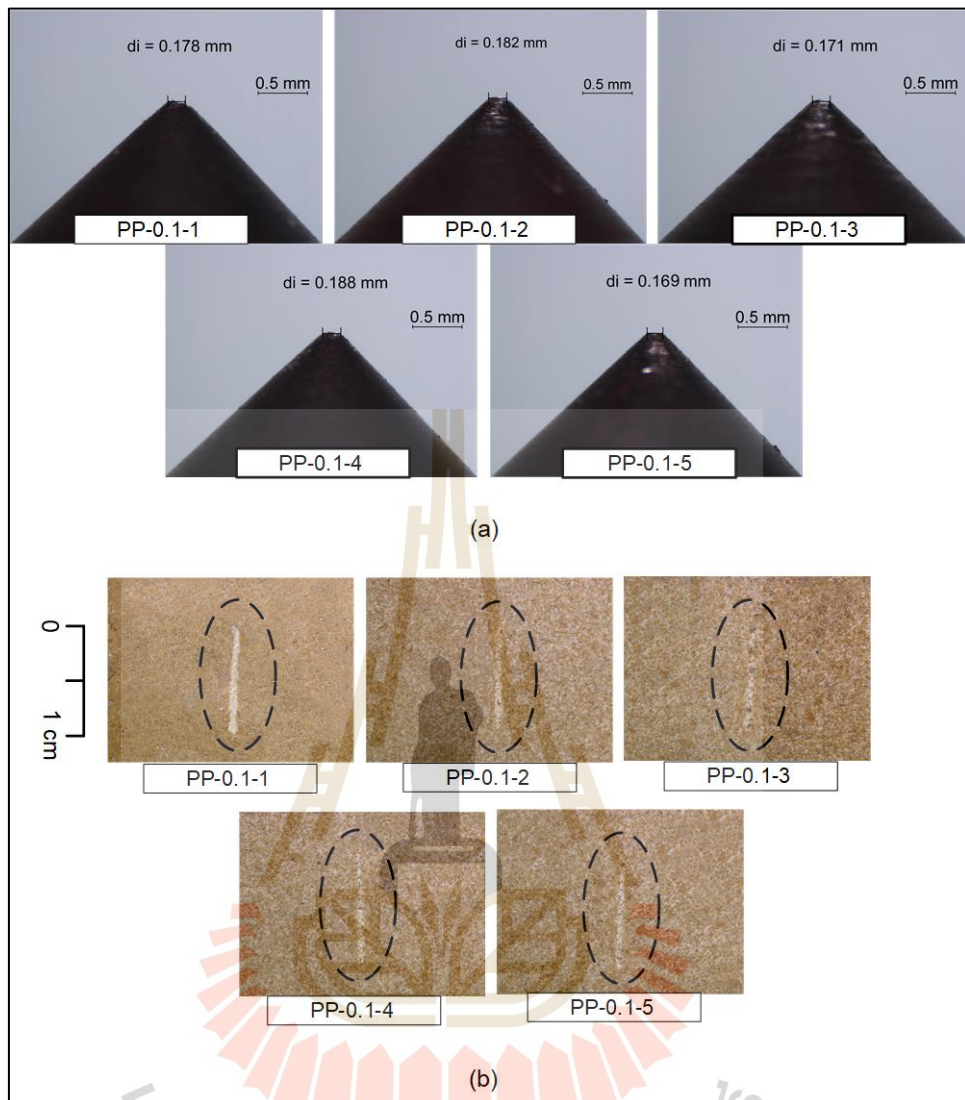


Figure A.14 CERCHAR stylus pins after testing on Phu Phan sandstone specimens (a) and their corresponding groove images (b) under scratching rate of 0.1 mm/s and saturated conditions.

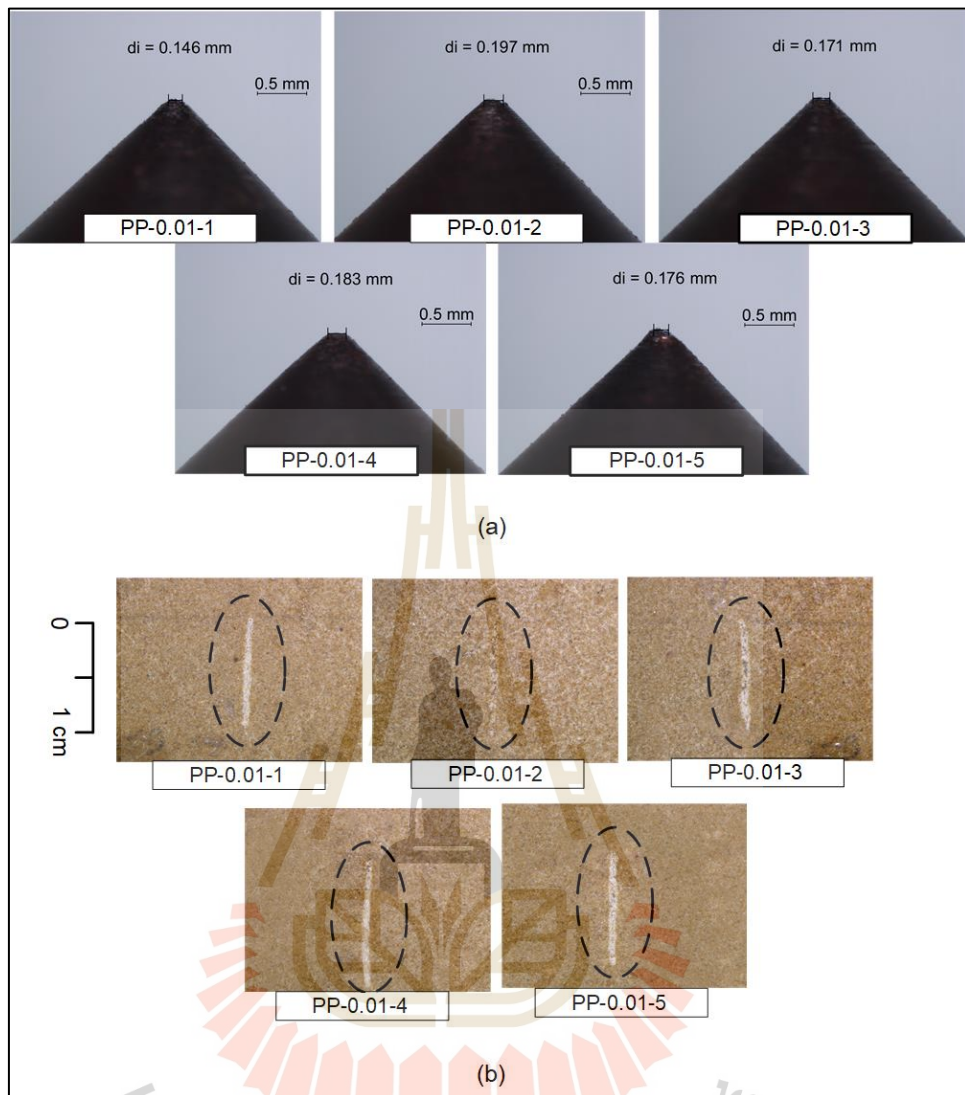


Figure A.15 CERCHAR stylus pins after testing on Phu Phan sandstone specimens (a) and their corresponding groove images (b) under scratching rate of 0.01 mm/s and saturated conditions.

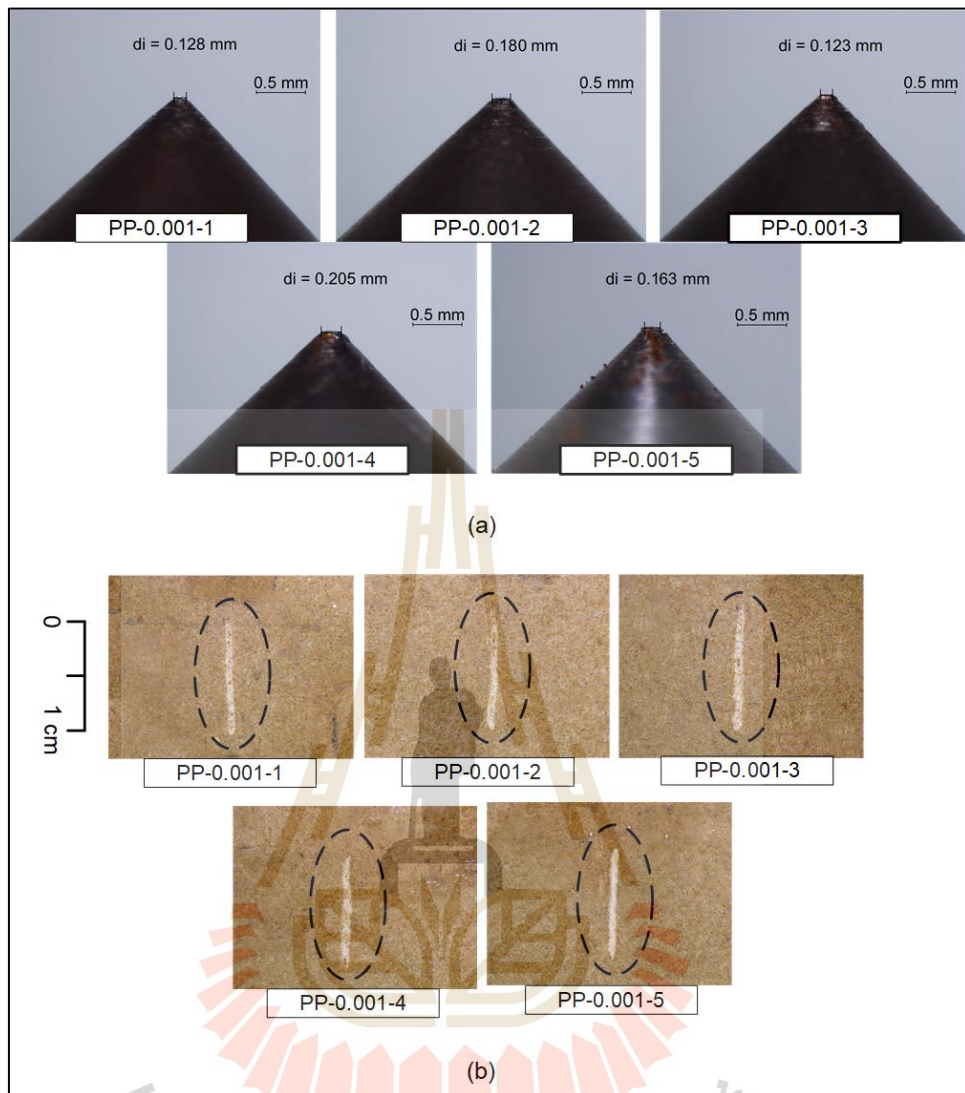


Figure A.16 CERCHAR stylus pins after testing on Phu Phan sandstone specimens (a) and their corresponding groove images (b) under scratching rate of 0.001 mm/s and saturated conditions.

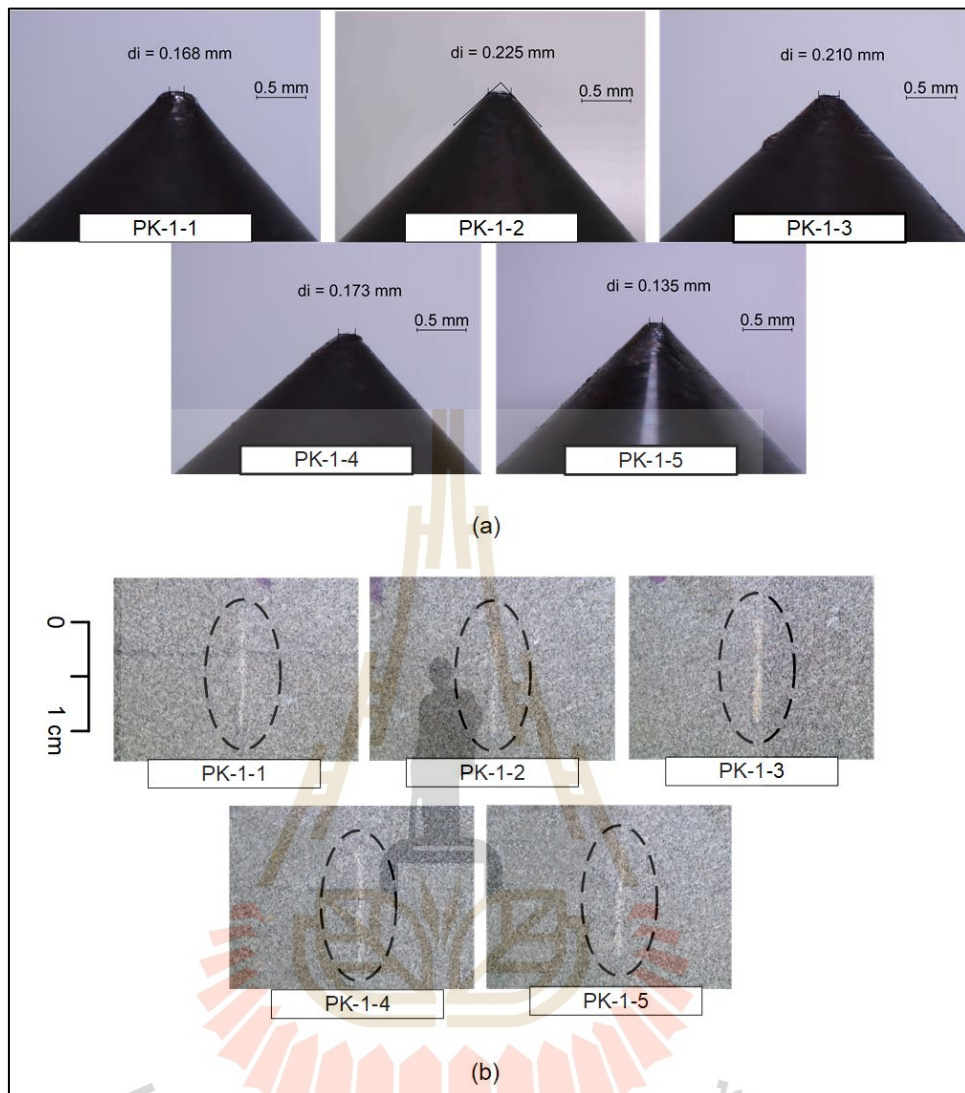


Figure A.17 CERCHAR stylus pins after testing on Phu Kradung sandstone specimens (a) and their corresponding groove images (b) under scratching rate of 1 mm/s and dry conditions.

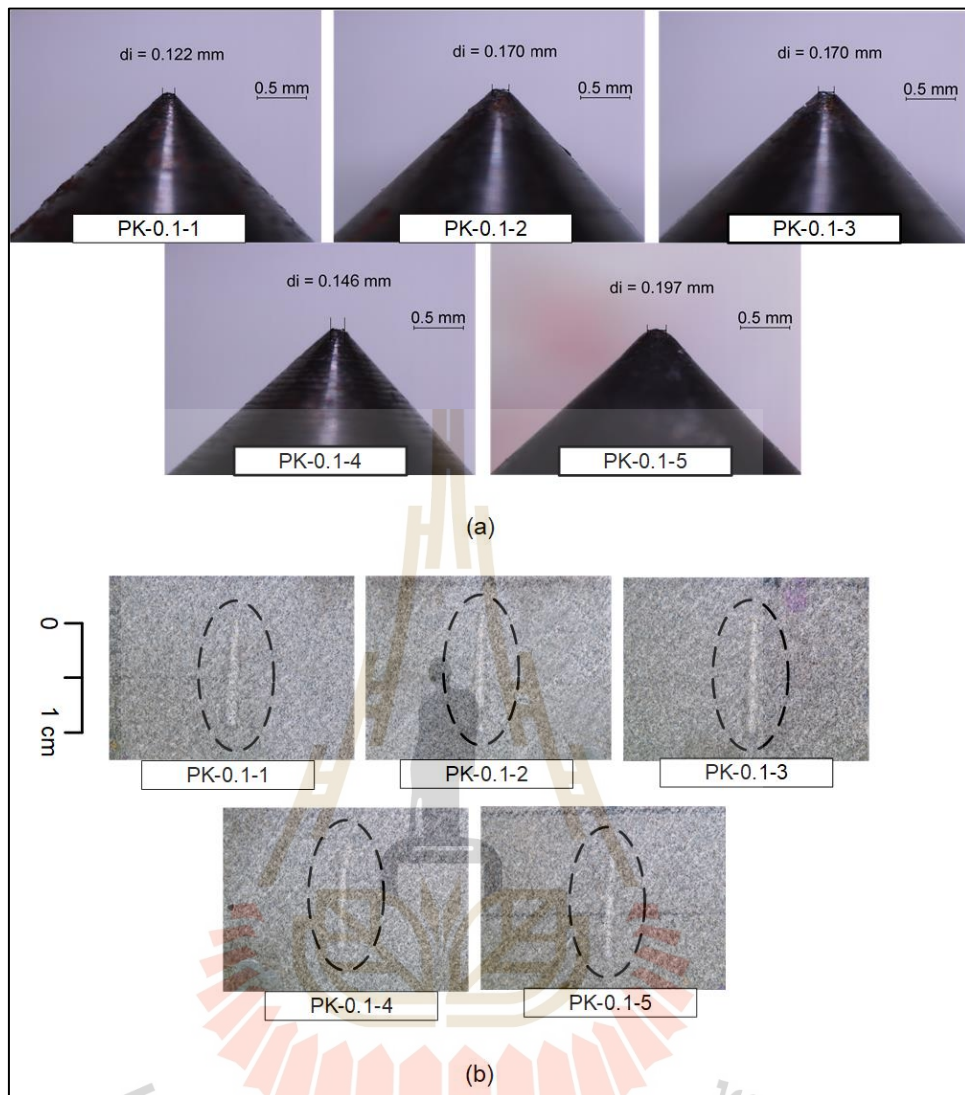


Figure A.18 CERCHAR stylus pins after testing on Phu Kradung sandstone specimens (a) and their corresponding groove images (b) under scratching rate of 0.1 mm/s and dry conditions.

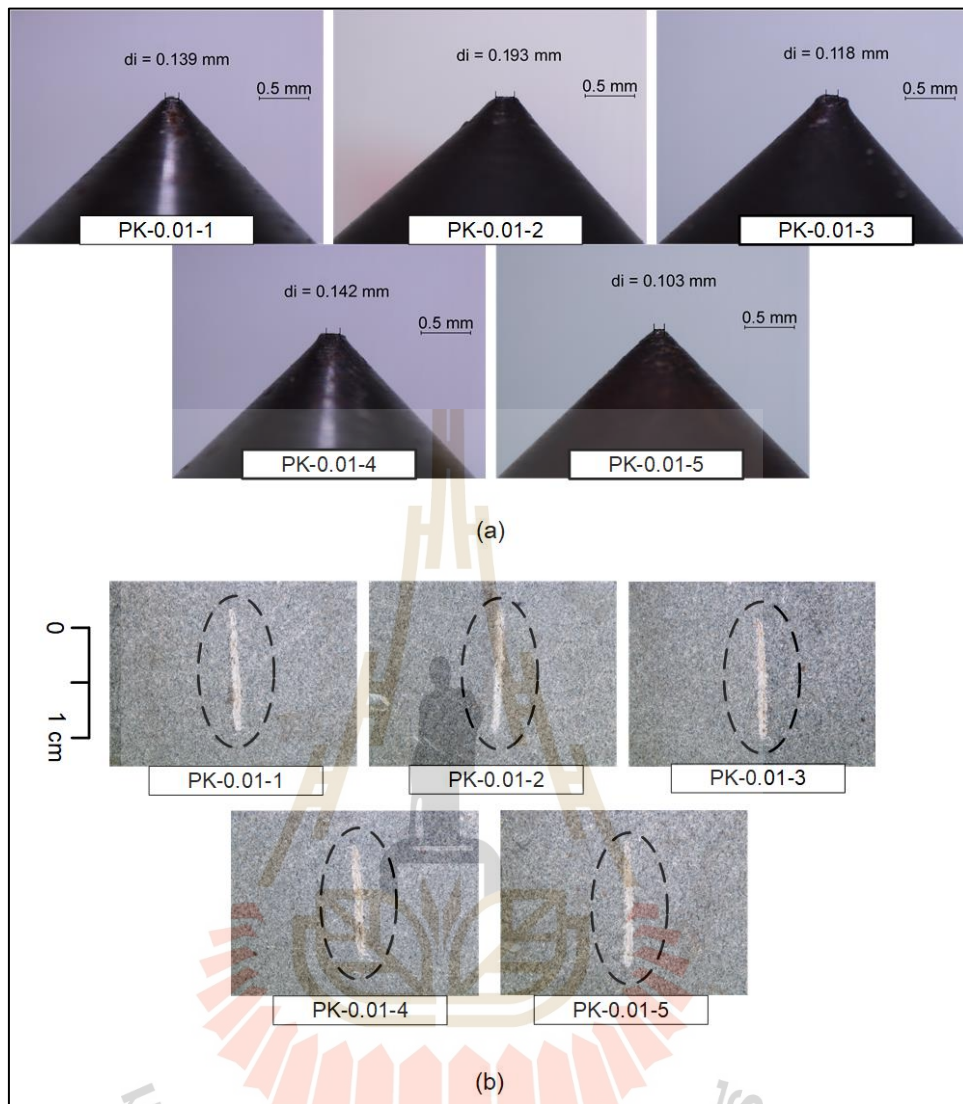


Figure A.19 CERCHAR stylus pins after testing on Phu Kradung sandstone specimens (a) and their corresponding groove images (b) under scratching rate of 0.01 mm/s and dry conditions.

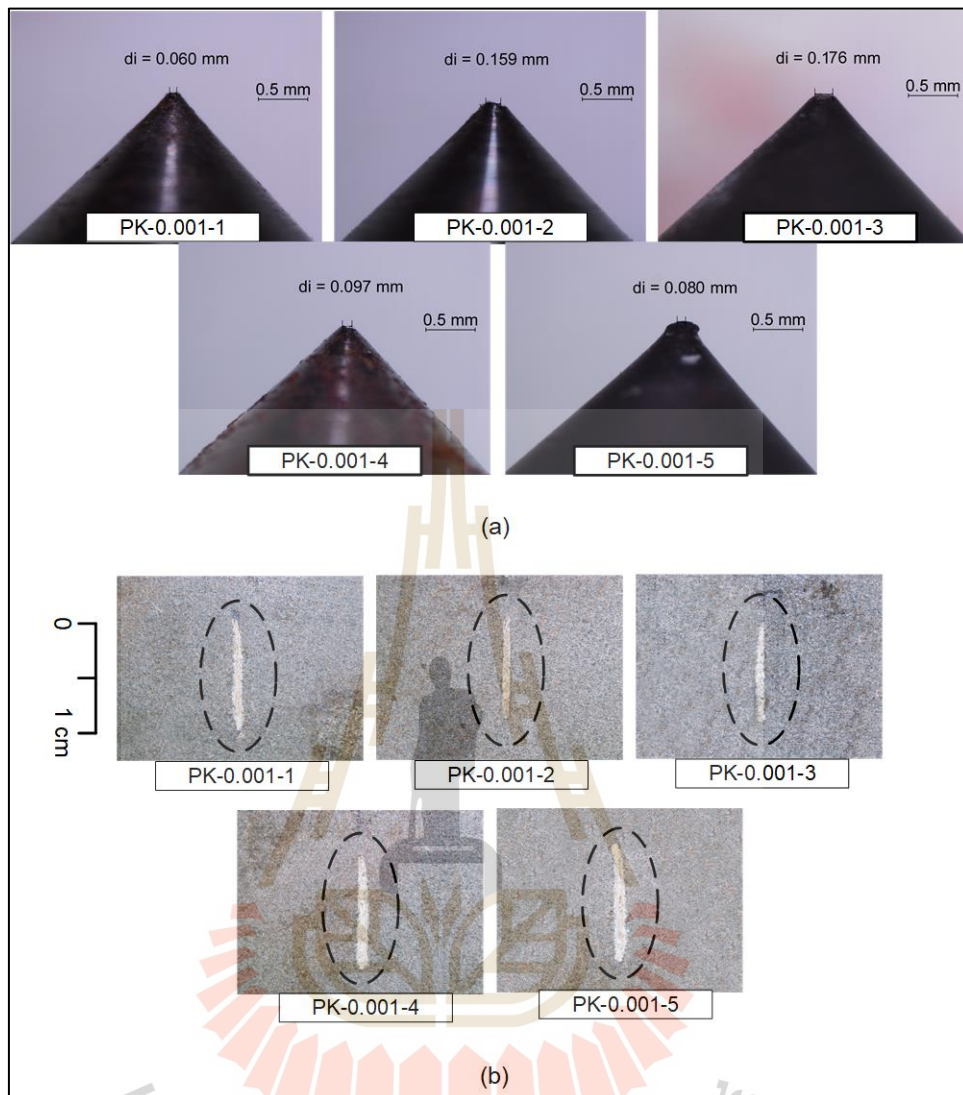


Figure A.20 CERCHAR stylus pins after testing on Phu Kradung sandstone specimens (a) and their corresponding groove images (b) under scratching rate of 0.001 mm/s and dry conditions.

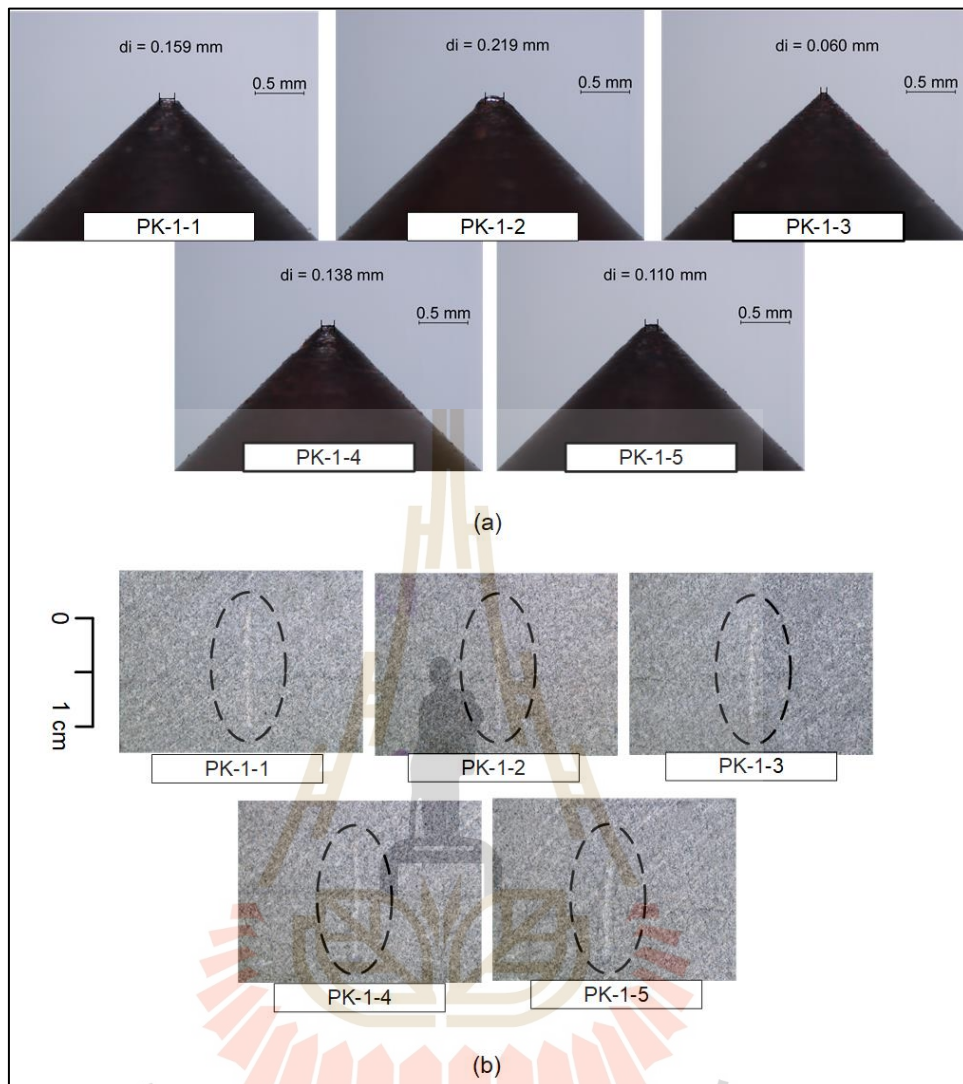


Figure A.21 CERCHAR stylus pins after testing on Phu Kradung sandstone specimens (a) and their corresponding groove images (b) under scratching rate of 1 mm/s and saturated conditions.

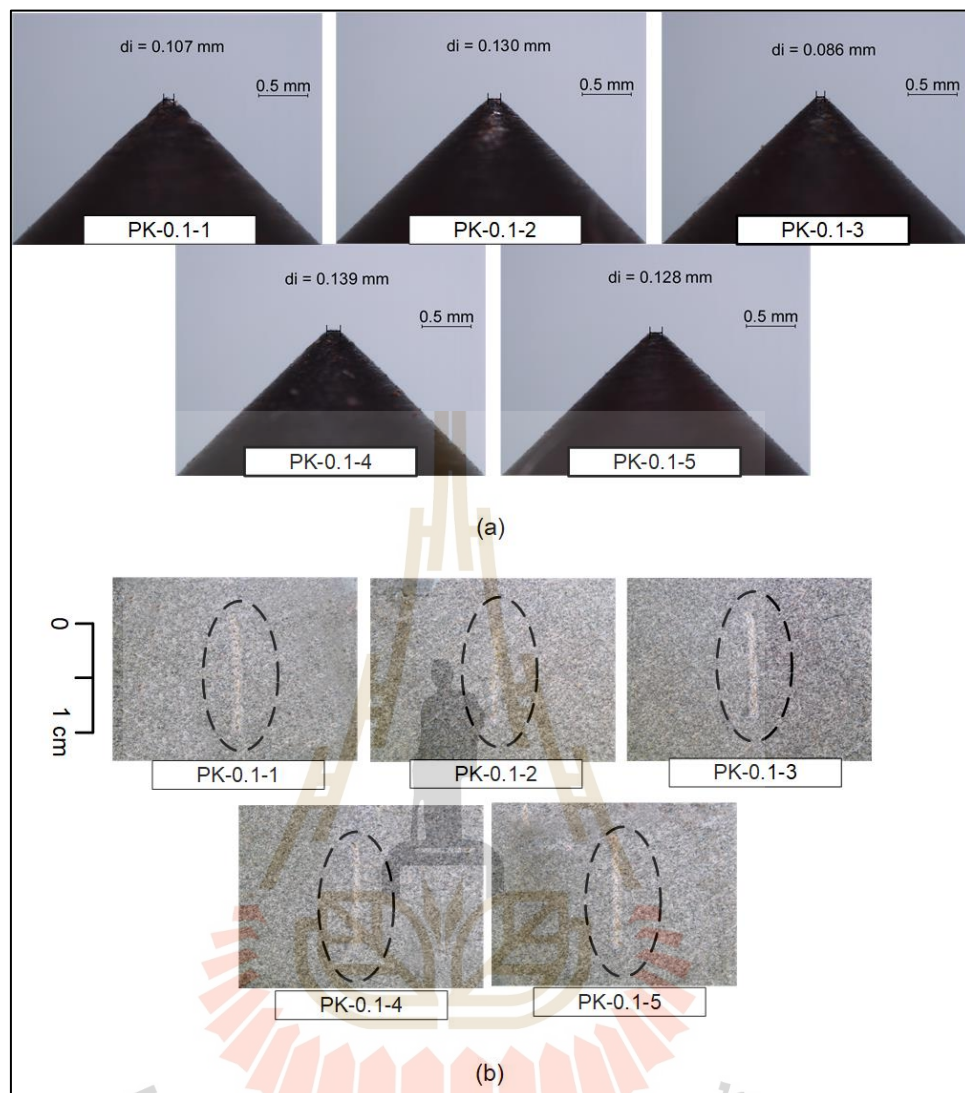


Figure A.22 CERCHAR stylus pins after testing on Phu Kradung sandstone specimens (a) and their corresponding groove images (b) under scratching rate of 0.1 mm/s and saturated conditions.

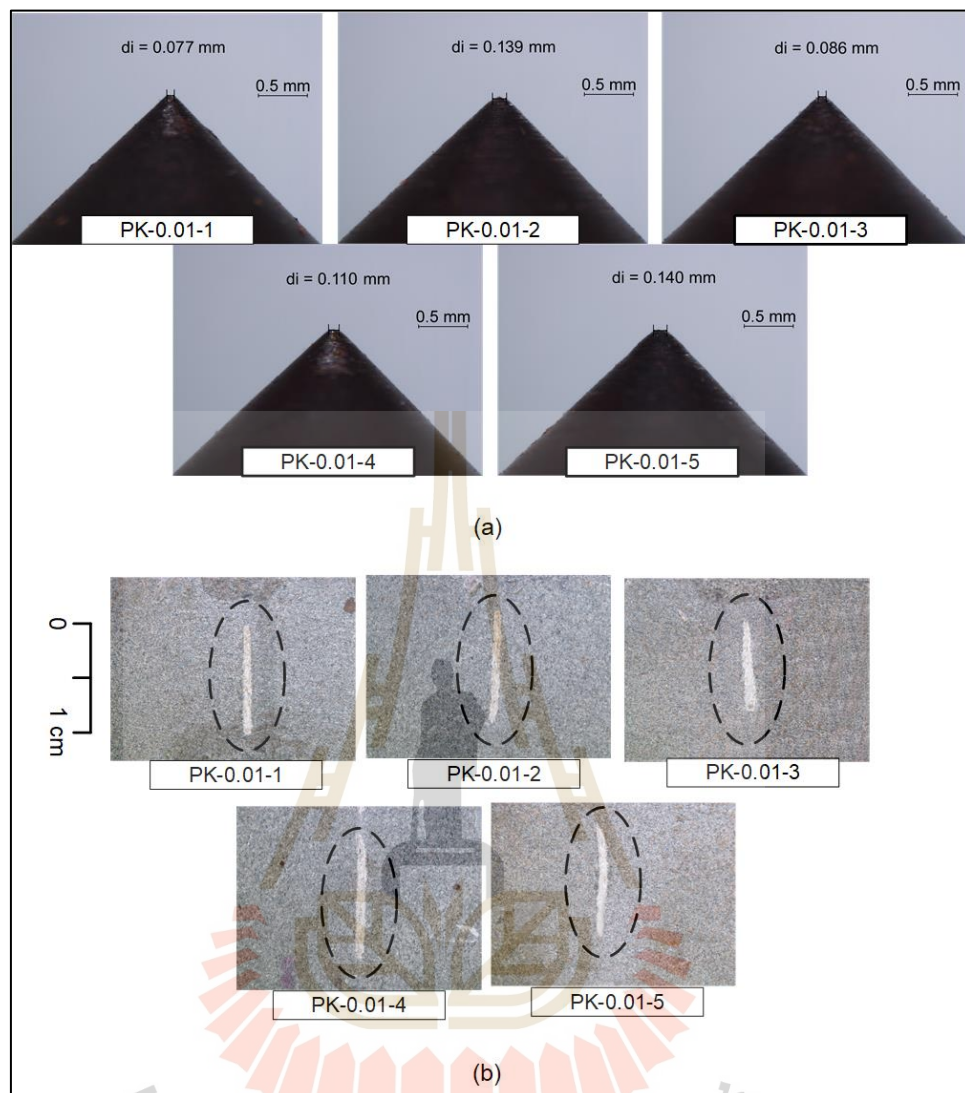


Figure A.23 CERCHAR stylus pins after testing on Phu Kradung sandstone specimens (a) and their corresponding groove images (b) under scratching rate of 0.01 mm/s and saturated conditions.

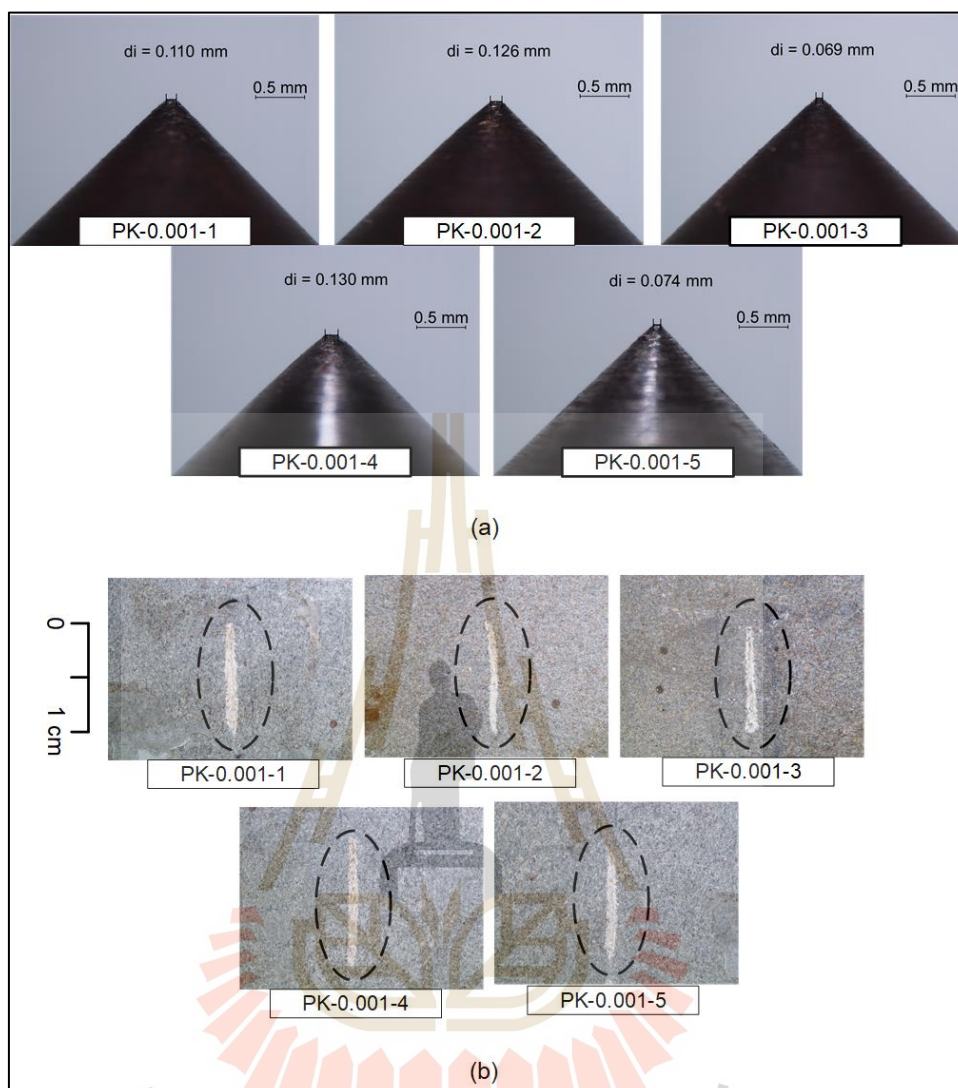


Figure A.24 CERCHAR stylus pins after testing on Phu Kradung sandstone specimens (a) and their corresponding groove images (b) under scratching rate of 0.001 mm/s and saturated conditions.

BIOGRAPHY

Miss. Taraporn Kotsombat was born on April 13, 1996 in Yasothon Province, Thailand. She received his Bachelor's Degree in Engineering (Geological Engineering) from Suranaree University of Technology in 2018. For her post-graduate, she continued to study with a Master's degree in the Geological Engineering Program, Institute of Engineering, Suranaree university of Technology. During graduation, 2018-2020, she was a part time worker in position of research assistant at the Geomechanics Research Unit, Institute of Engineering, Suranaree University of Technology.

